

MICROSCOPICAL ANALYSIS OF THE HEPATOPANCREAS IN WHITELEG SHRIMP (*Penaeus vannamei*) USING COMPUTER-ASSISTED IMAGE ANALYSIS

Fabio Cervellione

Department of Morphology
Faculty of Veterinary Medicine
Ghent University

Academic year 2016 – 2017

Fabio Cervellione (2017)

Microscopical analysis of the hepatopancreas in whiteleg shrimp (*Penaeus vannamei*) using computer-assisted image analysis

On the front cover: photo editing of a light microscopic image of the tubular structure of the hepatopancreas in whiteleg shrimp (*Penaeus vannamei*)

Printed by University Press, Zelzate, Belgium. www.universitypress.be

This thesis was funded by Skretting ARC and the Research Council of Norway. The author and promoters give the permission to consult and copy parts of this work for personal use only. Every other use is subject to copyright laws. Permission to reproduce any material should be obtained from the author.

**MICROSCOPICAL ANALYSIS OF THE HEPATOPANCREAS IN
WHITELEG SHRIMP (*Penaeus vannamei*)
USING COMPUTER-ASSISTED IMAGE ANALYSIS**

Fabio Cervellione

A dissertation submitted in partial fulfilment of the requirements for the
degree of Doctor in Veterinary Sciences (PhD)

Promoters

Prof. dr. Wim Van den Broeck
Dr. Charles McGurk

Department of Morphology
Faculty of Veterinary Medicine
Ghent University

Academic year 2016 - 2017



Promoters

Prof. dr. Wim Van den Broeck
Faculty of Veterinary Medicine, UGent

Dr. Charles McGurk
Skretting Aquaculture Research Centre, Norway

Members of the Examination Committee

Chair of the Examination Committee
Prof. dr. Geert Janssens
Faculty of Veterinary Medicine, UGent

Prof. dr. Koen Chiers
Faculty of Veterinary Medicine, UGent

Prof. dr. Dominique Adriaens
Faculty of Science, UGent

Prof. dr. Peter Bossier
Faculty of Bioscience Engineering, UGent

Dr. Dantas Lima João
IMAQUA, Gent

Table of contents

List of abbreviations	1
General Introduction	3
Scientific aims	47
Chapter 1	49
Optimization of fixation methods for image analysis of the hepatopancreas in whiteleg shrimp, <i>Penaeus vannamei</i> (Boone)	
Chapter 2	71
Use of computer-assisted image analysis for semi-quantitative histology of the hepatopancreas in whiteleg shrimp, <i>Penaeus vannamei</i> (Boone)	
Chapter 3	101
Effect of starvation and refeeding on the hepatopancreas of whiteleg shrimp <i>Penaeus vannamei</i> (Boone) using computer-assisted image analysis	
Chapter 4	127
Effect of starvation and refeeding on the ultrastructure of the hepatopancreas of whiteleg shrimp <i>Penaeus vannamei</i> (Boone) using transmission electron microscopy	
Chapter 5	151
“Perigastric organ”: a replacement name for the “hepatopancreas” in Decapoda	
General discussion	163
Summary/Samenvatting	179
Acknowledgments	187
Curriculum Vitae	188
Bibliography	189

List of abbreviations

The following list provides the full names of all abbreviations used in the test presented in this PhD thesis in alphabetical order.

1 in = single injection inside

4 in = four injections inside

4 out = four injections outside

APP = protocol for image analysis

CAIA = computer-assited image analysis

FCA = F-cell area

FE = fed group

H&E = haematoxylin and eosin

HIA = haemocytic infiltration area

HP = hepatopancreas

IHC = immunohistochemistry

Mabs = monoclonal antibodies

MVB = multivescicular body

Ob1/Ob2 = observer 1/ observer 2

PM = peritrophic membrane

PNR = point of no return

PO = perigastric organ

REF = refed group

RER = rough endoplasmic reticulum

ROI = region of interest

SER = smooth endoplasmic reticulum

ST = starved group

TLA = total lumen area

TTA = total tissue area

VBA = vacuole B-cell area

WSH8 = monoclonal antibodies targeting haemocytes

General Introduction

1.1 Shrimp production

Modern shrimp farming began in the late 1960s, when French researchers in Tahiti developed techniques for intensive breeding and rearing of various shrimp species belonging to the family Penaeidae. Penaeid shrimp are decapods, possessing distinctive morphological features including an extensive rostrum that projects as far as the eye stalk and three pairs of clawed legs (Martin & Hose 2010). Early penaeid culture efforts in America concentrated on indigenous species including northern white shrimp (*Penaeus setiferus*) and blue shrimp (*Penaeus stylirostris*) in Panama, northern brown shrimp (*Penaeus aztecus*) and western white shrimp (*Penaeus occidentalis*) in Honduras, northern brown shrimp and northern pink shrimp (*Penaeus duorarum*) in southern USA, southern white shrimp (*Penaeus schmitti*) and redspotted shrimp (*Penaeus braziliensis*) in Brazil. In 1972, the initial work on whiteleg shrimp (*Penaeus vannamei*) gave much better results than the other species and eyestalk ablation techniques (used to stimulate female shrimp to develop mature ovaries and spawn) led to successful year-round production. Whiteleg shrimp were introduced into Asia experimentally in 1978-79, and commercially in 1996 (FAO 2004).

Farmed crustaceans contribute to a significant proportion of the total aquaculture sector with an annual production exceeding ten million metric tonnes yielding

first sale value of 40 billion US dollars. Average annual growth in penaeid shrimp production has been approximately 14% per annum since 1989 (Bondad-Reantaso *et al.* 2012). The sector is dominated by farmed tropical marine shrimp, the fastest growing sector of global aquaculture industry (Stentiford *et al.* 2012). The leading producers of farmed shrimp are primarily located in South East Asia (China, Thailand, Vietnam, Indonesia and India) and Central and South America (Ecuador, Mexico and Brazil). Main farmed species are whiteleg shrimp and giant tiger prawn (*Penaeus monodon*) (Lightner, *et al.* 2012).

Shrimp remain the most valuable farmed species in the seafood industry, with the highest trade value: the international market is concentrated in the USA, EU and Japan, with the major exporting countries consisting of Thailand, China and Vietnam. Trends in cultured shrimp production of whiteleg shrimp are summarized in Figure 1 (FAO 2017).

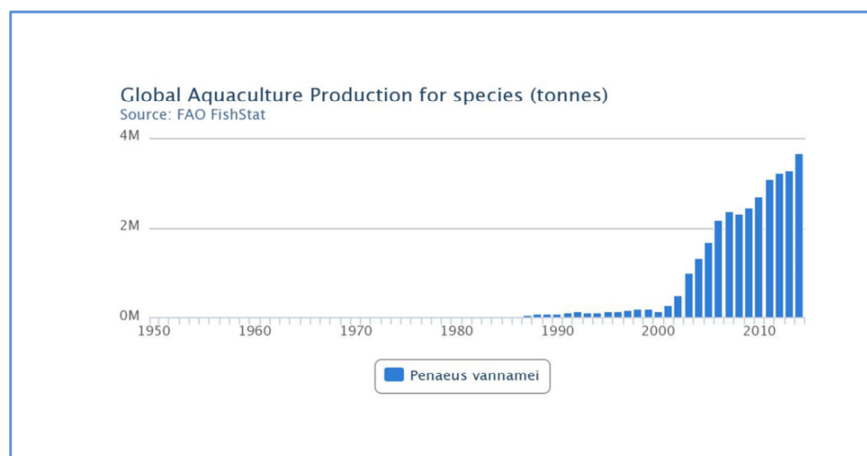


Fig. 1 Global aquaculture production of whiteleg shrimp (*Penaeus vannamei*) from 1950 to 2014 (FAO 2017).

1.2 Whiteleg Shrimp (*Penaeus vannamei*)

1.2.1 Taxonomy

The taxonomic position of whiteleg shrimp is outlined below (ITIS 2017).

Kingdom:	Animalia
Subkingdom:	Bilateria
Infrakingdom:	Ecdysozoa
Phylum:	Arthropoda
Subphylum:	Crustacea
Class:	Malacostraca
Subclass:	Eumalacostraca
Superorder:	Eucarida
Order:	Decapoda
Suborder:	Dendrobrachiata
Superfamily:	Penaeoidea
Family:	Penaeidae
Genus:	<i>Penaeus</i>
Species:	<i>Penaeus vannamei</i> , Boone 1931

1.2.2 Biology

Whiteleg shrimp live in tropical marine habitats (depth 0 to 72 m), native to the Eastern Pacific coast from Mexico to South America, where water temperature is normally over 20°C all year-round. Maximum total body length is 230 mm and maximum carapace length is 90 mm (Holthuis 1980). Adults live and spawn in the open ocean, while post larvae migrate inshore to spend their sub-adult stages in coastal estuaries. Males become mature from 20 g and females from 28 g onwards at the age of six–seven months. Females weighing 30–45 g will spawn approximately 100.000–250.000 eggs (Ø 0.22 mm). Hatching occurs about 16 hours after spawning and fertilization. The first stage

larvae (nauplii) do not feed and live on their yolk reserves. They swim intermittently and are attracted by light (positively phototactic). The next larval stages (protozoa, mysis) remain planktonic and eat phytoplankton and zooplankton, carried towards the shore by tidal currents. Five days after moulting into post larvae, shrimp move inshore and start feeding on benthic detritus (FAO 2017). Farming of whiteleg shrimp offers some advantages over giant tiger prawn: the ability to close the life cycle and produce brood stock (allowing for domestication and genetic selection), rapid growth rate, tolerance to high stocking density and to low salinities and temperatures, and high larval survival during rearing (FAO 2017).

1.2.3 Morphology

Siebold (1848) was the first author to describe the general morphology of the Crustacea.

Figure 2 and Figure 3 show the original illustrations of the internal morphology of European crayfish (*Astacus fluviatilis*) published in 1880 by Huxley.

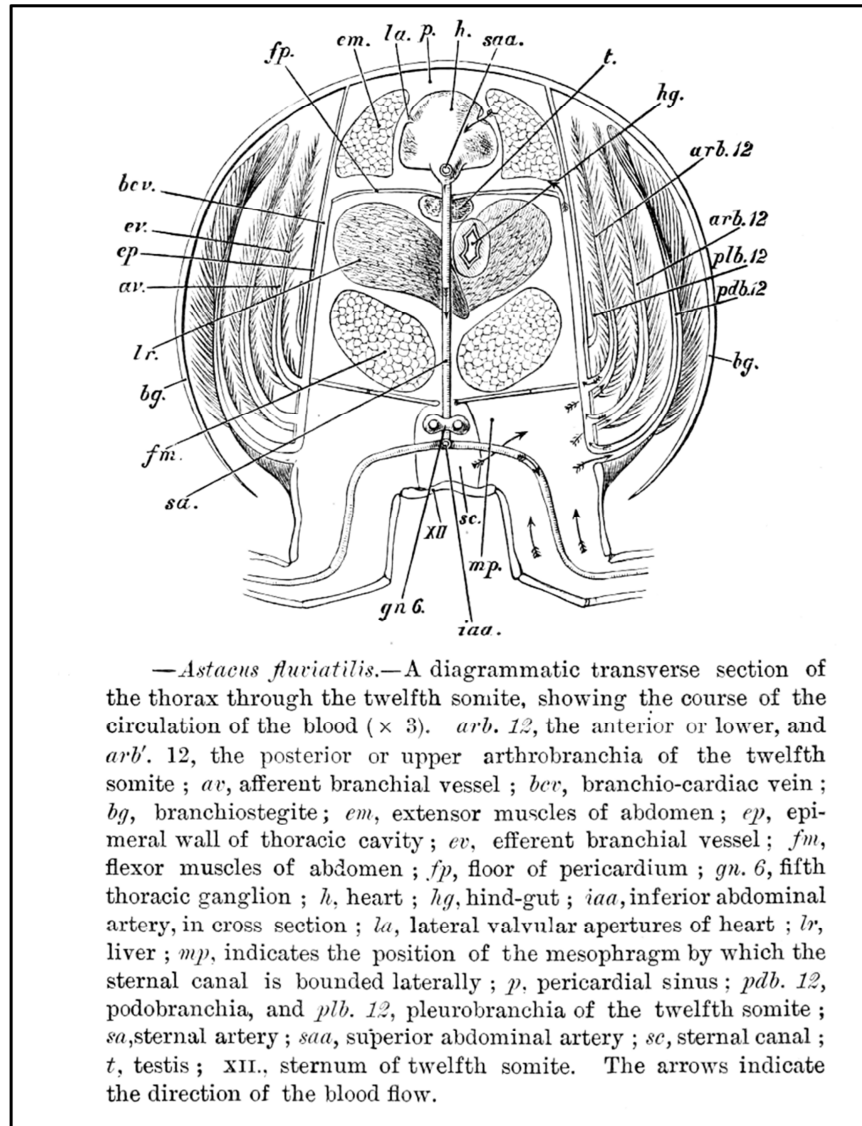


Fig. 2 Historical illustration of the internal morphology of the Decapoda (Huxley 1880).

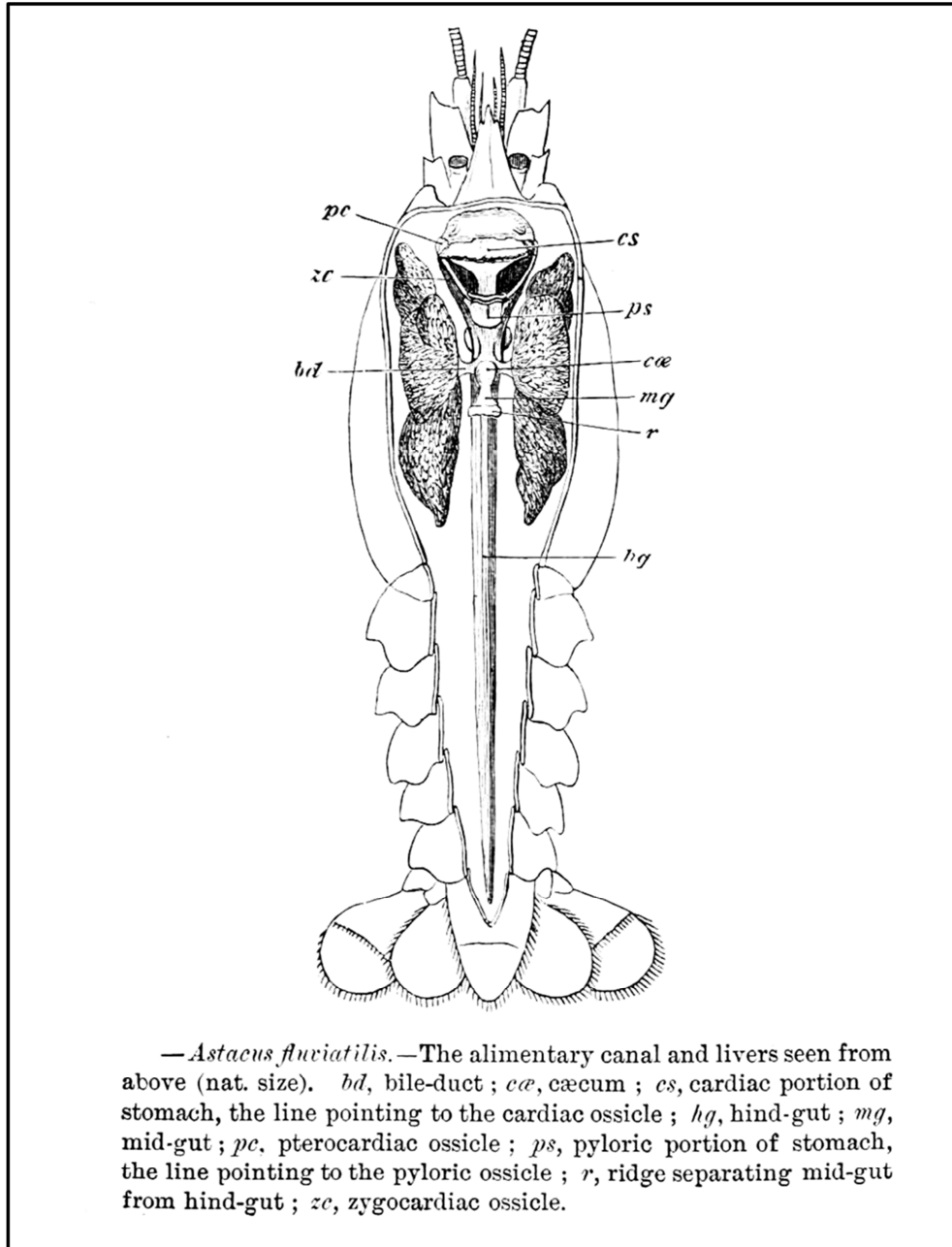


Fig. 3 Historical illustration of the digestive tract of the Decapoda (Huxley 1880).

1.2.3.1 External and internal morphology

The shrimp body is laterally compressed and divided into two regions: the cephalothorax and the abdomen. The anterior cephalothorax comprises the fusion of five head segments and eight thoracic segments. The abdomen is composed of six distinct segments. The external surface is covered by the exoskeleton (Martin & Hose 2010). External and internal morphology of the Decapoda are illustrated in Figure 4 and Figure 5.

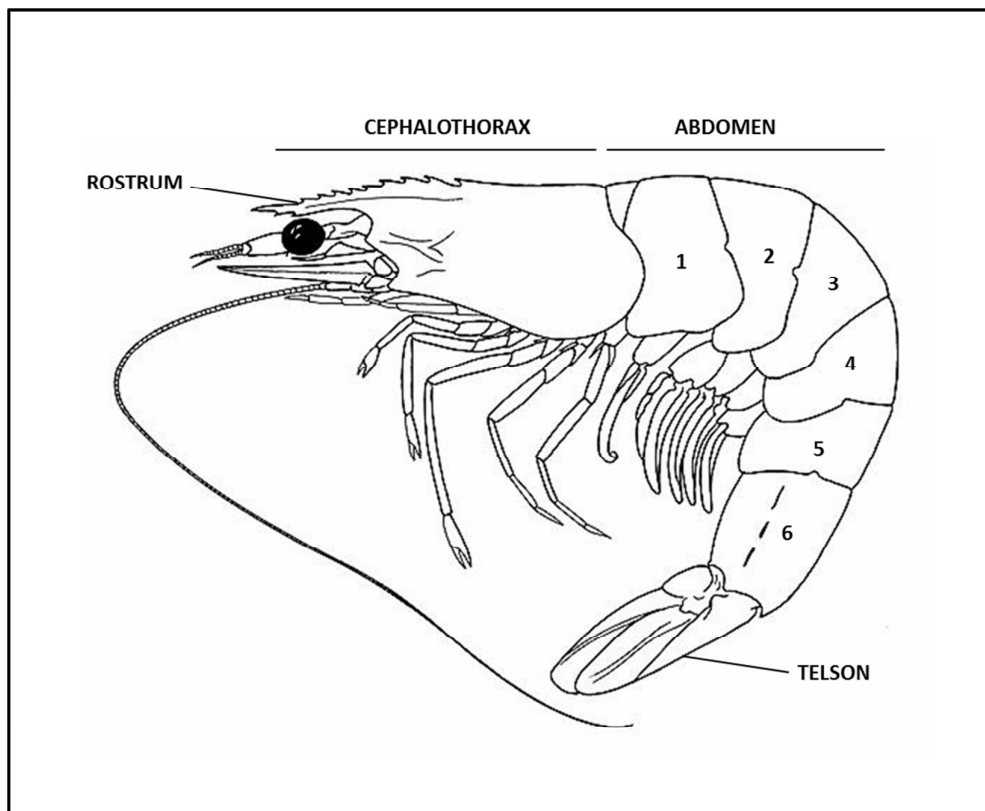


Fig. 4 External morphology of penaeid shrimp. Adapted from FAO (2017).

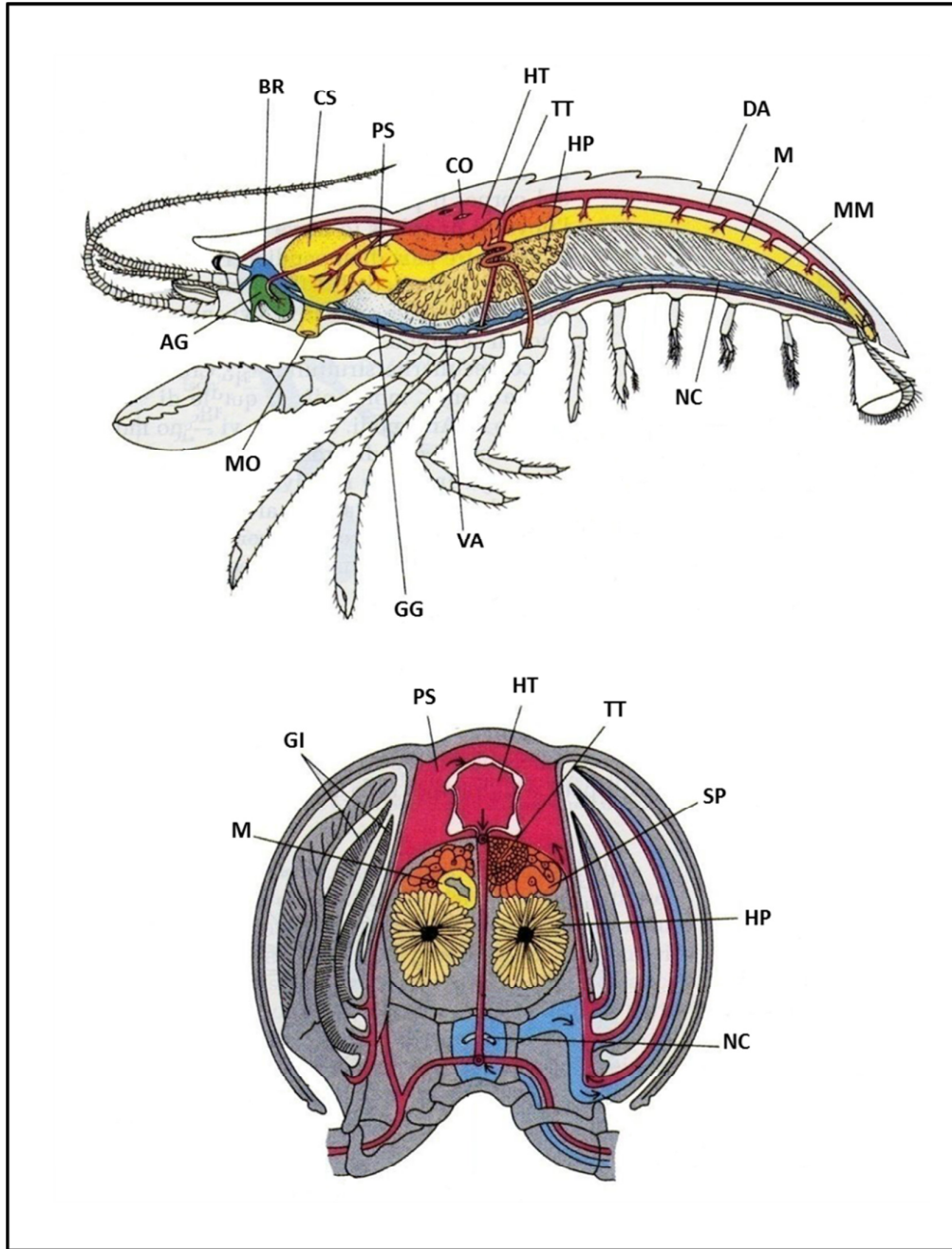


Fig. 5 Internal morphology of the Decapoda. AG = antennal gland; BR = brain; CO = cardiac ostium; CS = cardiac stomach; DA = dorsal artery; GG = ganglion; GI = gills; HP = hepatopancreas; HT = heart; M = midgut; MM = muscles; MO = mouth; NC = neural cord; PS = pyloric stomach; SP = sperm duct; TT = testicle; VA = ventral artery. Adapted from SlidePlayer (2017).

1.3 Digestive tract of the Decapoda

The digestive tract can be divided in three parts: foregut (mouth, oesophagus and stomach), midgut (including hepatopancreas and midgut caeca) and hindgut. It extends the length of the body from the anterior mouth to the posterior anus (Figure 6) (Gimenez 2013). The anatomy and cellular composition of the digestive tract of decapods is considerably different from vertebrates. Differences primarily include the gastric mill, a sophisticated filter apparatus in the stomach, and the tubules of the hepatopancreas (HP). Additional differences are the lack of strongly acid pH and pepsin in the stomach. The lumen of the digestive tract must be considered as being located outside the animal itself. The internal wall is impregnated, in its fore and hind parts (foregut and hindgut), with complexes of chitin and proteins forming a cuticle (comparable to the exoskeleton) which are removed with the exoskeleton at each moult. Tegumental glands are located along the walls of the oesophagus and the junction between midgut and hindgut. They secrete mucus that lubricates the wall and facilitates the transition of food and faeces (Felgenhauer 1992; McGaw & Curtis 2013).

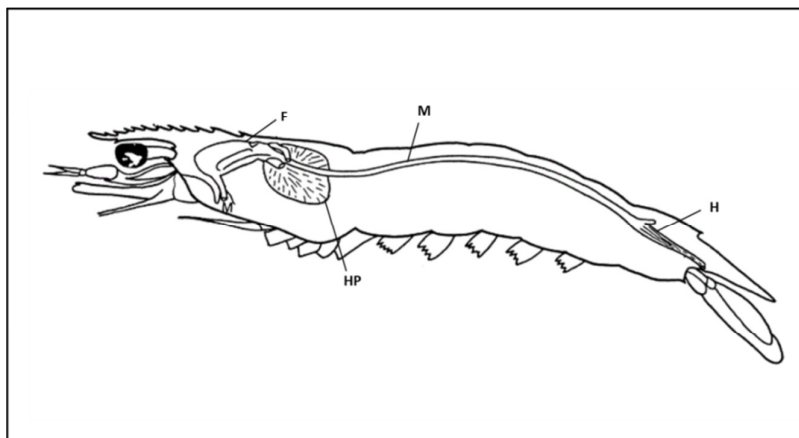


Fig. 6 Schematic representation of the digestive tract of the Decapoda. F = foregut; H = hindgut; HP = hepatopancreas; M = midgut. Adapted from Dall (1965).

1.3.1 Foregut

The foregut is composed of the mouth, oesophagus and stomach. The oesophagus is usually short, straight, positioned vertically, and lined by a thick cuticle (Ceccaldi 1989). The stomach is a dual-chambered, chitinous sac, divided into a larger anterior (or cardiac) chamber and a narrower posterior (or pyloric) chamber. The anterior chamber is a spacious sac facilitating mastication and sorting ingested food. It bears a longitudinal row of small ridges which lead to the lateral teeth and the larger dorsal median tooth. The cardio-pyloric valve separates the anterior chamber from the posterior chamber. The posterior chamber has a dorsal region which allows ingested material to pass directly into the midgut and a ventral region called the filter-press, which permits only the finest particles to enter the HP. Both chambers are composed of a varying number of chitinous plates/ossicles that differ in size and morphology (Felgenhauer 1992).

1.3.2 Midgut

The midgut is composed of the intestine and many evaginations, namely the HP, anterior and posterior midgut caeca (McLaughlin 1983). It starts in the cephalothorax at the junction with the pyloric sac of the stomach and ends in a coiled tube, the posterior midgut caecum, at the anterior half of the sixth abdominal segment (Ceccaldi 1989; McGaw & Curtis 2013). The midgut is the only region of the digestive tract which is not lined by cuticle and is in contact with the external environment. The midgut is lined by a columnar epithelium sitting on a basement membrane, usually exhibiting a prominent brush border. The functions of the midgut are not entirely clear, and include osmoregulation, limited nutrient absorption, and the production of the peritrophic membrane (PM). The PM is a

non-cellular membrane lining the midgut, which serves as a barrier between the contents of the gut lumen and the midgut epithelium, protecting the midgut from abrasive food particles and pathogens. The PM is composed of chitin fibrils associated to proteoglycans and assists digestion process by compartmentalization of the gut and immobilization of the digestive enzymes. It is an important component of the intestinal immune system, inactivates ingested toxin, and prevents oxidation (Wang *et al.* 2012). The midgut caeca are two blind ending extensions of the midgut, and histologically differ from the intestine in lacking longitudinal muscular fibres and in possessing considerably infolded walls. They play a role in ion and water regulation (Barker & Gibson 1977; Ceccaldi 1989).

1.3.3 Hepatopancreas

The HP is a large bi-lobed organ composed of many blindly ending tubules, which wrap over the dorsal and lateral sides of the posterior part of the stomach and the anterior part of the midgut (Franceschini-Vicentini *et al.* 2009; Martin & Hose 2010). It represents 2-6% of the total body weight and reaches its greatest degree of complexity in the Decapoda (Gibson & Barker 1979). Its colour (brown, red, green, yellow, blue) mainly depends on the stored reserves (carotene, zeaxanthine, astaxanthine, and cantaxantine) (Gibson & Barker 1979; Ceccaldi 1989). It has two separate lobes, enclosed together in a connective tissue capsule and separated by a thin septum. Each lobe is composed of two or three lobules and it is connected to the intestine through the corresponding principal duct (Esteve & Herrera 2000; Vasagam *et al.* 2007). Principal ducts divide in secondary ducts which branch in the HP tubules. Around each duct, there are fine circular and longitudinal muscular fibres, which allow for peristaltic and longitudinal contractions, facilitating the movement of liquids through the organ. The HP is well supplied with haemolymph: the hepatic arteries pass into the HP lobes where they subdivide among ducts and tubules (Herreid & Full 1988; Ceccaldi 1989). Transverse sections of the tubules through the medial region of the HP exhibit a normal star-shape lumen (Esteve & Herrera 2000; Vasagam *et al.* 2007).

Each hepatopancreatic tubule can be subdivided into a distal, medial and proximal zone relative to the distance from the midgut (Figure 7) (Felgenhauer 1992; Franceschini-Vicentini *et al.* 2009). Each tubule is made up of four basic cell types: E-, F-, R- and B-cells (Figure 8) (Nakamura 1987; Franceschini-Vicentini *et al.* 2009). Figure 9 shows the four cell types comprising the HP tubule observed under light microscope.

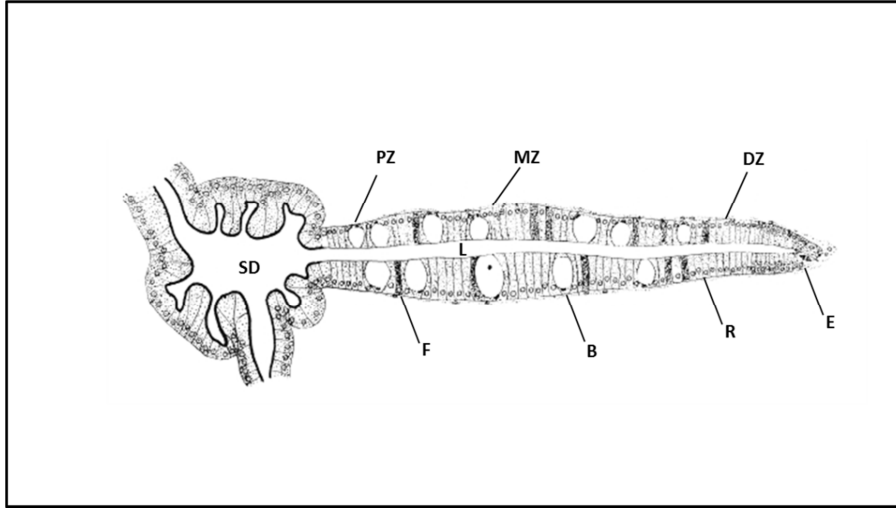


Fig. 7 Schematic representation of the hepatopancreas tubule structure in the Decapoda. = B-cell; DZ = distal zone; E = E-cell; F = F-cell; L = lumen; MZ = medial zone; PZ = proximal zone; R = R-cell; SD = secondary duct. Adapted from Van Weel (1955).

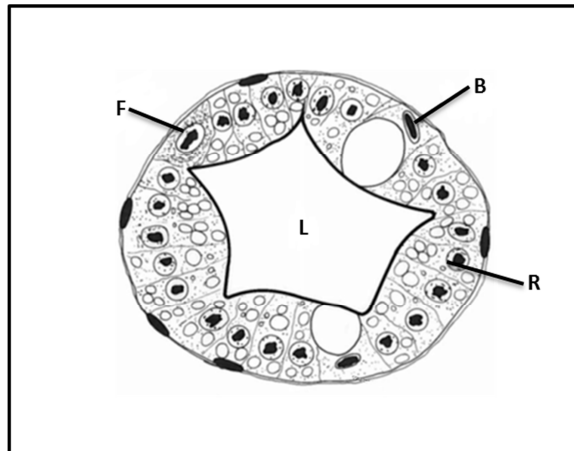


Fig. 8 Schematic representation of a cross section of the medial part hepatopancreatic tubule in the Decapoda. B = B-cell; F = F-cell; L = lumen; R = R-cell. Adapted from Johnson (1995).

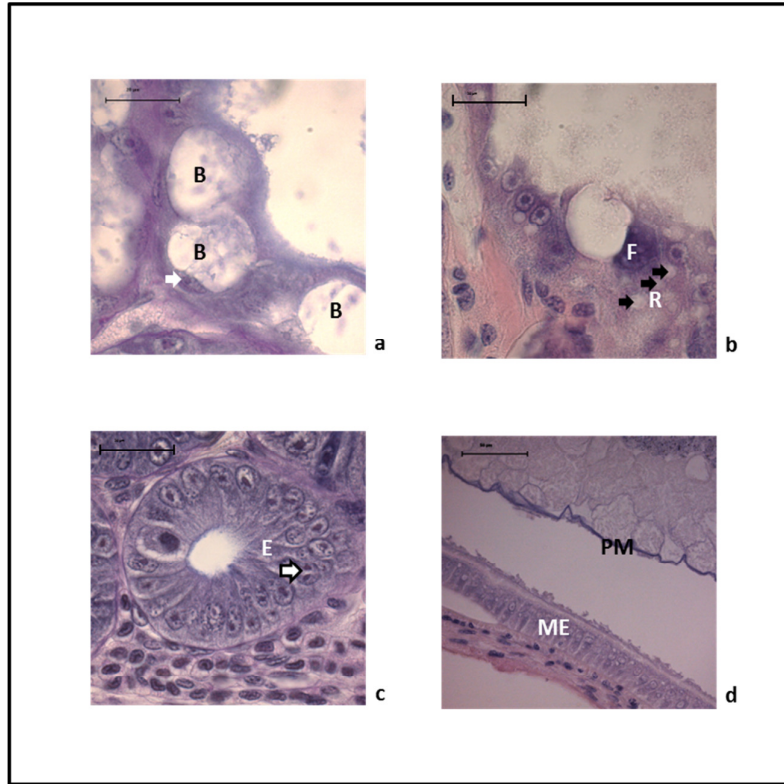


Fig. 9 Light microscopic structure of the hepatopancreas (a, b, c) and midgut (d) in whiteleg shrimp (*Penaeus vannamei*). Five μm paraffin sections. H&E. (a) B-cells, showing a single large vacuole and peripheral nucleus (white arrow); (b) F-cell with basophilic cytoplasm and R-cell with multiple lipid droplets (black arrows); (c) E-cells at the distal end of the tubule, in mitotic division (black/white arrow); (d) midgut, showing the epithelium and peritrophic membrane. B = B-cell; E = E-cell; F = F-cell; ME = midgut epithelium; PM = peritrophic membrane; R = R-cell. Scale bar = (a,b,c) 20 μm , (c) = 50 μm (Skretting ARC).

The E-cells, or embryonic cells, are small cuboidal cells found at the distal blind ends of the tubules and give rise to the other three cell types. E-cells are characterized by a large nucleus with prominent nucleolus and usually lack a brush border. The ultrastructure of the medial zone of the HP tubule is summarized in Figure 10. F-cells, or fibrillar cells, are cylindrical/prismatic cells located at the medial and proximal zones of the tubules among R-cells and B-cells. They have a basally located nucleus and a developed

rough endoplasmic reticulum (RER), giving them a fibrillar appearance, typically exhibiting a strong basophilia in H&E staining due to a high RNA content. They present small vesicles throughout the cytoplasm and have a prominent brush border (Barker & Gibson 1977) (Felgenhauer 1992). This cell type has a high rate of protein synthesis and is the only site of digestive enzyme synthesis (Franceschini-Vicentini *et al.* 2009). B-cells, or blister cells, are large, primary secretory cells, more frequent at the proximal zone of the tubules. They are defined by the presence of a single enormous vesicle surrounded by a dense cytoplasm filled with RER (Barker & Gibson 1977; Felgenhauer 1992; Cuartas *et al.* 2002). They are responsible for intracellular digestion, concentrating the absorbed materials in the large vacuole and secreting the vacuolar content at the end of the digestive process, and it is believed that the digestion-derived nutrients are released for reabsorption by R-cells (Franceschini-Vicentini *et al.* 2009). The R-cells are the most numerous cell type, located at medial and proximal zones. These tall, columnar cells are characterized by a prominent brush border and a large number of irregularly-shaped storage vesicles (primarily lipids) in their cytoplasm (Franceschini-Vicentini *et al.* 2009). These cells function in food absorption and storage of nutrients and minerals (Felgenhauer 1992).

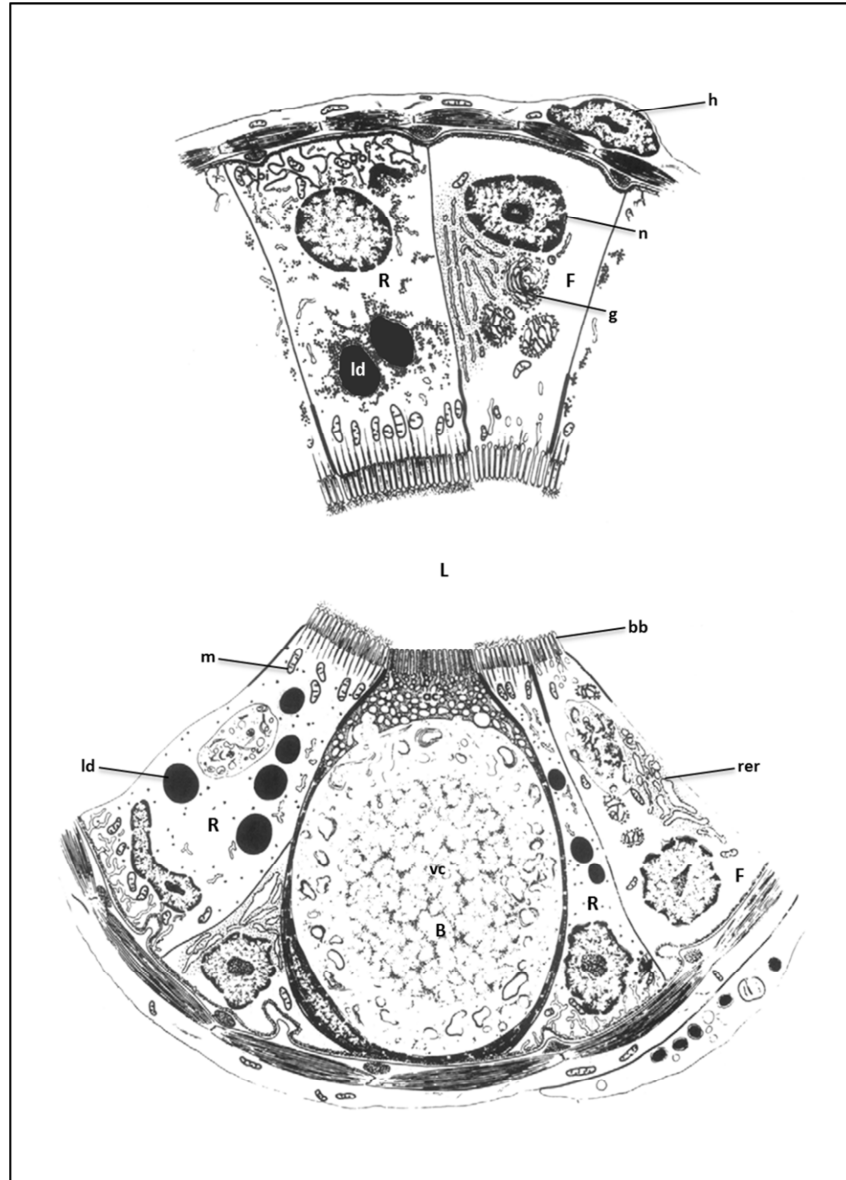


Fig. 10 Schematic representation of the ultrastructure of the medial zone of the hepatopancreas tubule in the Decapoda. B = B-cell; bb = brush boarder; F = F-cell; g = Golgi complex; h = haemocyte; L = lumen; ld = lipid droplet; m = mitochondria; n= nucleus; R = R-cell; rer = rough endoplasmic reticulum; vc = vacuole. Adapted from Dall & Moriarty (1983).

1.3.4 Hindgut

The hindgut is of ectodermal origin and consequently lined with chitin (Barker & Gibson 1977). It is located in the posterior half of the sixth abdominal segment and includes the rectum and anus (Ceccaldi 1989). It is characterized by the presence of cuticular scales or groups of spines, posteriorly directed facilitating the movement of the faecal mass towards the anus (Felgenhauer 1992).

1.4 Digestive physiology

The foregut, midgut and hindgut are specialized structures serving specific functions. The foregut is responsible for mechanical and extracellular enzymatic digestion (enzymes released by the HP into the anterior chamber), midgut regulates movements of digesta into the HP where intracellular digestion takes place, and peristaltic movements of the hindgut expel the PM containing faeces (Figure 11).

The mouth opens into a short oesophagus, lined with tegumental glands, secreting mucus that lubricates the food. The pyloric region filters out particulate matter, so that only liquid and particles less than 100 nm in diameter enter the HP (Martin & Hose 2010; McGaw & Curtis 2013). The primary role of the HP is the synthesis and secretion of digestive enzymes, final digestion of ingested food and uptake of nutrients (Laohabanjong *et al.* 2009). Enzymes from the HP are released into the anterior (cardiac) chamber and flow ventrally into the filter-press where setae filter particles. The excluded particles are passed posteriorly into the midgut, while the smallest particles and fluid enter the HP tubules for absorption (McGaw & Curtis 2013).

The microvilli in the midgut epithelia are involved with absorption of nutrients in larval shrimp, but minimal absorption occurs in adults. They synthesise the PM, a chitinous wrapper that encapsulates ingested materials as soon as they enter this region of the gut and persist around the faecal pellet (Martin & Hose 2010). Anterior and posterior midgut caeca play also a role in ion and water regulation, and maintain pH balance. The hindgut is involved in active ion uptake and transport. Tegumental glands along its length secrete mucus to lubricate the walls (McGaw & Curtis 2013).

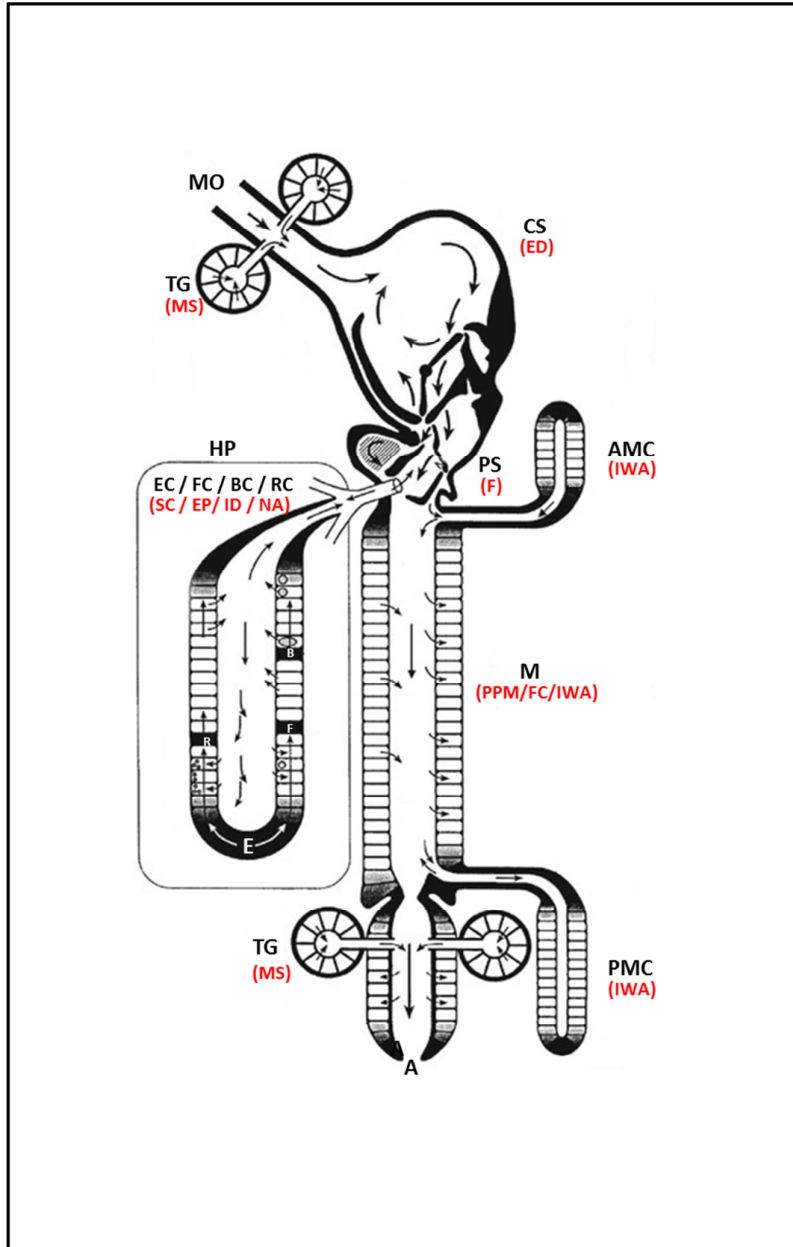


Fig. 11 Schematic diagram of digestive processes in the Decapoda. Organs (in black) and their main functions (in red between brackets). Organs: A = anus; AMC = anterior midgut caecum; BC = B-cells; CS = cardiac stomach; EC= E-cells; FC = F-cells; HP = hepatopancreas; M = midgut; MO = mouth; PMC = posterior midgut caecum; PS = pyloric stomach; RC = R-cells; TG = tegumental glands. Functions: ED = extracellular digestion; EP = enzyme production; F = filtration; FC = faecal compaction; ID = intracellular digestion; IWA = ion and water uptake; MS = mucus secretion; NA = nutrient absorption; PPM = production of peritrophic membrane; SC = staminal cells. Adapted from McGaw & Curtis (2013).

1.5 Feeding and moulting

Crustaceans alternate episodes of feeding and fasting during development, which occurs through moulting and results in growing by sequential steps. Increase in body size at each ecdysis is non-linear; this is a hormonally controlled process which might last days or weeks, is continuous and accompanied by morphological, physiological, and behavioral alterations occurring almost daily (Dall *et al.* 1990). Moulting is a natural continuous process used by crustaceans to shed their exoskeleton and grow. The moult cycle is divided into four major stages: pre-moult (D), moult (E), post-moult (A and B) and inter-moult (C). In stage A, the exoskeleton is soft and the shrimp is incapable of taking food. Feeding begins in stage B, when the exoskeleton is sufficient rigid to handle food. During stage C, shrimp feeds actively and exoskeleton becomes very rigid. Feeding declines during stage D, just before ecdysis (stage E), where the old cuticle is shed and the organism is unable to feed (Sánchez-Paz *et al.* 2007).

1.6 Immunology

Crustaceans lack true adaptive immunity and solely depend on innate immunity (cellular and humoral).

1.6.1 Cellular innate immunity

In crustaceans, the circulating haemocytes are crucial in protecting the animal against invading microorganisms by participating in recognition, phagocytosis, melanisation and cytotoxicity. Three morphologically different classes of haemocytes have been described: hyaline, semigranular and granular (Cerenius *et al.* 2010; Dantas Lima 2013; Musthaq & Kwang 2014).

Pathogen recognition stimulates the degranulation of granular and semigranular cells. The release of the prophenoloxidase system and other plasma factors from the stored granules promotes phagocytosis by hyaline cells or encapsulation by semigranular cells (Johansson *et al.* 2000).

Phagocytosis is the major cellular defence mechanism towards infection in crustaceans. If the number of the foreign entities invading the organism is too high or the sizes too large to be eliminated by phagocytosis, crustaceans apply nodulation (bacteria and fungus) or encapsulation (parasite). The process is characterized by trapping and isolating the foreign entities by attachment of concentric layers of adherent haemocytes around them. It follows the killing of the invaders by asphyxiation and action of toxic compounds and enzymatic cascades (Dantas Lima 2013).

1.6.2 Humoral innate immunity

Humoral defences of invertebrates are a multiplicity of serum or plasma factors which act against micro-organisms, foreign cells or abiotic materials. These factors include agglutinins, lytic agents, bactericidal peptides, cytokines, micro-biocidal pigments, antiviral, cytotoxic, clotting, and prophenoloxidase factors (Smith & Chisholm 1992).

1.6.3 Mucosal immunity

In vertebrates the mucosal immunity is composed of mechanical and chemical barriers preventing the entry of foreign bodies or potential pathogens. The PM constitutes a clear example of non-vertebrate barrier epithelia. The inflammatory process involves changes in vascular tissue and the rapid recruitment and activation of immune cells to damaged or

infected tissue. The main mechanisms of mucosal immunity in the gut of crustaceans are: receptors of pathogen recognition, as PI-PET (thioester containing protein), and antimicrobial peptides (Garcia-Garcia *et al.* 2013).

1.6.4 Innate immunity with specificity

There is increasing evidence that shrimp and other arthropods exhibit immune specificity and immune memory. Invertebrate host, after its first exposure to a pathogen, acquires memory that gives the host an enhanced immunity when the same pathogen is encountered again. The invertebrate immune response is now called “innate immunity with specificity” or “immune priming”, and its mechanisms are still unclear. While vertebrate antibodies have no invertebrate homolog, the Down syndrome cell adhesion molecule (Dscam) can function as a pathogen-specific recognizing molecule in arthropods (Ng *et al.* 2014).

1.7 Health issues related to shrimp farming

The aquaculture of penaeid shrimp has grown from its experimental beginnings roughly three decades ago into a major industry. Almost from the start, diseases were recognized as a biological threat to the shrimp industry, causing serious economic losses. The diseases of cultured penaeid shrimp include syndromes with infectious (viral, bacterial, fungal, parasitic) and non-infectious aetiologies (environmental stressors, nutritional imbalances, toxicants and genetic factors) (Lightner & Redman 1998).

According to a survey conducted by the Global Aquaculture Alliance, approximately 60% of the disease losses in shrimp aquaculture could be attributed to viral diseases and approximately 20% to bacterial diseases. The remaining 20% of losses can be attributed to a variety of other pathogens (parasites and fungi) and to abiotic or unknown causes (Flegel 2012).

Very recently shrimp farming has been affected by a new syndrome, targeting the HP, called acute hepatopancreatic necrosis disease (AHPND). AHPND was first reported in 2009 (officially in 2010) in China and initially named early mortality syndrome (EMS). The disease has rapidly spread to Vietnam, Malaysia, Thailand, Mexico and the Philippines (Leaño 2016). This disease specified with mass mortality (up to 100%) 20-30 days after stocking. The most important clinical symptoms consist of lethargy, low speed growth rate, spiral swimming, as well as empty gut (Lightner *et al.* 2013). Affected shrimp consistently show an abnormal HP, shrunken and discolored. The key diagnostic feature for diagnosis is the sloughing off of the HP cells observed in histological sections (Leaño 2016). The disease is caused by a highly virulent strain of *Vibrio parahaemolyticus*,

carrying plasmids containing the genes that code for the toxins *pirA* and *pirB* (Tran *et al.* 2013).

1.8 Pathophysiology of the hepatopancreas

1.8.1 Structural changes observed with light microscopy

The HP is routinely examined by pathologists and monitored for health (Johnson 1995; Laohabanjong *et al.* 2009; Calvo *et al.* 2011). Morphological changes in the HP have been described in response to physiological demands (Adiyodi & Adiyodi 1972), imbalanced diets (Gimenez *et al.* 2004; Vasagam *et al.* 2007; Laohabanjong *et al.* 2009), food deprivation (Vogt *et al.* 1985; Nakamura 1987; Ong & Johnston 2006; Leser *et al.* 2008; Berillis *et al.* 2013; Sacristán *et al.* 2016), environmental stressors (Diaz *et al.* 2010; Kuhn *et al.* 2010), and diseases (Frelier *et al.* 1992; Lightner & Redman 1994; Del Rio-Rodriguez *et al.* 2006; Joshi *et al.* 2014).

Haemocyte infiltration in the intertubular spaces is the response of the immune system to HP tissue damage (traumatic or due to infection), toxicity and environmental stress (Johnson 1980; Chiodi Boudet *et al.* 2015; Longo & Diaz 2015). Main morphological changes reported in the HP literature are: atrophy of the tubular epithelium, reduction of the epithelium thickness, desquamation of the epithelium, enlargement of the tubular lumen, reduction of the number of R-, F-, and B-cells, reduction of lipid droplets, damage and infolding of the basal lamina, enlargement of B-cell vacuole, nodule formation, loss of the normal star-like shape of the lumen.

1.8.2 Ultrastructural changes observed with electron microscopy

A few studies have described the ultrastructural changes occurring in the HP of decapods and, to our best knowledge, none of them in whiteleg shrimp during food deprivation. Three types of cell death have been described in literature so far: necrosis, apoptosis and autophagy (Sonakowska *et al.* 2016).

Ultrastructural changes in the HP have been described in response to imbalanced diets (Gopinath *et al.* 2012), food deprivation (Storch & Anger 1983; Elendt & Storch 1990; Storch *et al.* 1984; Tam & Avenant-Oldewage 2009; Yoshida *et al.* 2009; Sonakowska *et al.* 2016), environmental stressors (Diaz *et al.* 2010), toxic compounds (Znidarsic, Strus & Drobne 2003; Abdelmeguid, Awad, Ibrahim & Yousef 2009) and diseases (Frelier *et al.* 1992).

The main ultrastructural changes described in the HP are: depletion of lipid droplets within R-cells, swelling of organelles (mitochondria, RER, Golgi complex), rupture of the brush boarder and cell membranes, infolding and thickening of the basal lamina, nuclear fragmentation and vacuolation, chromatin condensation, autophagy, haemocytic infiltration in the intertubular spaces, and tubular necrosis.

1.9 Histological analysis

1.9.1 Fixatives and fixation methods

Histology has proved to be an essential discipline in the medical and veterinary professions since cellular pathology was initially described by Virchow in 1858 (Mawdesley-Thomas 1972). The foundation of all good histological preparations is adequate and complete sample fixation. Faults in fixation cannot be remedied at any later

stage, and the finished section can only be as good as its primary fixation. The object of fixation is to preserve the tissues as much as possible by preventing autolysis and putrefaction. The most important reaction for maintaining morphology is the stabilization of proteins. Fixatives have the property of forming cross-links between proteins, thereby forming a gel, ideally keeping everything in their *in vivo* relations to each other. In conventional histological techniques, lipids are largely removed during preparation of tissues: if they are to be visualized, then frozen sections should be used (Bancroft & Marylin 2002). Fixation can be performed using physical (heat, freezing) and chemical methods (liquid fixatives). Liquid fixatives affect the tissues both physically and chemically. The principal changes produced are swelling or shrinkage, and most of the fixatives are formulated to balance these two effects. Dehydration and paraffin embedding produce some further shrinkage and hardening (Kiernan 2008). Solid specimens are fixed by immersion in at least ten times their own volumes of the appropriate solution or by perfusion of the fixative through the vascular system, or by injection of the fixative in the target tissue (Kiernan 2008).

1.9.2 Fixatives in crustaceans

The HP undergoes rapid autolysis immediately after death. Delays of even a few seconds in fixative penetration into this organ can result in the whole specimen being useless for diagnosis. Thus, specimens must be immersed or injected with fixative while still alive. In tropical areas, it is best to use cold fixative to help arrest autolysis and secondary microbial proliferation. Larvae and early post larvae should be immersed directly in a minimum of ten volumes of fixative to one volume of shrimp tissue. This 10:1 ratio is critical for effective preservation (Bondad-Reantaso *et al.* 2001). Larger shrimp should be

injected before being immersed in fixative (Bell & Lightner 1988). The chitinous exoskeleton of juvenile and adult crustaceans does not allow for adequate fixative penetration by simple immersion: following removal from the water, specimens should be fixed immediately by injecting the fixative into vital areas (Bell & Lightner 1988).

Various fixatives have been used for preservation of crustaceans: Helly's, Bouin's, Dietrich's, and Davidson's fixatives, and 4% formaldehyde (Nakamura 1987; Bell & Lightner 1988; Sindermann & Lightner 1988; Esteve & Herrera 2000; Lewbart 2006; Ong & Johnston 2006; Alexandre *et al.* 2014).

Helly's fixative (25 g potassium dichromate, 10 g sodium sulphate, 50 g mercuric chloride, 1000 mL distilled water; before use, add 40% formaldehyde) is considered excellent for bone marrow and intercalated discs of cardiac muscle. Helly's is used mainly to fix cytoplasmic elements such as mitochondria and granules. The non-coagulant components (formaldehyde, dichromate at neutral pH) offset the coagulant action of the mercuric chloride so that the organelles are not destroyed by coarse coagulation of the cytoplasm. It produces mercury pigments which should be removed from sections before staining (Kiernan 2008; Leica Biosystem 2017). Bouin's fixative (750 mL picric acid saturated aqueous solution 2.1%, 250 mL formaldehyde, 50 mL acetic acid glacial) gives good results with trichrome staining and is recommended for gastro-intestinal biopsies and endocrine gland tissue. Bouin's fixative preserves morphological features, especially of nuclei and connective tissue. The fixative reacts with basic proteins and forms crystalline picrates with amino acids (Hopwood 2002). Physical distortion of tissues is minimal and paraffin sections are easy to cut. Because of its acidic nature it will slowly remove small calcium and iron deposits (Kiernan 2008; Leica Biosystem 2017).

4% formaldehyde is the most widely used fixative for routine histology. Many epitopes require antigen retrieval for successful immunohistochemistry following its use (Leica Biosystems 2017). Davidson's fixative (30 mL 95% ethanol, 20 mL 37% formaldehyde, 10 mL glacial acetic acid, and 30 mL distilled water) is the most common fixative used in crustaceans (Bell & Lightner 1988; Lightner *et al.* 1993; Cuartas *et al.* 2002; Gimenez *et al.* 2004; Hasson *et al.* 2009; Diaz *et al.* 2010; Kuhn *et al.* 2010; Andrade *et al.* 2008 Joshi *et al.* 2014). The swelling caused by acetic acid is present to counter the shrinkage caused by ethanol. Most lipids are extracted using this fixative (Kiernan 2008; Leica Biosystem 2017). Carnoy's fixative (60 mL absolute ethanol, 30 mL chloroform, and 10 mL glacial acetic acid) is recommended for the preservation of nucleic acids and macromolecular carbohydrates. The fixative penetrates rapidly coagulating protein and nucleic acids. It extracts lipids but maintains many carbohydrate components (Kiernan 2008). Zinc salt fixation (0.05 g calcium acetate, 0.5 g zinc acetate, 0.5 g zinc chloride, 1.2 g 0.1 M tris buffer, bidistilled water to 100 mL) has been reported to work excellently for the preservation of fixation-sensitive antigens in immunohistochemistry (Rieger *et al.* 2013).

1.9.3 Fixation protocols for crustaceans

Bell and Lightner's (1988) and the CEFAS (European Union reference laboratory for crustacean diseases) protocols are the fixation protocols most commonly used for shrimp histology (CEFAS 2013).

1.9.3.1 Bell's and Lightner's protocol

Bell and Lightner's protocol (1988) is considered by many researchers to be the reference protocol for shrimp histology. The protocol is here briefly described.

For post larvae (>20mm in length) use a fine needle to make a small shallow incision at the cuticular junction between the cephalothorax and first abdominal segment to allow the fixative to penetrate quickly. For larger post larvae, juveniles and adults, place the shrimp briefly in ice water to sedate them. Immediately after sedation, inject Davidson's fixative (approximately 10% of the shrimp's body weight) at the following sites: the HP, region anterior to the HP, anterior and posterior abdominal regions. The HP should receive a larger proportion of the injected fixative than the abdominal region. In larger shrimp it is better to inject the HP at several points. All signs of life should cease and the colour should change at the injection sites. Immediately following injection slit the cuticle with dissecting scissors along the side of the body from the sixth abdominal segment to the cuticle overlying the "head region" (cephalothorax). From there, angle the cut forward and upward until it reaches the base of the rostrum. Avoid cutting too deeply into the underlying tissue. Shrimp over 12 g should be transversely dissected, at least once, posterior of the abdomen/cephalothorax junction or again mid-abdominally. The tissues should then be immersed in a 10:1 volume ratio of fixative to tissue, at room temperature. The fixative can be changed after 24-72 hours to 70% ethanol, for long term storage.

1.9.3.2 European Union reference laboratory for crustacean diseases protocol

CEFAS is the reference European laboratory for crustacean diseases. The protocol is here briefly described (CEFAS 2013).

Ensure that the area around the cephalothorax is injected several times with small amounts of Davidson's fixative, to ensure good fixation of the HP. Place in Davidson's fixative and allow fixation for at least 24 hours after the last shrimp was placed in the fixative before sectioning samples. Using razor blade, carefully remove antennae and pereopods, leaving the base of appendages attached to enable any protozoan infections to be identified in section. Remove eyes, rostrum and mandible, tail and cut shrimp along the mid-sagittal line. Place half of the cephalothorax into the cassette. Remove pleopods from tail and section transversally first and third abdominal segments. Longitudinally cut sixth segment in half as shown above to include midgut posterior caecum and hindgut in the block. Place one half of the sixth segment (longitudinally sectioned) and the first and third segment (transversally sectioned) into the cassette. Take the second half of the cephalothorax and section across the middle line to include the lymphoid organ in the block. Place this second half into cassette. Remove the carapace from the remaining cephalothorax and section gills, place segment in the cassette.

1.9.4 Stainings

In many biological fields, tissue samples are treated with dyes that have selective affinities for different biological substances (Macenko *et al.* 2009). Stainings are chosen for their efficacy in differentiating normal elements in tissues, their ability to demonstrate abnormal conditions and to ease the detection of microorganisms and viral inclusions (Johnson 1980). Affinity describes the tendency of a stain to transfer from solution onto a section. The affinity's magnitude is affected by every factor aiding or hindering this process. Main factors are: stain-tissue (coulombic attractions, Van der Waal's forces hydrogen and

covalent bonding, solvent-solvent (hydrophobic bonding), stain-solvent, and stain-stain interactions (Horobin 2002).

1.9.4.1 Stainings in crustacean

In crustaceans, the main stainings reported in literature to study the digestive tract are: Mayer's hematoxylin-eosin, sudan B for lipids, bromophenol blue for proteins, von Kossa for calcium detection, PAS/alcian blue for detection of neutral and acid polysaccharides, phloxine-eosin, and Massons trichromic technique (Barker & Gibson 1977; Bell & Lightner 1988; Frelie *et al.* 1993; Lightner & Redman 1994; Karunasagar *et al.* 1997; Ong & Johnston 2006; Vasagam *et al.* 2007; Bortolini & Alvarez 2008; Li *et al.* 2008; Ding *et al.* 2013; Alexandre *et al.* 2014; Nunes *et al.* 2014).

1.10 Image analysis

Histological analysis is the standard method for pathology investigations and disease diagnosis (Silva *et al.* 2015). In current practice, histological analysis is based on qualitative features interpreted by pathologists (Miedema *et al.* 2012). Pathologists' quantification is in general time-consuming, poorly objective with significant discrepancies in scoring results reported between pathologists (He *et al.* 2012; Higgins 2015). This has motivated the development of computer-assisted image analysis (CAIA) methods for producing unbiased, reproducible, and reliable data (Nativ *et al.* 2014; Silva *et al.* 2015). The goal of CAIA in histopathology is to increase the amount and quality of data derived from a specimen (Fuchs & Buhmann 2011; He *et al.* 2012; Miedema *et al.* 2012; Nativ *et al.* 2014). CAIA assists but not replaces experienced pathologists as additional

morphological features need to be considered for clinical appraisal (He *et al.* 2012; Miedema *et al.* 2012; Nativ *et al.* 2014). The basic principle of automated image analysis for histology is the use of a series of mathematical algorithms to process images, enabling the segmentation of picture elements into regions of interest based on their colour, texture and/or context (Webster & Dunstan 2014). CAIA is currently used by Skretting Aquaculture Research Centre for investigating different organs (gills, gut and skin) in some fish species.

1.10.1 Image analysis in crustaceans

A limited amount of research has been done on the use of CAIA in crustacean and no studies have been conducted in whiteleg shrimp (Odendaal & Reinecke 2007; Berillis *et al.* 2013). Berillis *et al.* (2013) described an image-processing method for determining the nutritional condition in the HP of lobsters. However, the method proposed was not completely automated.

1.11 Terminology for the HP

The use of name “hepatopancreas” still remains controversial in crustacean and authors continue to refer to it using various names, often interchangeably (Cornelius 1985; Warburg 2012). Authors have been referring to the “hepatopancreas” of crustaceans as: “midgut gland”, “gastric gland”, “digestive gland”, “hepatic gland”, “pancreatic gland”, “racemose gland”, “pancreas”, “liver”, “liver diverticulum”, “midgut diverticulum”, “branched midgut caeca”, “branched diverticula”, “hepatopancreatic caeca”, “intestinal caecum”, “hepatic caecum”, “lateral caecum”, “pyloric caecum”, “midgut organ”, “digestive organ”, “digestive diverticula”, “gland diverticulum”, and “caeca anteriores” (Van Weel 1974; Gibson & Barker 1979; McLaughlin 1980; Bliss 1983; McLaughlin 1983; Cornelius 1985; Herreid & Full 1988). The most accepted name is “hepatopancreas”. In vertebrates, this name is used in some fish species when the exocrine pancreas forms islets of tissue dispersed in the liver. This exocrine pancreatic tissue is formed around the portal vein, and it penetrates deeply into the liver parenchyma during ontogenesis, separated from the rest of the liver by a thin layer of connective tissue (Seyrafi *et al.* 2013). The use of the name “hepatopancreas” for the putative analogue invertebrate structure has resulted in some confusion (Dall & Moriarty 1983; Cornelius 1985). The name “hepatopancreas” is not appropriate, because this organ differs from the vertebrate liver and pancreas (Vonk 1960; Warburg 2012; Röszer 2014).

1.12 Conclusions

The fast growth in shrimp farming in the last decades was followed by the increase of mortality outbreaks. Adverse environmental conditions and disease outbreaks force farmers to starve shrimp for several days. The HP is the main organ of the gastrointestinal tract of decapods, and it is frequently checked by pathologists for diseases and for health monitoring. Pathologist evaluation is subjective and time consuming. CAIA has the potential to support the pathologist in the slide interpretation. However, CAIA requires proper fixation and staining uniformity of the sections before scanning and image processing. Bell and Lightner's (1988) and the CEFAS protocols are the fixation protocols most commonly used for shrimp histology (CEFAS 2013). However, the use of these protocols do not allow to process sections for CAIA due to the incomplete fixation of the HP. Moreover, these protocols do not specify the volume of the fixative that has to be injected and the number of injection within the HP.

Many stainings have been used in shrimp and crustaceans in the past. However, staining protocols are not optimized for CAIA, which requires consistent staining uniformity of the sections.

References

- Abdelmeguid, N.E., Awad, H.E., Ibrahim, A.H. & Yousef, N.A. (2009) Ultrastructural changes in hepatopancreas of *Palaemon serratus*, following treatment with petroleum carcinogenic compounds. *Pakistan Journal of Nutrition*, **8**: 770-781.
- Adiyodi, R.G. & Adiyodi, K.G (1972) Hepatopancreas of *Paratelphusa hydrodromous* (Herbst): histopathology and the pattern of proteins in relation to reproduction and molt. *The Biological Bulletin*, **142** (3), 359-369.
- Alexandre, D., Ozorio, R.A., Derner, R.B., Fracalossi, D.M., Oliveira, G.B., Samuels, R.I., Terra, W.R. & Silva, C.P. (2014) Spatial distribution of digestive proteinases in the midgut of the Pacific white shrimp (*Litopenaeus vannamei*) indicates the existence of endo-ectoperitrophic circulation in Crustacea. *Comparative Biochemistry and Physiology B-Biochemistry & Molecular Biology*, **172**, 90-95.
- Andrade, T.P.D., Redman, R.M. & Lightner, D.V. (2008) Evaluation of the preservation of shrimp samples with Davidson's AFA fixative for infectious myonecrosis virus (IMNV) in situ hybridization. *Aquaculture*, **278**, 179-183.
- Bancroft, J.D. & Marylin, G. (2002) *Theory and practice of histological techniques*, Churchill Livingstone, Edinburgh, Scotland, UK.
- Barker, P.L. & Gibson, R. (1977) Observation on feeding mechanism, structure of gut, and digestive physiology of european lobster *Homarus gammarus* (L) (Decapoda-Nephropidae). *Journal of Experimental Marine Biology and Ecology*, **26**, 297-324.
- Bell, T.A. & Lightner, D.V. (1988) *A handbook of normal penaeid shrimp histology*, The World Aquaculture Society, Baton Rouge.
- Berillis, P., Simon, C., Mente, E., Sofos, F. & Karapanagiotidis, I.T. (2013) A novel image processing method to determine the nutritional condition of lobsters. *Micron*, **45**, 140-144.
- Bliss, D.E. (1983) General preface. In: *The Biology of Crustacea: systematics, the fossil record and biogeography*, Vol. 1, (ed. D.E. Bliss), pp. xiii–xiv. Academic Press, New York.
- Bondad-Reantaso, M.G., Mcgladdery, S.E., East, I. & Subasinghe, R.P. (2001) Asia Diagnostic Guide to Aquatic Animal Diseases. In: *FAO Fisheries Technical Paper No. 402, Supplement 2*, pp. 154-191, Rome.
- Bondad-Reantaso, M.G., Subasinghe, R.P., Josupeit, H., Cai, J.N. & Zhou, X.W. (2012) The role of crustacean fisheries and aquaculture in global food security: Past, present and future. *Journal of Invertebrate Pathology*, **110**, 158-165.

- Bortolini, J.L. & Alvarez, F. (2008) Hepatopancreas alteration of the blue crab *Callinectes sapidus* by the rhizocephalan barnacle *Loxothylacus texanus*. *Journal of Invertebrate Pathology*, **103**, 144-144.
- Calvo, N.S., Stumpf, L., Pietrokovsky, S. & Greco, L.S.L. (2011) Early and late effects of feed restriction on survival, growth and hepatopancreas structure in juveniles of the red claw crayfish *Cherax quadricarinatus*. *Aquaculture*, **319**, 355-362.
- Ceccaldi, H.J. (1989) Anatomy and physiology of digestive tract of crustacean decapods reared in aquaculture. In: *Advances in Tropical Aquaculture*, pp. 243-259, Tahiti, French Polynesia.
- CEFAS (2013) Method for testing crustaceans for White Spot Disease, Yellowhead Disease and Taura Syndrome by histological analysis. Weymouth, U.K.
- Cerenius, L., Jiravanichpaisal, P., Liu, H. & Söderhäll, I. (2010) Crustacean immunity. In: *Invertebrate Immunity* (ed. by K. Söderhäll), pp. 239-259. Springer Science, New York.
- Chiodi Boudet, L.N., Polizzi, P., Romero, M.B., Robles, A., Marcovecchio, J.E. & Gerpe, M.S. (2015) Histopathological and biochemical evidence of hepatopancreatic toxicity caused by cadmium in white shrimp, *Palaemonetes argentinus*. *Ecotoxicology and Environmental Safety*, **113**, 231-240.
- Cornelius, C.E. (1985) Hepatic ontogenesis. *Hepatology*, **5**, 1213-1221.
- Cuartas, E.I., Diaz, A.C. & Petriella, A.M. (2002) Morphological and histological study of the hepatopancreas of shrimp *Pleoticus muelleri* (Bate) (Crustacea, Penaeoidea). *Revista de Investigacion y Desarrollo Pesquero*, **15**, 5-13.
- Dall, W. (1965) Studies on the physiology of a shrimp, *Metapenaeus* sp. (Crustacea Decapoda: Penaeidae), Carbohydrate metabolism. *Australian Journal of Marine & Freshwater Research*, **16**:163–80.
- Dall, W. & Moriarty, D.J.W. (1983) Functional aspects of nutrition and digestion. In: *The Biology of Crustacea: internal anatomy and physiological regulation*, **Vol. 5** (ed. D.E. Bliss), pp. 215–261. Academic Press, New York.
- Dantas Lima, J. (2013) Development of Techniques to Culture Shrimp Haemocytes and Purify White Spot Syndrome Virus (WSSV) in Order to Study WSSV-Haemocyte Interactions. In: *Department of Virology, Parasitology and Immunology*, p. 173. Ghent University.
- Del Rio-Rodriguez, R.E., Soto-Rodriguez, S., Lara-Flores, M., Cu-Escamilla, A.D. & Gomez-Solano, M.I. (2006) A necrotizing hepatopancreatitis (NHP) outbreak in a shrimp farm in Campeche, Mexico: A first case report. *Aquaculture*, **255**, 606-609.

- Diaz, A.C., Sousa, L.G. & Petriella, A.M. (2010) Functional cytology of the hepatopancreas of *Palaemonetes argentinus* (Crustacea, Decapoda, Caridea) under osmotic stress. *Brazilian Archives of Biology and Technology*, **53**, 599-608.
- Ding, Z.F., Yao, W., Du, J., Ren, Q., Li, W.J., Wu, T., Xiu, Y.J., Meng, Q.G., Gu, W., Xue, H., Tang, J.Q. & Wang, W. (2013) Histopathological characterization and in situ hybridization of a novel spiroplasma pathogen in the freshwater crayfish *Procambarus clarkii*. *Aquaculture*, **380**, 106-113.
- Elendt, B.-P. & Storch, V. (1990) Starvation-Induced Alterations of the Ultrastructure of the Midgut of *Daphnia Magna* Straus, 1820 (Cladocera). *Journal of Crustacean Biology*, **10**, 79-86.
- Esteve, M. & Herrera, F.C. (2000) Hepatopancreatic alterations in *Litopenaeus vannamei* (Boone, 1939) (Crustacea-Decapoda-Penaeidae) experimentally infected with a *Vibrio alginolyticus* strain. *Journal of Invertebrate Pathology*, **76**, 1-5.
- FAO (2004) Introductions and movements of *Penaeus vannamei* and *Penaeus stylirostris* in Asia and the Pacific. *RAP Publication 2004/10*, Bangkok.
- FAO (2017) Cultured Aquatic Species Information Programme. *Penaeus vannamei*. Cultured Aquatic Species Information Programme. In: *FAO Fisheries and Aquaculture Department* [online], <http://www.fao.org/fishery/species/3404/en>.
- Felgenhauer, B.E. (1992) Internal Anatomy of the Decapods: An Overview. In: *Microscopic Anatomy of Invertebrates*, pp. 45-75. Wiley-Liss, New York.
- Flegel, T.W. (2012) Historic emergence, impact and current status of shrimp pathogens in Asia. *Journal of Invertebrate Pathology*, **110**, 166-173.
- Franceschini-Vicentini, I.B., Ribeiro, K., Papa, L.P., Marques, J., Vicentini, C.A. & Valenti, P. (2009) Histoarchitectural features of the hepatopancreas of the amazon river prawn *Macrobrachium amazonicum*. *International Journal of Morphology*, **27**, 121-128.
- Frelier, P.F., Loy, J.K. & Kruppenbach, B. (1993) Transmission of necrotizing hepatopancreatitis in *Penaeus vannamei*. *Journal of Invertebrate Pathology*, **61**, 44-48.
- Frelier, P.F., Sis, R.F., Bell, T.A. & Lewis, D.H. (1992) Microscopic and ultrastructural studies of necrotizing hepatopancreatitis in pacific white shrimp (*Penaeus vannamei*) cultured in Texas. *Veterinary Pathology*, **29**, 269-277.
- Fuchs, T.J. & Buhmann, J.M. (2011) Computational pathology: challenges and promises for tissue analysis. *Computerized Medical Imaging and Graphics*, **35**, 515-530.
- Gibson, R. & Barker, P.L. (1979) The decapod hepatopancreas. *Oceanography and Marine Biology an Annual Review*, **17**, 285-346.

Gimenez, A.V.F. (2013) Digestive physiology of three species of decapod crustaceans of Argentina. *Journal of Shellfish Research*, **32**, 767-777.

Gimenez, A.V.F., Fenucci, J.L. & Petriella, A.M. (2004) The effect of vitamin E on growth, survival and hepatopancreas structure of the Argentine red shrimp *Pleoticus muelleri* Bate (Crustacea, Penaeidea). *Aquaculture Research*, **35**, 1172-1178.

Gopinath, R., Paul Raj, R., George, K.C. & Sanil, N.K. (2012) Ultrastructural changes in the hepatopancreas of *Penaeus monodon* Fabricius 1798 given aflatoxin B1 diets. *Aquaculture Research*, **43**, 32-43.

Garcia-Garcia, E., Galindo-Villegas, J. & Mulero, V. (2013) Mucosal immunity in the gut: The non-vertebrate perspective. *Developmental and Comparative Immunology*, **40**, 278-288.

Hasson, K.W., Wyld, E.M., Fan, Y.P., Lingsweiller, S.W., Weaver, S.J., Cheng, J.L. & Varner, P.W. (2009) Streptococcosis in farmed *Litopenaeus vannamei*: a new emerging bacterial disease of penaeid shrimp. *Diseases of Aquatic Organisms*, **86**, 93-106.

He, L., Long, L.R., Antani, S. & Thoma, G.R. (2012) Histology image analysis for carcinoma detection and grading. *Computer Methods and Programs in Biomedicine*, **107**, 538-556.

Herreid, C.F., & Full, R.J. (1988) Energetic and locomotion. In: *Biology of the land crabs* (eds. W.W Burggren & B.R. McMahon), pp. 341–345. Cambridge University Press, Cambridge, UK.

Higgins, C. (2015) Applications and challenges of digital pathology and whole slide imaging. *Biotech Histochem*, **90**, 341-347.

Holthuis, L.B. (1980) FAO specie catalogue, volume 1 – Shrimps and prawns of the world. *FAO Fisheries Synopsis n. 125*. Rome.

Huxley, T.H. (1880). The crayfish. Appleton, New York.

ITIS (2017) *Litopenaeus vannamei* (Boone, 1931) Taxonomic Serial number 551682. *Integrated Taxonomic Information System (ITIS)* [online], <http://www.itis.gov>.

Johansson, M.W., Keyser, P., Sritunyalucksana, K. & Soderhall, K. (2000) Crustacean haemocytes and haematopoiesis. *Aquaculture*, **191**, 45-52.

Johnson, P.T. (1980) *Histology of the blue crab Callinectes sapidus. A model for the Decapoda*, Praeger Publishers, New York.

Johnson, S.K. (1995) *Handbook of Shrimp Diseases*, Texas A&M University, Texas.

Joshi, J., Srisala, J., Truong, V.H., Chen, I.T., Nuangsaeng, B., Suthienkul, O., Lo, C.F., Flegel, T.W., Sritunyalucksana, K. & Thitamadee, S. (2014) Variation in *Vibrio parahaemolyticus* isolates from a single Thai shrimp farm experiencing an outbreak of acute hepatopancreatic necrosis disease (AHPND). *Aquaculture*, **428**, 297-302.

Karunasagar, I., Otta, S.K. & Karunasagar, I. (1997) Histopathological and bacteriological study of white spot syndrome of *Penaeus monodon* along the west coast of India. *Aquaculture*, **153**, 9-13.

Kiernan, J.A. (2008) *Histological and histochemical methods - Theory and practice*. Cold Spring Harbor Laboratory Press, New York.

Kuhn, D.D., Smith, S.A., Boardman, G.D., Angier, M.W., Marsh, L. & Flick, G.J. (2010) Chronic toxicity of nitrate to Pacific white shrimp, *Litopenaeus vannamei*: Impacts on survival, growth, antennae length, and pathology. *Aquaculture*, **309**, 109-114.

Laohabanjong, R., Tantikitti, C., Benjakul, S., Supamattaya, K. & Boonyaratpalin, M. (2009) Lipid oxidation in fish meal stored under different conditions on growth, feed efficiency and hepatopancreatic cells of black tiger shrimp (*Penaeus monodon*). *Aquaculture*, **286**, 283-289.

Leaño, E. M. (2016). Regional response on AHPND and other emerging shrimp diseases in the Asia-Pacific. Proceedings of the ASEAN Regional Technical Consultation on EMS/AHPND and Other Transboundary Diseases for Improved Aquatic Animal Health in Southeast Asia: pp. 24-32. Makati City, Philippines.

Leica Biosystem (2017) Fixation and fixatives – popular fixative solutions. www.leicabiosystem.com.

Leser, V., Drobne, D., Vilhar, B., Kladnik, A., Znidarsic, N. & Strus, J. (2008) Epithelial thickness and lipid droplets in the hepatopancreas of *Porcellio scaber* (Crustacea: Isopoda) in different physiological conditions. *Zoology*, **111**, 419-432.

Lewbart, G.A. (2006) *Invertebrate medicine*. Blackwell Publishing, Oxford, UK.

Li, E.C., Chen, L.Q., Zeng, C., Yu, N., Xiong, Z.Q., Chen, X.F. & Qin, J.G. (2008) Comparison of digestive and antioxidant enzymes activities, haemolymph oxyhemocyanin contents and hepatopancreas histology of white shrimp, *Litopenaeus vannamei*, at various salinities. *Aquaculture*, **274**, 80-86.

Lightner, D.V., Redman, R.M., Moore, D.W. & Park, M.A. (1993) Development and application of a simple and rapid diagnostic method to studies on hepatopancreatic parvovirus in Penaeid shrimp. *Aquaculture*, **116**, 15-23.

-
- Lightner, D.V. & Redman, R.M. (1994) An epizootic of necrotizing hepatopancreatitis in cultured penaeid shrimp (Crustacea: decapoda) in northwestern Peru. *Aquaculture*, **122**, 9-18.
- Lightner, D.V. & Redman, R.M. (1998) Shrimp diseases and current diagnostic methods. *Aquaculture*, **164**, 201-220.
- Lightner, D.V. (2012) Global transboundary disease politics: The OIE perspective. *Journal of Invertebrate Pathology*, **110**, 184-187.
- Lightner, D.V., Redman, R.M., Pantoja, C.R., Tang, K.F.J., Noble, B.L., Schofield, P., Mohny, L.I., Nunan, L.M. & Navarro, S.A. (2012) Historic emergence, impact and current status of shrimp pathogens in the Americas. *Journal of Invertebrate Pathology*, **110**, 174-183.
- Lightner, D.V., Redman, R.M., Pantoja, C.R., Noble, B.L., Nunan, L.M. & Tran (2013). Documentation of an Emerging Disease (Early Mortality Syndrome) in SE Asia & Mexico. OIE Reference Laboratory for Shrimp Diseases, Department of Veterinary Science & Microbiology, School of Animal and Comparative Biomedical Sciences.
- Longo, M.V. & Diaz, A.O. (2015) Histological and Histochemical Study of the Hepatopancreas of Two Estuarine Crab Species, *Cyrtograpsus angulatus* and *Neohelice granulata* (Grapsoidae, Varunidae): Influence of Environmental Salinity. *Zoological Science*, **32**, 163-170.
- Macenko, M., Niethammer, M., Marron, J.S., Borland, D., Woosley, J.T., Guan, X.J., Schmitt, C., Thomas, N.E. & Ieee (2009) *A method for normalizing histology slides for quantitative analysis*, Ieee, New York.
- Martin, G.G. & Hose, H. (2010) Functional anatomy of Penaeid shrimp. In: *The Shrimp Book* (V. Alday-Sanz, ed), Nottingham University Press, UK.
- Mawdesley-Thomas, L.E. (1972) Diseases of fish. In. Academic Pres Inc., New York.
- McGaw, I.J. & Curtis, D.L. (2013) A review of gastric processing in decapod crustaceans. *Journal of Comparative Physiology B-Biochemical Systemic and Environmental Physiology*, **183**, 443-465.
- McLaughlin, P.A. (1980). Comparative morphology of Recent Crustacea. W.H Freeman, San Francisco.
- McLaughlin, P.A. (1983) Internal anatomy. In: *The biology of Crustacea: internal anatomy and physiological regulation*, **Vol. 5** (ed. D.E. Bliss), pp. 1–41. Academic Press, New York.

- Miedema, J., Marron, J.S., Niethammer, M., Borland, D., Woosley, J., Coposky, J., Wei, S., Reisner, H. & Thomas, N.E. (2012) Image and statistical analysis of melanocytic histology. *Histopathology*, **61**, 436-444.
- Musthaq, S.K.S. & Kwang, J. (2014) Evolution of specific immunity in shrimp - A vaccination perspective against white spot syndrome virus. *Developmental and Comparative Immunology*, **46**, 279-290.
- Nativ, N.I., Chen, A.I., Yarmush, G., Henry, S.D., Lefkowitz, J.H., Klein, K.M., Maguire, T.J., Schloss, R., Guarrera, J.V., Berthiaume, F. & Yarmush, M.L. (2014) Automated image analysis method for detecting and quantifying macrovesicular steatosis in hematoxylin and eosin-stained histology images of human livers. *Liver Transplant*, **20**, 228-236.
- Nakamura, K. (1987) Classification of diverticular cells of the midgut gland in the prawn *Penaeus japonicus*. *Memoirs of Faculty of Fisheries Kagoshima University*, **36**, 207-214.
- Nejedli, S. & Tlak Gajger, I. (2013) Hepatopancreas in some sea fish from different species and the structure of the liver in teleost fish, common pandora, *Pagellus erythinus* (Linnaeus, 1758) and whiting, *Merlangius merlangus euxinus* (Nordmann, 1840). *Veterinarski Archiv*, **83**, 441-452.
- Ng, T.H., Chiang, Y-A., Yeh, Y-C. & Wang, H-C. (2014) Review of Dscam-mediated immunity in shrimp and other arthropods. *Developmental and Comparative Immunology*, **46**: 129-138.
- Nunes, E.T., Braga, A.A. & Camargo-Mathias, M.I. (2014) Histochemical study of the hepatopancreas in adult females of the pink-shrimp *Farfantepenaeus brasiliensis* Latreille, 1817. *Acta Histochemica*, **116**, 243-251.
- Odendaal, J.P. & Reinecke, A.J. (2007) Quantitative assessment of effects of zinc on the histological structure of the hepatopancreas of terrestrial isopods. *Archives of Environmental Contamination and Toxicology*, **53**, 359-364.
- Ong, B.L. & Johnston, D. (2006) Influence of feeding on hepatopancreas structure and digestive enzyme activities in *Penaeus monodon*. *Journal of Shellfish Research*, **25**, 113-121.
- Peeler, E.J. (2012) Costs and benefits of freedom from shrimp diseases in the European Union. *Journal of Invertebrate Pathology*, **110**, 188-195.
- Rieger, J.; Twardziok, S.; Huenigen, H., Hirschberg, RM. & Plendi, J. (2013) Porcine intestinal mast cells. Evaluation of different fixatives for histochemical staining techniques considering tissue shrinkage. *European Journal of Histochemistry*, **57** (3): 133-142.

- Rószter, T. (2014) The invertebrate midintestinal gland (“hepatopancreas”) is an evolutionary forerunner in the integration of immunity and metabolism. *Cell and Tissue Research*, **358**, 685-695..
- Sacristán, H.J., Ansaldo, M., Franco-Tadic, L.M., Gimenez, A.V.F. & Greco, L.S.L. (2016) Long-Term starvation and posterior feeding effects on biochemical and physiological responses of midgut gland of *Cherax quadricarinatus* Juveniles (Parastacidae). *PloS one*, **11**, e0150854.
- Sánchez-Paz, A., García-Carreño, F., Hernández-López, J., Muhlia-Almazán, A. & Yepiz-Plascencia, G. (2007) Effect of short-term starvation on hepatopancreas and plasma energy reserves of the Pacific white shrimp (*Litopenaeus vannamei*). *Journal of Experimental Marine Biology and Ecology*, **340**, 184-193.
- Seyrafi, R., Najafi, G., Rahmati-Holasoo, H., Hajimohammadi, B. & Shamsadin, A.S. (2009) Histological Study of Hepatopancreas in Iridescent Shark Catfish (*Pangasius hypophthalmus*). *Journal of Animal and Veterinary Advances*, **8**, 1305-1307.
- Siebold, C.TH. (1848) *Lehrbuch der vergleichenden Anatomie der Wirbellosen Thiere*, Veir, Berlin.
- Silva, P.F., McGurk, C., Thompson, K.D., Jayasuriya, N.S. & Bron, J.E. (2015) Development of a quantitative semi-automated system for intestinal morphology assessment in Atlantic salmon, using image analysis. *Aquaculture*, **442**, 100-111.
- Sindermann, C.J. & Lightner, D.V. (1988) Disease diagnosis and control in North American marine aquaculture. *Developments in Aquaculture and Fisheries Science*, **17**, 1-431.
- SlidePlayer (2017). Artropodi Crostacei. Canale alimentare negli insetti: intestino completo e differenziato [online] <http://slideplayer.it/slide/5544006/>
- Smith, V.J. & Chisholm, J.R.S. (1992) Non-cellular immunity in crustaceans. *Fish & Shellfish Immunology*, **2**, 1-31.
- Sonakowska, L., Wlodarczyk, A., Wilczek, G., Wilczek, P., Student, S. & Rost-Roszkowska, M.M. (2016) Cell Death in the Epithelia of the Intestine and Hepatopancreas in *Neocaridina heteropoda* (Crustacea, Malacostraca). *PloS one*, **11**, e0147582.
- Stentiford, G.D., Neil, D.M., Peeler, E.J., Shields, J.D., Small, H.J., Flegel, T.W., Vlaskin, J.M., Jones, B., Morado, F., Moss, S., Lotz, J., Bartholomay, L., Behringer, D.C., Hauton, C. & Lightner, D.V. (2012) Disease will limit future food supply from the global crustacean fishery and aquaculture sectors. *Journal of Invertebrate Pathology*, **110**, 141-157.

- Storch, V. & Anger, K. (1983) Influence of starvation and feeding on the hepatopancreas of larval *Hyas araneus* (Decapoda, Majidae). *Helgoländer Meeresuntersuchungen*, **36**, 67-75.
- Storch, V., Juario, J.V. & Pascual, F.P. (1984) Early effects of nutritional stress on the liver of milkfish, *Chanos chanos* (Forsskal), and on the hepatopancreas of the tiger prawn, *Penaeus monodon* (Fabricius). *Aquaculture*, **36**, 229-236.
- Tam, Q. & Avenant-Oldewage, A. (2009) The effect of starvation on the ultrastructure of the digestive cells of *Dolops ranarum* (Stuhlmann, 1891) (Crustacea: Branchiura). *Arthropod Structure & Development*, **38**, 391-399.
- Tran, L., L. Nunan, R.M. Redman, L.L.Mohney, C.R. Pantoja, K. Fitzsimmons & Lightner D.V. (2013) Determination of the infectious nature of the agent of acute hepatopancreatic necrosis syndrome affecting penaeid shrimps. *Disease of Aquatic Organisms*, **105**:45-55.
- Van Weel, P. (1955). Processes of Secretion, Restitution, and Resorption in Gland of Mid-Gut (*Glandula Media Intestini*) of *Atya spinipes* Newport (Decapoda-Brachyura). *Physiological Zoology*, **28**(1), 40-54.
- Van Weel, P.B. (1974) Hepatopancreas? *Comparative Biochemistry and Physiology Part A: Physiology*, **47**, 1-9.
- Vasagam, K.P.K., Balasubramanian, T. & Venkatesan, R. (2007) Apparent digestibility of differently processed grain legumes, cow pea and mung bean in black tiger shrimp, *Penaeus monodon* Fabricius and associated histological anomalies in hepatopancreas and midgut. *Animal Feed Science and Technology*, **132**, 250-266.
- Vonk, H.J. (1960) Digestion and metabolism. In: *The physiology of the Crustacea*, **Vol. 1** (T.H. Waterman, ed.), pp. 291–311. Academic Press, New York.
- Vogt, G., Storch, V., Qunitio, E.T. & Pascual, F.P. (1985) Midgut gland as monitor organ for the nutritional value of diets in *Penaeus monodon* (Decapoda). *Aquaculture*, **48**, 1-12.
- Wang, L.Y., Li, F.H., Wang, B. & Xiang, J.H. (2012) Structure and partial protein profiles of the peritrophic membrane (PM) from the gut of the shrimp *Litopenaeus vannamei*. *Fish & Shellfish Immunology*, **33**, 1285-1291.
- Warburg, M.R. (2012) Reviewing the structure and function of the scorpion's hepatopancreas. *Arthropods*, **1**, 79-93.
- Webster, J.D. & Dunstan, R.W. (2014) Whole-slide imaging and automated image analysis: considerations and opportunities in the practice of pathology. *Veterinary Pathology*, **51**, 211-223.

Yoshida, T., Kawagushi, S., Meyer, B., Virtue, P., Penschow, J. & Nash, G. (2009) Structural changes in the digestive glands of larval Antarctic krill (*Euphausia superba*) during starvation. *Polar Biology*, **32**, 503-507.

Znidarsic, N., Strus, J. & Drobne, D. (2003) Ultrastructural alterations of the hepatopancreas in *Porcellio scaber* under stress. *Environmental Toxicology and Pharmacology*, **13**, 161-174.

Scientific aims

The hepatopancreas (HP) is a key organ of the gastro-intestinal tract in crustaceans, serving five functions: the absorption of nutrients, secretion of digestive enzymes, storage of metabolic reserves, breakdown of toxic substances, and elimination of waste products. It is routinely checked by pathologists being vulnerable to diseases, environmental and dietary changes.

The general aim of this thesis was to study if it was possible to monitor health in whiteleg shrimp based on histological analysis of the morphology of the HP.

The particular aims of this thesis were:

- (1) To optimize sampling and fixation methods for paraffin and frozen sections of the HP that can be used for computer-assisted image analysis (CAIA).
- (2) To investigate which morphological parameters can be used to monitor the health status of whiteleg shrimp using CAIA.
- (3) To develop a standardized starvation trial to validate the developed CAIA methodology and to describe the ultrastructural changes using transmission electron microscopy.
- (4) To propose a new terminology for the HP, based on the differences between vertebrates and invertebrates (Decapoda).

Chapter 1

**Optimization of fixation methods for image analysis of the
hepatopancreas in whiteleg shrimp, *Penaeus vannamei* (Boone)**

F Cervellione¹, C McGurk¹, P Silva¹, MAG Owen¹, W Van den Broeck²

¹Skretting Aquaculture Research Centre, Stavanger, Norway.

²Department of Morphology, University of Ghent, Ghent, Belgium.

Journal of Fish Disease 2016, DOI:10.1111/jfd.12531

Abstract

Pathology in Penaeid shrimps relies on histology, which is subjective, time consuming and difficult to grade in a reproducible manner. Automated image analysis is faster, objective and suitable for routine screening, however it requires standardized protocols. The first critical step is proper fixation of the target tissue. Bell and Lightner's (1988) fixation protocol, widely used for routine histology of paraffin sections, is not optimized for image analysis and no protocol for frozen sections is described in the available literature. Therefore the aim of this study was to optimize fixation of the hepatopancreas from whiteleg shrimp (*Penaeus vannamei*) for both paraffin and frozen sections using a semi-quantitative scoring system. For paraffin sections four injection volumes and three injection methods were compared, for frozen sections four freezing methods and four fixation methods. For paraffin sections optimal fixation was achieved by increasing three fold the fixative volume recommended by Bell and Lightner, from 10% to 30% of the shrimp body weight, combined with single injection into the hepatopancreas. Optimal fixation for frozen sections was achieved by freezing the cephalothorax with liquid nitrogen, followed by fixation of the section with 60% isopropanol. These optimized methods enable the future use of image analysis and improve classical histology.

Keywords: histology; hepatopancreas; fixation methods; *Penaeus vannamei*; whiteleg shrimp; penaeid.

Introduction

Pathologists studying penaeid shrimp rely mainly on well-established diagnostic methods, such as macroscopic examination, classical microbiology and microscopic analysis, including routine histology and histochemistry (Bell & Lightner 1988; Lightner, Hasson *et al.* 1996). Routine histological assessments are core to shrimp pathology diagnostic laboratories (Lightner & Redman 1998).

Histology is defined as the study of the microscopic anatomy of cells and tissues of organisms, and is performed by examining a thin section of tissue under microscope. Classic diagnostic methods have limitations, due to the methods being subjective. The analysis of tissue sections depends on the experience and expertise of histopathologists, and it is laborious and difficult to grade in a reproducible manner. It is known that there are substantial intra- and inter-observation variations between experts (Asaoka *et al.* 2016). Computer assisted image analysis refers to the field of using computer algorithms to extract quantitative information from digital images of sections (Kårsnäs 2014). Image analysis can be faster than traditional methods, generating objective numerical data and can be suitable for routine screening of high number of samples, both for diagnostic and research applications (Gurcan *et al.* 2009). However, image analysis requires standardization of histology procedures for preparation of the sample: the first critical step is to achieve proper fixation of the target tissue (He *et al.* 2012). The basis of high quality histological preparation is complete and adequate fixation. The purpose of fixation is to preserve tissues by preventing autolysis and putrefaction: inadequate fixation cannot be remedied at any later stage, and the finished section can only be as good as its primary fixation (Bucke 1972). In crustaceans, the hepatopancreas (HP) is affected by multiple

diseases and is routinely examined by pathologists (Johnson 1995). The HP is also assessed as a general indicator of health, being the site of digestion, nutrient absorption, detoxification, reserve storage, synthesis and secretion of digestive enzymes (Laohabanjong *et al.* 2009; Calvo *et al.* 2011). However, the HP undergoes rapid autolysis immediately after death, and delays of even a few seconds in fixative penetration into this organ can result in the whole specimen being unsuitable for diagnosis (Bondad-Reantaso *et al.* 2012). Inadequate or improper fixation can often lead to misinterpretation of the sectioned material (Bell & Lightner 1988). Therefore the aim of the present study was to semi-quantitatively optimize the fixation of the HP in whiteleg shrimp (*Penaeus vannamei*), so that it can be used later on for histological computer assisted image analysis.

Materials and methods

Shrimp and rearing conditions

Experiments were conducted in collaboration with IMAQUA, located at the Faculty of Veterinary Medicine (Ghent, Belgium). Specific pathogen-free whiteleg shrimp were imported from Shrimp Improvement Systems (Florida, USA). Shrimp were housed in 50 L glass tanks, each supplied with constant aeration and independent biological/mechanical filters. Water temperature was kept at 27 ± 1 °C, with a pH of 7.8 – 8.1 and salinity of 20 ± 1 g L⁻¹. The biological filters and regular water exchanges kept the total ammonium concentrations below 0.5 mg L⁻¹ and the total nitrites below 0.15 mg L⁻¹. The room was illuminated 12 h d⁻¹ by a dimmed luminescent light-tube. Shrimp were fed a commercial diet for 30 d, at 5% of the body weight (bw), 4 times per day. Thereafter, shrimp of 2 ± 1 g, within the C-intermoult stage (Corteel *et al.* 2009) were collected and transported to the Department of Morphology (Ghent University, Belgium) in aerated buckets. Shrimp were then euthanized as described by Lightner (2015) for paraffin sections and euthanized in cold ice for frozen sections.

Paraffin sections

In a previous experiment (data not shown), through comparison of different fixatives (Davidson's, Bouin's, formaldehyde, Carnoy and Zinc salt based fixatives) it was ascertained that Davidson's fixative resulted in the best fixation quality.

Shrimp were individually weighed, fixed with Davidson's solution (30 mL 95% ethanol, 20 mL 37% formaldehyde, 10 mL glacial acetic acid, and 30 mL distilled water), and further processed according to the protocol of Bell and Lightner (1988). Four distinct volumes of Davidson's fixative were compared, using a 1 mL syringe with a 26 G needle: 10%, 20%, 30%, and 40% of the bw were injected (15 shrimp per volume). The speed of injection was approximately 0.02 mL s^{-1} . Seventy-five percent of the fixative was allocated to the cephalothorax (from which 50% into or around the HP and the other 50% into the region anterior to the HP) and 25% to the abdomen (from which 50% into the posterior abdominal region and 50% into the anterior abdominal region). For each volume, three different injection methods into or around the HP were tested (five shrimp per method): single injection into the HP (1 in), four injections into the HP (4 in), and four injections around the HP (4 out). After injection and lateral slitting of the cuticle from the sixth abdominal segment to the base of the rostrum, shrimp were immersed in Davidson's fixative (ratio of fixative to tissue volume of 10:1) for 48 h at 22 °C. The shrimp were then bisected transversally at the junction of the cephalothorax and abdomen, the cephalothorax bisected longitudinally on the mid-line, and both parts placed in tissue processing cassettes. Tissues were dehydrated in a graded series of alcohol baths (70%, 80%, 95%, and 100%) and cleared in xylene, using an automated tissue processor (Microm STP420D, ThermoScientific™). Then, the tissues were embedded in paraffin (melting point 54 – 56 °C, Paraclean Klinipath BV, VWR International®) using manual embedding station (Microm EC350, ThermoScientific™). Based on a previous experiment (data not shown) comparing different thicknesses of the section, eight μm thick longitudinal sections were cut with an automated microtome (Microm HM 360,

ThermoScientific™), placed on APES (3-Aminopropyltriethoxysilane) coated glass slides, dried for 1 h at 56 °C and kept at 37 °C overnight. Sections were then stained with Mayer's haematoxylin and eosin combination (Wilson & Gamble 2002) through an automated slide-stainer (Gemini AS, ThermoScientific™) and mounted in non-aqueous medium (DPX, Sigma-Aldrich®).

Frozen sections

Shrimp were bisected transversally at the junction of the cephalothorax and the abdomen, and immediately anterior to the HP. Four freezing methods were compared (five animals per method): (i) immersion and storing in pre-cooled (-20 °C) isopentane (2-Methylbutane); (ii) injection and storing in pre-cooled isopentane (single injection laterally into the HP); (iii) immersion for 20 s in liquid nitrogen followed by immersion and storing in pre-cooled isopentane; (iv) immersion for 20 s in liquid nitrogen and storing in dry air. After freezing, all samples were kept at -80 °C. Samples were embedded in water-soluble media (Tissue-Tek® OCT, VWR International®) and, based on a previous experiment (data not shown) comparing different thicknesses of the section (5-8-10-12-14 and 16 µm), 16 µm thick longitudinal sections cut, by use of an automated cryostat (Microm HM505E, ThermoScientific™) at -25 °C and placed on glass slides (HistoBond®+, Marienfeld). Sections were fixed for 10 s in 70% alcohol at 22 °C, stained with Mayer's haematoxylin and eosin combination (Wilson & Gamble 2002) using an automated slide-stainer (Gemini AS, ThermoScientific™) and mounted in aqueous media (Aquatex®, VWR International®). In addition, aiming to optimize the lipid staining for sections frozen according to method (iv), four different fixation methods were employed: (a) 10 s in 60% isopropanol at 22 °C; (b) 10 s in 70% alcohol at 22 °C; (c) air drying for 30 min at 45 °C;

(d) air drying for 10 min at 22 °C. Thereafter, sections were stained with Lillie and Ashburn's isopropanol Oil Red O staining (Culling 1974) using the same automated stainer and mounted in aqueous media (Aquatex®, VWR International®).

Microscopic visualization

All sections were label-coded, blindly observed and randomized to avoid any bias potentially caused by personal preferences. One experienced examiner evaluated every slide (each five times) over a period of five consecutive days, under light microscope (BX53, Olympus®). A semi-quantitative scoring system was developed to evaluate the fixation of the HP. Criteria are summarized in Tables 1 and 2, and Figures 1 and 2.

Statistical analysis

Slide scores were treated as non-parametric data. One-way ANOVA (Kruskal-Wallis) was applied for testing equality of score medians among treatments (Gibson-Corley *et al.* 2013). Dunn's multiple comparisons test with median ranks ($p = 0.05$) was used to compare injection methods (Säfhlo *et al.* 2016).

Table 1. Semi-quantitative scoring system for light microscopic evaluation of the hepatopancreas of whiteleg shrimp (*Penaeus vannamei*) in paraffin sections. H&E = haematoxylin and eosin; na = not applicable.

SEMI-QUANTITATIVE SCORING SYSTEM OF PARAFFIN SECTIONS							
CRITERIA		SCORE					
	Description	0	1	2	3	4	5
Adhesion (H&E)	Adhesion of the tissue to the slide	Extremely poor <5%	Poor 5%<x<25%	Scarce 25%<x<50%	Moderate 50%<x<75%	Good 75%<x<95%	Excellent 100%
Morphology and Architecture (H&E)	Tubules: normal morphology and attachment to the basal membrane	Extremely poor <5%	Poor 5%<x<25%	Scarce 25%<x<50%	Moderate 50%<x<75%	Good 75%<x<95%	Excellent 100%
Tissue Integrity (H&E)	Tissue damage due to the needle; artifacts	Severe	Moderate	Light	Absent	na	na

Table 2. Semi-quantitative scoring system for light microscopic evaluation of the hepatopancreas of whiteleg shrimp (*Penaeus vannamei*) in frozen sections. H&E = haematoxylin and eosin.

SEMI-QUANTITATIVE SCORING SYSTEM OF FROZEN SECTIONS							
CRITERIA		SCORE					
	Description	0	1	2	3	4	5
General Morphology (H&E)	Appearance and morphology of tubules	Extremely poor <5%	Poor 5%<x<25%	Scarce 25%<x<50%	Moderate 50%<x<75%	Good 75%<x<95%	Excellent 100%
Lipid droplets (Oil Red O)	Morphology and location of lipid droplets	Not present	Widespread in the whole section	Not uniform in size and location	Not uniform and present in the lumen	Uniform in size and present in the lumen	Uniform in size and inside tubules

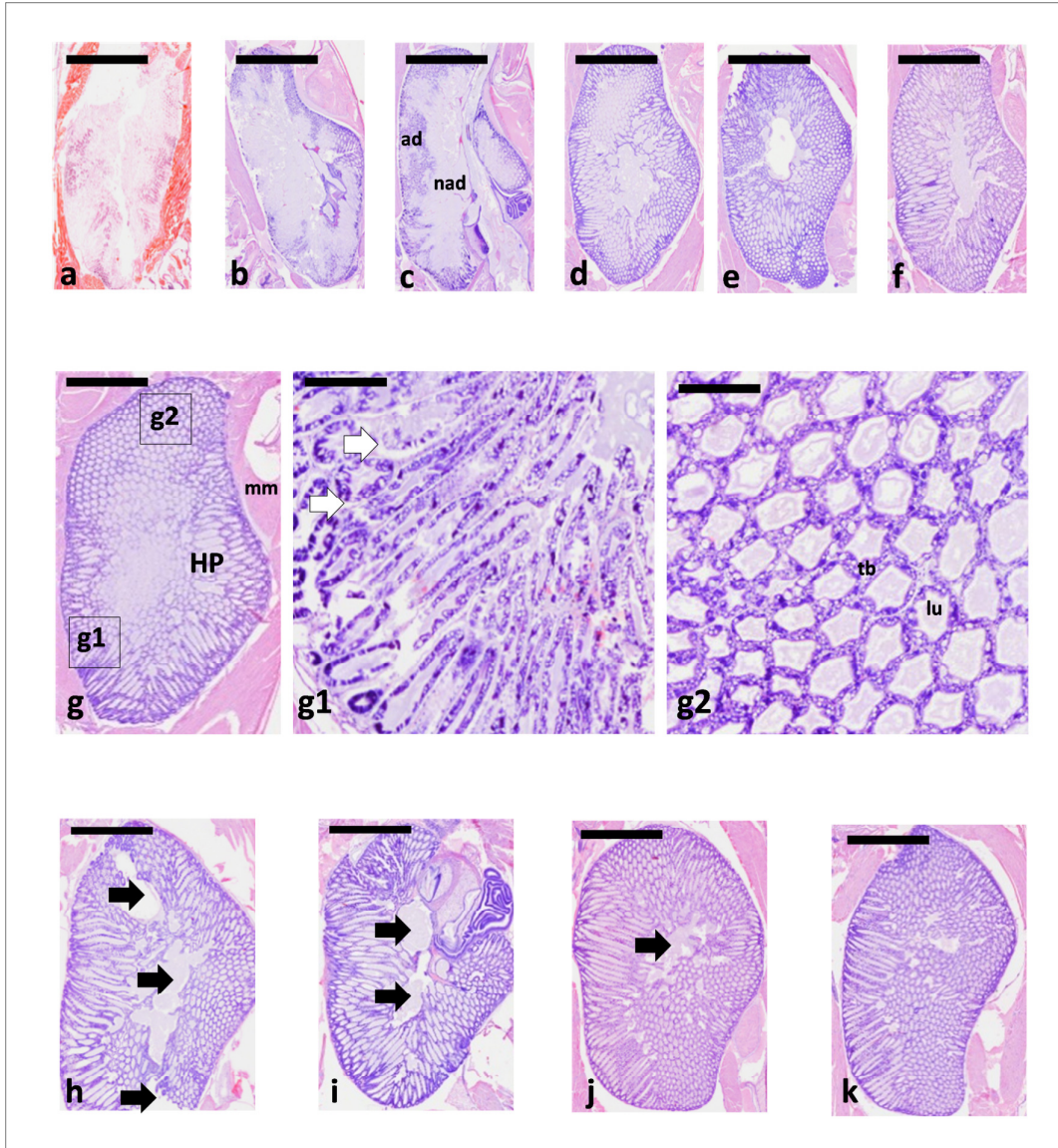


Figure 1. Criteria for light microscopic evaluation of paraffin sections of the hepatopancreas in whiteleg shrimp (*Penaeus vannamei*). Adhesion (a - f), morphology and architecture (g, g1 and g2), and tissue integrity (h - k); ad = tissue adhesion; HP = hepatopancreas; lu = tubular lumen; mm = muscles; nad = tissue adhesion not present; tb = hepatopancreatic tubule; white arrows = detachment of tubule from the basal membrane; black arrows = tissue damage. H&E. 8 μ m section. Scale bar a - f = 2500 μ m; scale bar g1 - g2 = 200 μ m; scale bar g - k = 700 μ m. **Adhesion:** a = score 0 (extremely poor); b = score 1 (poor); c = score 2 (scarce); d = score 3 (moderate); e = score 4 (good); f = score 5 (excellent). **Morphology and architecture:** g = score 2 (scarce); g1 = magnification of g, showing detachment of the tubules from the basal membrane; g2 = magnification of g, showing the complete attachment of the tubules to the basal membrane. **Tissue integrity:** h = score 0 (severe tissue damage); i = score 1 (moderate tissue damage); j = score 2 (light tissue damage); k = score 3 (no tissue damage).

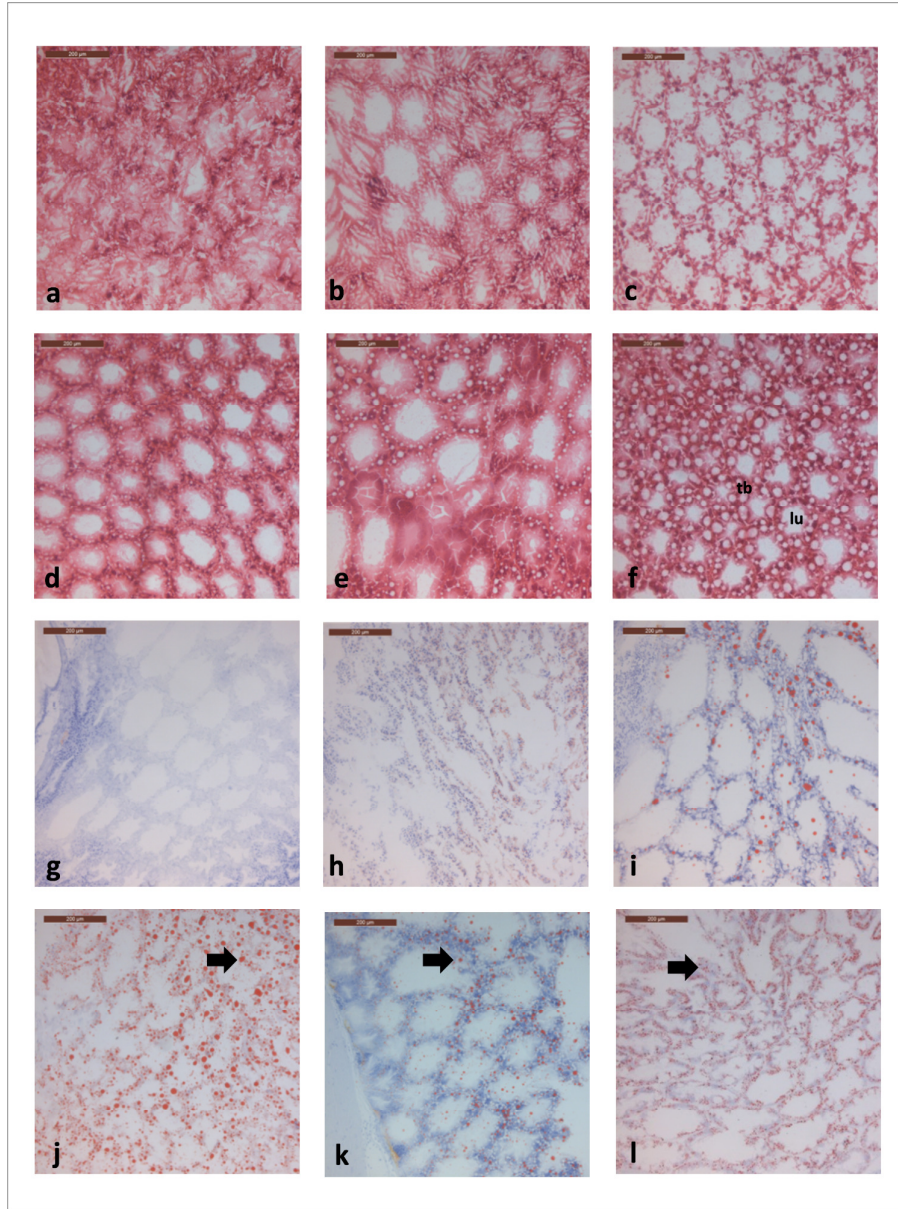


Figure 2. Criteria for light microscopic evaluation of frozen sections of the hepatopancreas in whiteleg shrimp (*Penaeus vannamei*). General morphology (a-f), location and morphology of lipid droplets (g-l). lu = tubular lumen; tb = hepatopancreatic tubule; black arrows = lipid droplets in red. H&E (a-f); Oil Red O (g-l). 16 μ m section. Scale bar a – l =200 μ m. **General morphology:** a = score 0 (extremely poor); b = score 1 (poor); c = score 2 (scarce); d = score 3 (moderate); e = score 4 (good); f = score 5 (excellent). **Location and morphology of lipid droplets:** g = score 0 (not present); h = score 1 (widespread in the whole section); i = score 2 (not uniform in size and location); j = score 3 (not uniform in size and present in the lumen); k = score 4 (uniform in size and present in the lumen); l = score 5 (uniform in size and inside tubules).

Results

Paraffin sections

The effect of volume and injection method on adhesion to the glass slide is shown in Figure 3. Adhesion improved as the injection volumes increased from 10% to 30%, while it slightly decreased when 40% was injected. This tendency was seen with every injection method. Furthermore, 1 in always provided slightly better scores than 4 in, and it was significantly higher than 4 out. The effect of volume and injection method on the morphology and tissue architecture is shown in Figure 4. Method 1 in was always significantly better than method 4 out. Method 1 in provided slightly better scores than 4 in when 10% and 30% were injected, slightly worse than 4 in with 20% and similar to 4 in with 40%. Slide score for 4 in slightly increased from 10% to 30% while it decreased when 40% was injected. Slide score for 4 out was not highly influenced by the volume injected. Morphology and tissue architecture had highest scores when 30% was injected using methods 1 in and 4 in. Finally, Figure 5 shows the effect of volume and injection methods on tissue integrity. When 10% was injected no differences in slide score was observed, while for 20%, 30% and 40% 4 in was generally worse than 4 in and 4 out. Method 1 in was better than 4 in when 30% and 40% were injected.

Frozen sections

The effect of freezing methods on general morphology is shown in Figure 6. Immersion in isopentane (i) and injection with isopentane (ii) gave a slide score significantly lower than did the freezing in liquid nitrogen (iii and iv). Furthermore, the use of liquid nitrogen followed by storing in dry air (iv) gave the highest slide scores. The effect of the fixation methods on the morphology and location of the lipid droplets is shown in Figure 7. Lipid droplets displayed the characteristic morphology and appropriate location into the hepatopancreatic tubules when frozen slides were fixed with 60% isopropanol. Slide scores worsened progressively when frozen slides were fixed with 70% alcohol, with heat and air-dried. Fixation with 60% isopropanol was significantly higher than the heating and air drying methods

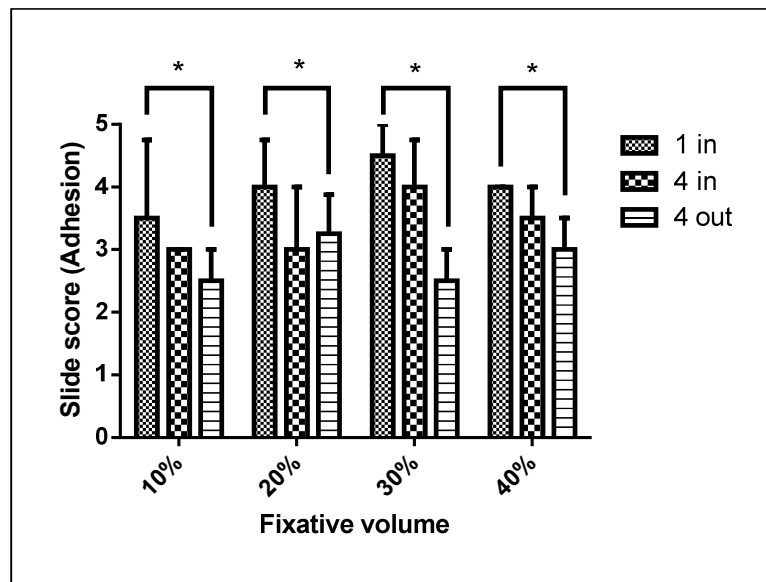


Figure 3. Effect of volume and injection methods on adhesion of hepatopancreas (HP) in paraffin sections from whiteleg shrimp (*Penaeus vannamei*). Single injection into the HP (1 in); four injections into the HP (4 in); four injections around the HP (4 out). 1 in and 4 out are significantly different (* = $p < 0.05$). Error bars indicate the standard deviation of the median. Sample size for each bar is $n=5$.

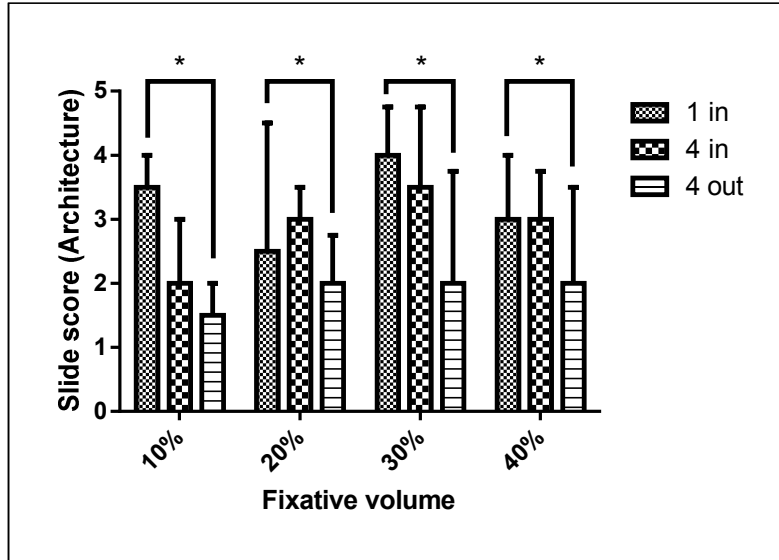


Figure 4. Effect of volume and injection method on morphology and architecture of hepatopancreas (HP) in paraffin sections from whiteleg shrimp (*Penaeus vannamei*). Single injection into the HP (1 in); four injections into the HP (4 in); four injections around the HP (4 out). 1 in and 4 out are significantly different ($* = p < 0.05$). Error bars indicate the standard deviation of the median. Sample size for each bar is $n=5$.

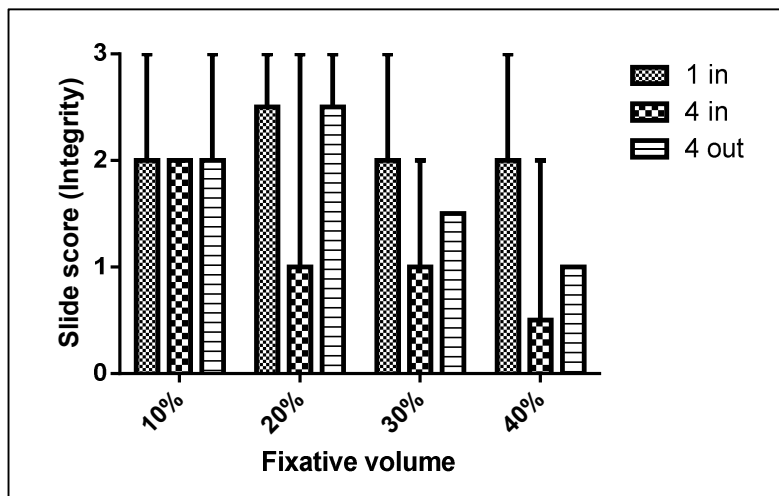


Figure 5. Effect of volume and injection method on tissue integrity of hepatopancreas (HP) in paraffin sections from whiteleg shrimp (*Penaeus vannamei*). Single injection into the HP (1 in); four injections into the HP (4 in); four injections around the HP (4 out). No statistically significant differences were observed. Error bars indicate the standard deviation of the median. Sample size for each bar is $n=5$.

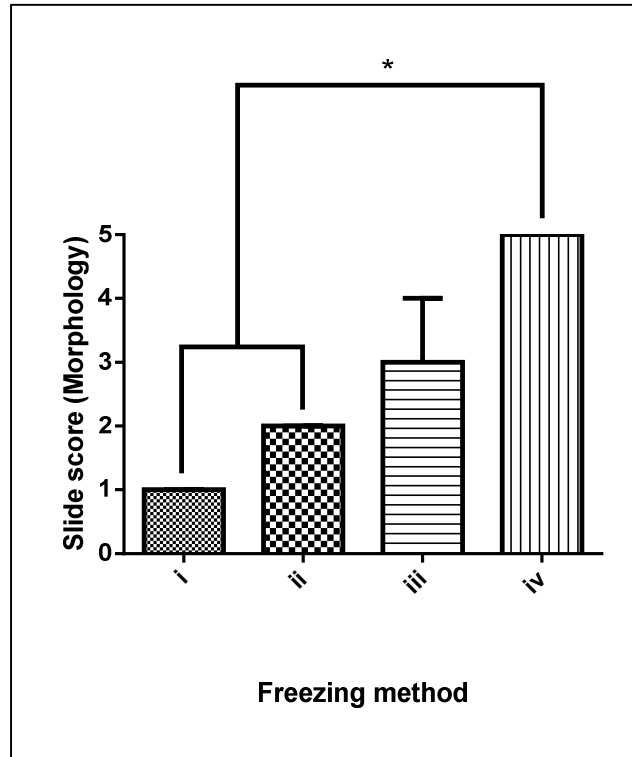


Figure 6. Effect of freezing method on general morphology of hepatopancreas (HP) in frozen sections from whiteleg shrimp (*Penaeus vannamei*). Freezing method: (i) immersion and storing in pre-cooled (-20 °C) isopentane; (ii) injection and storing in pre-cooled isopentane (single injection laterally into the HP); (iii) immersion for 20 s in liquid nitrogen followed by immersion and storing in pre-cooled isopentane; (iv) immersion for 20 s in liquid nitrogen and storing in dry air. i and ii are significantly lower than iv (* = $p < 0.05$). Error bars indicate the standard deviation of the median. Sample size for each bar is $n=5$.

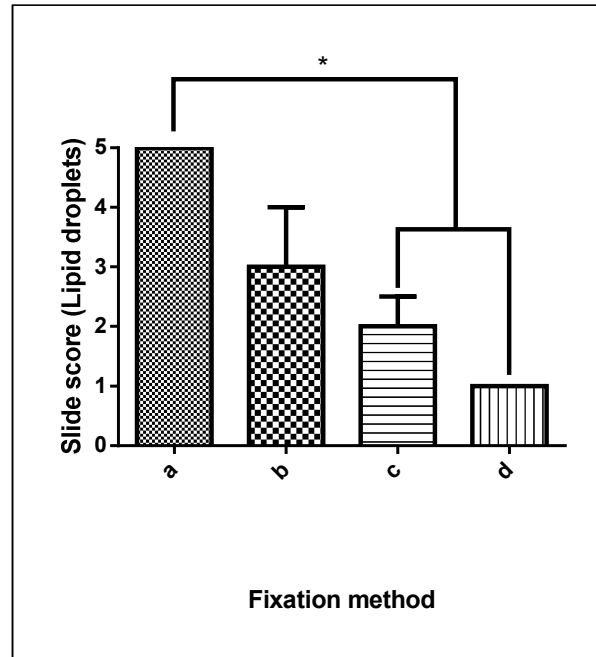


Figure 7. Effect of fixation method on morphology and location of lipid droplets of hepatopancreas in frozen sections from whiteleg shrimp (*Penaeus vannamei*). Tissue samples were immersed in liquid nitrogen for 20 s and stored in dry air. Fixation method: (a) 10 seconds in 60% isopropanol at 22 °C; (b) 10 s in 70% alcohol at 22 °C; (c) air drying for 30 minutes at 45 °C; (d) a drying for 10 min at 22 °C. a is significantly higher than c and d (* = $p < 0.05$). Error bars indicate the standard deviation of the median. Sample size for each bar is $n=5$.

Discussion

Computer-assisted image analysis requires effective consistent fixation of the sections (He *et al.* 2012). Established histological protocols for the HP of crustaceans are not satisfactory for this purpose. Therefore, the aim of the present study was to optimize fixation for paraffin sections and for frozen sections. The chitinous exoskeleton of crustaceans does not allow for adequate fixative penetration by simple immersion:

following removal from the water, specimens should be fixed immediately for paraffin sections by injecting the fixative into vital areas (Bell & Lightner 1988).

In the present study, a semi-quantitative scoring system evaluated fixation in paraffin sections assessing three parameters: adhesion of the section to the glass slide, general structural morphology and architecture of the tubules (attachment of tubules to the basal membrane), and tissue integrity of the HP (damage due to the needle and fixative penetration, and artifacts). Bell and Lightner's protocol (1988) is considered by many shrimp health practitioners to be the reference work for shrimp histology: it recommends injecting fixative at 5 - 10% volume relative to the bw of the shrimp, with a single injection into the HP. Different methods have been implemented and suggested as standard operating procedures for shrimp histology diagnostic laboratories, however all are adapted from Bell and Lightner's protocol. The Centre for Environment, Fisheries and Aquaculture Science (CEFAS) in the United Kingdom suggests injecting the cephalothorax several times, with small amounts of fixative to ensure good fixation of the HP region (CEFAS 2014). The Food and Agriculture Organization of the United Nations (FAO) recommends injecting the HP at several points (Bondad-Reantaso *et al.* 2001). The World Organization for Animal Health (OIE) recommends injecting the HP at two or more sites (Lightner 2015). In all these manuals the number of injections into the HP is not specified.

The present study showed that 1 in fixed the HP better than 4 in and 4 out. We suggest following Bell and Lightner's protocol but increasing the volume of the fixative being injected. Although 30% might appear to be a large relative volume, it allows complete fixation of the HP without compromising morphology. The protocol described in the

present study can be used not only in the research environment but also in a farm site, where animals can be easily fixed and then sent to diagnostic laboratories to be processed.

Paraffin wax continues to be the most popular embedding medium for histology (Anderson & Bancroft 2002). However, alcohol soluble tissue lipids are extracted during the dehydration process. Some alternatives were proposed to overcome lipid extraction, including plastic embedding (Van Goor *et al.* 1986) and fixation of lipids in formalin fixed samples (Tracy & Walia 2002). Both methodologies were tested in a previous experiment (data not shown) but were found to be time consuming and without generating successful results. Cryosectioning is the standard method for lipid preservation in histology (Hopwood 2002). This is a simple and rapid procedure but adversely affects morphological features, because crystal formation disrupts the cells, and freezing rate is critical to control ice crystal formation and thus cell disruption (Frederick & Busing 1981). This limitation of the method dissuades many researchers from using it in their studies (Xu & Xu 2001).

For the first time, in the present study a standardized protocol for cryopreservation and cryosectioning of the HP was described in crustaceans. A semi-quantitative scoring system evaluated fixation in frozen sections assessing two parameters: general morphology of the HP and tubules (freezing method), and morphology and location of the lipid droplets in the HP (fixation method). Immediate immersion in liquid nitrogen was demonstrated to be the best freezing method. Slow freezing of tissues produces artifacts, due to aggregation of water molecules into the ice crystals, which is significantly reduced with immediate immersion in liquid nitrogen (Steu *et al.* 2008). Based on a previous

experiment (data not shown), dissection of the HP before freezing is not recommended: surprisingly the morphology of the HP is poor when the organ is direct exposed to liquid nitrogen. When cephalothorax is immersed in liquid nitrogen, the exoskeleton might act as a mechanical barrier, preventing direct exposure of the HP to the freezing media. In the present study, optimal fixation for lipid staining was achieved with 60% isopropanol. There are a number of fixatives in use for frozen sections (*e.g.*: 95% ethanol, methanol, formalin, acetone, and various mixtures of ethanol or methanol with formalin and acetic acid) but the use of the fixative has to be compatible with the staining technique used (Peters & Delia 2010). In the present study, the utilization of isopropanol in Lillie and Ashburn's isopropanol Oil Red O staining (Culling 1974) could support optimal fixation of the section achieved with 60% isopropanol.

In the present study, fixation methods were tested on shrimp with a mean body weight of 2 ± 1 g in C-intermoult stage: the same fixation methods should be validated in shrimp of different sizes and molting stages. Different injection velocities should be compared to evaluate the potential tissue damage due to pressure of the fixative injected. Optimized fixation methods were described for both paraffin sections and frozen sections of the HP in whiteleg shrimp. These standardized methods have a broad range of applications for image analysis in both routine diagnostic pathology and research studies.

References

- Anderson G. & Bancroft J. (2002) Tissue processing and microtomy. In: *Theory and practice of histological techniques* (ed. by J. D. Bancroft & G. M. Gamble), pp. 85-99. Elsevier Health Publications, Edinburgh.
- Asaoka Y., Togashi Y., Mutsuga M., Imura N. & Miyoshi T. & Miyamoto Y. (2016) Histological image analysis of chemical-induced hepatocellular hypertrophy in mice. *Experimental and Toxicologic Pathology* **68**, 233-239.
- Bell T.A. & Lightner D.V. (1988) *A handbook of normal penaeid shrimp histology*, pp. 2-6. The World Aquaculture Society, Baton Rouge.
- Bondad-Reantaso M.G., McGladdery S.E., East I. & Subasinghe R.P. (2001) Asia Diagnostic Guide to Aquatic Animal Diseases. In: *FAO Fisheries Technical Paper No. 402, Supplement 2*, pp. 154-191. FAO and NACA, Rome.
- Bondad-Reantaso M.G., Subasinghe R.P., Josupeit H., Cai J. & Zhou X. (2012) The role of crustacean fisheries and aquaculture in global food security: Past, present and future. *Journal of Invertebrate Pathology* **110**, 158-165.
- Bucke D. (1972) Some histological techniques applicable to fish tissues. In: *Diseases of Fish* (ed. by L.E. Mawdesley-Thomas), pp. 153-189. *Symposia of The Zoological Society of London, number 30*. Academic Press, New York.
- Calvo N.S., Stumpf L., Pietrokovsky S. & López Greco L.S. (2011) Early and late effects of feed restriction on survival, growth and hepatopancreas structure in juveniles of the red claw crayfish *Cherax quadricarinatus*. *Aquaculture* **319**, 355-362.
- CEFAS (2014) Sampling of crustaceans for infectious diseases. In: *Standard Operating Procedure SOP 2014, Revision number 1*, pp. 10. Center for Environment Fisheries and Aquaculture Science, Weymouth.
- Corteel M., Dantas-Lima J.J., Wille M., Alday-Sanz V., Pensaert M.B., Sorgeloos P. & Nauwynck H.J. (2009) Molt stage and cuticle damage influence white spot syndrome virus immersion infection in penaeid shrimp. *Veterinary Microbiology* **137**, 209-216.
- Culling C.F.A. (1974) Identification of Lipids. In: *Handbook of Histopathological and Histochemical Techniques*, pp. 360-361. Butterworths & Co. Ltd, London.
- Frederick P.M. & Busing W.M. (1981) Ice crystal damage in frozen thin sections: freezing effects and their restoration. *Journal of Microscopy* **121** (2), 191-199.
- Gibson-Corley K.N., Olivier A.K. & Meyerholz D.K. (2013) Principles for Valid Histopathologic Scoring in Research. *Veterinary Pathology* **50**, 1007-1015.

Gurcan M.N., Boucheron L., Can A., Madabhushi A., Rajpoot N. & Yener B. (2009) Histopathological image analysis: a review. *IEEE reviews in biomedical engineering* **2**, 147-171.

He L., Long L.R., Antani S. & Thoma G.R. (2012) Histology image analysis for carcinoma detection and grading. *Computer Methods and Programs in Biomedicine* **107**, 538-556.

Hopwood D. (2002) Fixation and fixatives. In: *Theory and practice of histological techniques* (ed. by J. D. Bancroft & GM. Gamble), pp. 67-68. Elsevier Health Publications, Edinburgh.

Johnson S.K. (1995) *Handbook of Shrimp Diseases*, pp. 10. Texas A&M University, Texas.

Kårnsnäs A. (2014) Image analysis methods and tools for digital histopathology applications relevant to breast cancer diagnosis. *Digital Comprehensive Summaries of Uppsala Dissertations from the Faculty of Science and Technology* 1128, pp. 129. Uppsala.

Laohabanjong R., Tantikitti C., Benjakul S., Supamattaya K. & Boonyaratpalin M. (2009) Lipid oxidation in fish meal stored under different conditions on growth, feed efficiency and hepatopancreatic cells of black tiger shrimp (*Penaeus monodon*). *Aquaculture* **286**, 283-289.

Lightner D.V., Hasson K.W., White B.L. & Redman R.M. (1996) Chronic toxicity and histopathological studies with Benlate®, a commercial grade of benomyl, in *Penaeus vannamei* (Crustacea: Decapoda). *Aquatic Toxicology* **34**, 2: 105-118.

Lightner D.V. & Redman R.M. (1998) Shrimp diseases and current diagnostic methods. *Aquaculture* **164**, 201-220.

Lightner D.V. (2015) Diseases of Crustaceans. In: *Manual of Diagnostic Tests for Aquatic Animals* (ed. by OIE), Section 2.2.0, pp. 1-10. World Organization of Animal Health, Paris.

Peters, S.R. & Delia C. S. (2010) Fixation, staining and coverslipping of frozen section slides. In: *A Practical Guide to Frozen Section Technique* (ed. by S. R. Peter), pp. 117-129. Springer, New York.

Säfholm M., Jansson E., Fick J. & Berg C. (2016) Molecular and histological endpoints for developmental reproductive toxicity in *Xenopus tropicalis*: Levonorgestrel perturbs anti-Müllerian hormone and progesterone receptor expression. *Comparative Biochemistry and Physiology, Part C* **181-182**, 9-18.

Steu S., Baucamp M., Von Dach G., Bawohl M., Dettwiler S., Storz M., Moch H. & Schraml P. (2008) A procedure for tissue freezing and processing applicable to both intra-

operative frozen section diagnosis and tissue banking in surgical pathology. *Virchows Archiv* **452**, 305-312.

Tracy R.E. & Walia P. (2002) A method to fix lipids for staining fat embolism in paraffin sections. *Histopathology* **41**, 75-79.

Van Goor H., Gerrits P.O. & Grond J. (1986) The application of lipid-soluble stains in plastic-embedded sections. *Histochemistry* **85**, 251-253.

Wilson I. & Gamble M. (2002) The Hematoxylins and Eosin. In: *Theory and practice of histological techniques* (ed. by J. D. Bancroft & GM. Gamble), pp. 125-138. Elsevier Health Publications, Edinburgh.

Xu X. & Xu P.X. (2001) A modified cryosection method for mouse testis tissue. *Tissue and Cell* **33**, 208-210.

Chapter 2

Use of computer assisted image analysis for semi-quantitative histology of the hepatopancreas in whiteleg shrimp, *Penaeus vannamei* (Boone)

Fabio Cervellione¹, Charles McGurk¹, Tommy Berger Eriksen¹, Wim Van den Broeck²

¹Skretting Aquaculture Research Centre, Stavanger, Norway

²Department of Morphology, Ghent University, Ghent, Belgium

Journal of Fish Disease 2016, DOI:10.1111/jfd.12599

Abstract

Despite the increasing use of novel molecular techniques in pathology; histology remains the standard method for monitoring tissue alterations and for assessing pathology. Histopathological evaluation is generally laborious and subjective with risk of discrepancies in semi-quantitative scoring between pathologists. In contrast, computer assisted image analysis (CAIA) is potentially faster, more objective and thus suitable for routine screening. Limited research has been done on CAIA in crustacean histopathology and the methods described were not fully automated. Therefore, the aim of the present study was to develop CAIA in whiteleg shrimp (*Penaeus vannamei*) for the study of the hepatopancreas. Paraffin sections were immunohistochemically stained with monoclonal antibodies WSH8 against haemocytes and counterstained with Mayer's haematoxylin for detection of haemocytes and B-cell vacuoles, and modified Toluidine Blue protocol was used for detection of F-cells; frozen sections were stained with Oil Red O for detection of lipid droplets within R-cells. Visiopharm® software was used to develop and validated protocols for the quantification of morphological parameters (areas of haemocyte infiltration, F-cells, B-cell vacuoles, lipid droplets and their ratios to total tissue area and total lumen area). These protocols enable the future use of CAIA for determining the degree of severity of morphological changes reflecting a pathological or nutritional alteration of the organ.

Key words: computer assisted image analysis, semi-quantitative histology, hepatopancreas, whiteleg shrimp, *Penaeus vannamei*.

Introduction

In crustaceans, the hepatopancreas (HP) is a large bilobed organ, located in the cephalothorax, composed of many blindly ending tubules, which wrap over the dorsal and lateral sides of the posterior part of the stomach and the anterior part of the midgut trunk (Franceschini-Vicentini *et al.* 2009; Alday-Sanz 2010). The primary role of the HP is the synthesis and secretion of digestive enzymes, final digestion, uptake of nutrients and detoxification (Laohabanjong *et al.* 2009). In decapods, two separate lobes are enclosed together in a connective tissue capsule and are separated by a thin septum. The lobes are connected separately to the intestine through the corresponding principal duct (Esteve & Herrera 2000; Vasagam *et al.* 2007). Hepatopancreatic tubules diverge dendritically and each tubule can be subdivided into distal, medial and proximal zones relative to the distance from the midgut (Nakamura 1987; Felgenhauer 1992; Franceschini-Vicentini *et al.* 2009). From the distal to the proximal zone of the tubules the epithelium becomes smaller and the lumen larger (Cuartas *et al.* 2002). Tubules are lined up by an epithelium which, apart from the distal closed end, is only a single layer thick (Gibson & Barker 1979). The simple columnar epithelium is made up of four basic cell types: E-, F-, R- and B-cells (Nakamura 1987; Franceschini-Vicentini *et al.* 2009). Normal structure of the HP is shown in Figure 1.

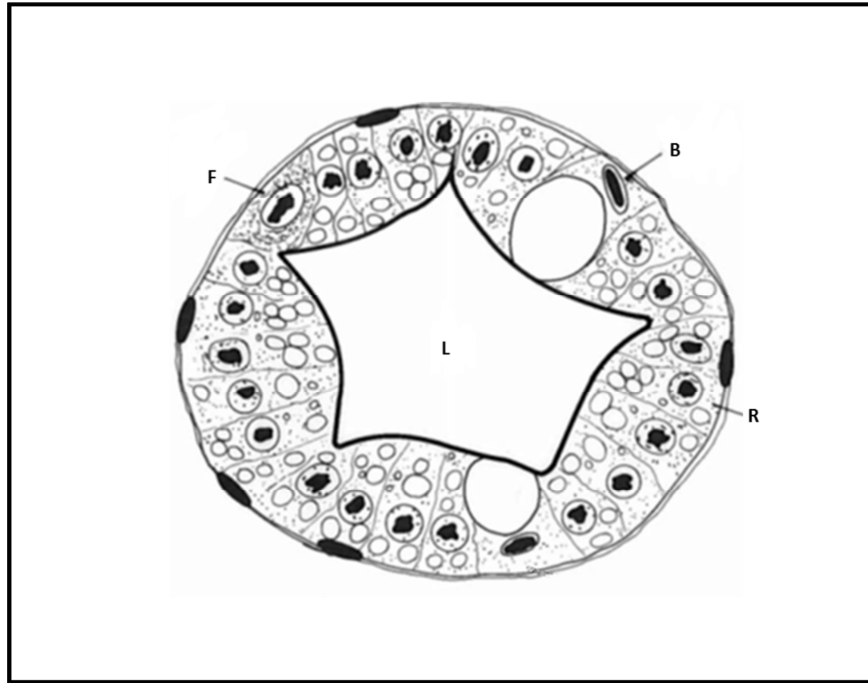


Figure 1. Normal structure of the medial zone of the hepatopancreas tubule. Cross section. lu = lumen. Adapted from Johnson (1995).

The E-cells, or embryonic cells, are small cuboidal cells entirely confined to the distal blind ends of the tubules and give rise to the other three cell types of the organ. F-cells, or fibrillar cells, are cylindrical/prismatic cells located at the medial and proximal zones of the tubules among R- and B-cells, and are characterized by a strong basophilia due to a well-developed rough endoplasmatic reticulum, giving them a fibrillar appearance. This cell type has a high rate of protein synthesis and synthesizes enzyme for extracellular digestion (Barker & Gibson 1977; Felgenhauer 1992; Sousa *et al.* 2005; Franceschini-Vicentini *et al.* 2009). B-cells, or blister cells, are large primary secretory cells more frequent at the proximal zone of the tubules and are defined by the presence of a single large membrane-bound vesicle surrounded by a dense cytoplasm. These cells produce digestive enzymes in the HP and are responsible for intracellular digestion, concentrating

the absorbed materials in the large vacuole and secreting the vacuolar content into the tubular lumen at the end of the digestive process for reabsorption by R-cells (Barker & Gibson 1977; Gibson & Barker 1979; Felgenhauer 1992; Franceschini-Vicentini *et al.* 2009). The R-cells, or reabsorption cells, are the most numerous cell types in the HP. These tall, columnar cylindrical cells are located, as F-cells, at medial and proximal zones and characterized by a large numbers of irregularly-shaped storage vesicles (primarily lipids) in their cytoplasm. These cells function in food absorption, storing lipid droplets, glycogen and mineral deposits (Felgenhauer 1992; Sousa *et al.* 2005; Franceschini-Vicentini *et al.* 2009).

Although new molecular methods in pathology are developing fast, histology remains the standard method for pathology investigations and disease diagnosis (Silva *et al.* 2015). In current practice, histological analysis is based most commonly on qualitative features as interpreted by pathologists (Miedema *et al.* 2012). Pathologists' quantification is in general time-consuming, poorly objective with significant discrepancies in scoring results reported between pathologists (He *et al.* 2012; Higgins 2015). This has motivated the development of computer-assisted image analysis (CAIA) methods for producing unbiased, reproducible, and reliable data (Nativ *et al.* 2014; Silva *et al.* 2015). This method could assist but not replace experienced pathologists as additional morphological features need to be considered for clinical appraisal (He *et al.* 2012; Miedema *et al.* 2012; Nativ *et al.* 2014). This methodology requires optimization of histological procedures for preparation of samples. In a previous study, our research group proposed a standardized protocol for paraffin and frozen sections of the HP in whiteleg shrimp (*Penaeus vannamei*) for image analysis (Cervellione *et al.* 2016). A limited amount of

research has been done on the application of CAIA in crustacean histopathology and to our best knowledge, no studies have been conducted in whiteleg shrimp (Odendaal & Reinecke 2003; Odendaal & Reinecke 2007; Berillis *et al.* 2013). Therefore, the aim of the present study was to develop CAIA in whiteleg shrimp for the study of the HP structure and future determination of the nutritional and pathological status of this organ.

Materials and Methods

Shrimp and rearing conditions

Experiments were conducted in collaboration with IMAQUA, located at the Faculty of Veterinary Medicine (Ghent, Belgium). Specific pathogen-free whiteleg shrimp were imported from Shrimp Improvement Systems (Florida, USA). Shrimp were housed in 50 L glass tanks, each supplied with constant aeration and independent biological/mechanical filters. Water temperature was kept at 27 ± 1 °C, with a pH of 7.8 – 8.1 and salinity of 20 ± 1 g L⁻¹. The biological filters and regular water exchanges kept the total ammonium concentrations below 0.5 mg L⁻¹ and the total nitrites below 0.15 mg L⁻¹. The room was illuminated 12 h d⁻¹ by a dimmed luminescent light-tube. Shrimp were fed a commercial diet for 30 d, at 5% of the body weight (bw), four times per day. Thereafter, shrimp of 2 ± 1 g, within the C-intermoult stage (Corteel *et al.* 2009) were collected and transported to the Department of Morphology (Ghent University, Belgium) in aerated buckets. Shrimp were then euthanized as described by Lightner (2015) for paraffin sections and euthanized in cold ice for frozen sections.

Preparation of paraffin and frozen sections

Ten shrimp were individually weighed, fixed with Davidson's solution (30 mL 95% ethanol, 20 mL 37% formaldehyde, 10 mL glacial acetic acid, and 30 mL distilled water), as described by Cervellione *et al.* (2016). After injection and lateral slitting of the cuticle from the sixth abdominal segment to the base of the rostrum, shrimp were immersed in Davidson's fixative (ratio of fixative to tissue volume of 10:1) for 48 h at 22 °C. The shrimp were then bisected transversally at the junction of the cephalothorax and abdomen, the cephalothorax bisected longitudinally on the mid-line, and both parts placed in tissue processing cassettes. Tissues were dehydrated in a graded series of alcohol baths (70%, 80%, 95%, and 100%) and cleared in xylene, using an automated tissue processor (Microm STP420D, ThermoScientific™). Then, the tissues were embedded in paraffin (melting point 54 – 56 °C, Paraclean Klinipath BV, VWR International®) using manual embedding station (Microm EC350, ThermoScientific™). After further optimization of section thickness, five µm thick longitudinal sections were cut with an automated microtome (Microm HM 360, ThermoScientific™), placed on APES (3-Aminopropyltriethoxysilane) coated glass slides, dried for 1 h at 56 °C and kept at 37 °C overnight.

For frozen sections, ten shrimp were processed as described by Cervellione *et al.* (2016). Shrimp were bisected transversally at the junction of the cephalothorax and the abdomen, and immediately anterior to the HP. Cephalothorax was frozen by immersion for 20 s in liquid nitrogen and storing in dry air. After freezing, all samples were kept at -80 °C. Samples were embedded in water-soluble media (Tissue-Tek® OCT, VWR International®) and 16 µm thick longitudinal sections cut, by use of an automated

cryostat (Microm HM505E, ThermoScientific™) at -25 °C and placed on glass slides (HistoBond®, Marienfeld). Then frozen sections were fixed for 10 s in 60% isopropanol at 22 °C.

Selection of morphometric parameters for CAIA

In crustaceans, the HP is routinely examined by pathologists and assessed as a general indicator of health (Johnson 1995; Laohabanjong et al. 2009; Calvo *et al.* 2011). Morphological alterations of the HP, such as reduction of the tubular area and enlargement of the lumen area, variation in the number of B-cells, F-cells and R-cells, infiltration of haemocytes in the intertubular spaces, have been described by different authors in case of pathogens, food deprivation, changes in salinity and food ingredients (Nakamura 1987; Sánchez-Paz *et al.* 2007; Tam & Avendant-Oldewage 2009; Diaz *et al.* 2010; Masson *et al.* 2012; Sacristán *et al.* 2016). Haemocyte infiltration has been reported as initial response of the HP to tissue damage (traumatic or due to infection), toxicity and environmental stress (Johnson 1980; McGallery 2011; Chiodi Boudet *et al.* 2015; Longo & Diaz 2015). F-cells have a high rate of protein synthesis, producing enzymes for extracellular digestion (Barker & Gibson 1977). The quantification of F-cells (enzymatic activity of the HP) could help to understand how the HP copes with different diets, feeding regimes and starvation periods. Morphometric parameters were selected for the development of protocols (APPs) and quantification of the main morphological changes occurring in the HP (Table 1). Total Tissue Area (TTA) represented the total area covered by tubular epithelium, composed by B-, F- and R-cells, and Total Lumen Area (TLA) represented the area covered by tubular lumen. The ratio TLA:TTA indicated the variation of tubular lumen. Haemocyte Infiltration Area (HIA) indicated the area of

haemocytes infiltrating the intertubular spaces of the HP, and ratio HIA:TTA indicated the response of the HP to noxa. Vacuoles B-cells Area (VBA) represented the area of the tubule composed by vacuole of the B-cells, and ratio VBA:TTA measured the intracellular digestion taking place in the HP. F-Cell Area (FCA) represented the area of the tubule composed by F-cells, and ratio FCA:TTA indicated the enzymatic activity of the HP. Finally, Lipid Droplet Area (LDA) indicated the area of the tubule composed by lipid droplets within R-cells, and ratio LDA:TTA measured the lipid reserves in the HP. All ratios were indicated as % of TTA.

Table 1. Selection of morphometric parameters and their ratios used for the development of computer assisted image analysis of the hepatopancreas in whiteleg shrimp (*Penaeus vannamei*).

Morphometric parameter	Description
Total Tissue Area (TTA)	Total area covered by tubular epithelium, composed by B-cells, F-cells and R-cells
Total Lumen Area (TLA)	Total area covered by lumen
TLA:TTA	Ratio of Total Lumen Area to Total Tissue Area, as measure of the variation of the tubular lumen, expressed as %
Haemocyte Infiltration Area (HIA)	Area of the haemocytes infiltrating the intertubular spaces of the HP
HIA:TTA	Ratio of Haemocyte Infiltration Area to Total Tissue A, as measure of the HP response to noxa, expressed as %
Vacuoles of B-cells Area (VBA)	Area of the tubule composed by vacuoles of B-cells
VBA:TTA	Ratio of Vacuoles of B-cells Area to Total Tissue Area, as measure of intra-cellular digestion of the HP, expressed as %
F-Cells Area (FCA)	Area of the tubule composed by F-cells
FCA:TTA	Ratio of F-Cells Area to Total Tissue Area, as measure of the enzymatic activity of the HP, expressed as %
Lipid Droplets Area (LDA)	Area of the tubule composed by lipid droplets within R-cells
LDA:TTA	Ratio of Lipid Droplets Area to Total Tissue Area, as measure of the lipid reserves in the HP, expressed as %

Note: HP = hepatopancreas.

Stainings

Stainings used for the development of APPs for CAIA are reported in Table 2. Detection of haemocytes in the intertubular spaces was based on immunohistochemistry (IHC). WSH8 monoclonal antibodies (Mabs) were produced by the Wageningen Institute of Animal Science (Wageningen University, The Netherlands) immunizing mice with membrane lysates of tiger shrimp (*Penaeus monodon*, Fabricus 1798) haemocytes (Van de Braak *et al.* 2000). A previous experiment (data not shown) proved the specificity of WSH8 for whiteleg shrimp haemocytes. After deparaffination in xylene and rehydration in ethanol series, paraffin sections (one section per shrimp) were subjected to heat-induced epitope retrieval using citrate solution in microwave for 150 s at 750 W followed by 10 min at 160 W and stored for 30 min at 4 °C. Then sections were incubated for 5 min at 22 °C with Dako REAL™ Peroxidase-Blocking Solution followed by incubation with 30% rabbit serum blocking solution for 30 min at 22 °C. After incubation of the slides for 1h at 22 °C with the Mabs dilution (100x), peroxidase-conjugated reaction was carried out using Dako REAL™ EnVision™ Labelled Polymer HRP anti-mouse for 30 min at 22 °C, followed by DAB chromogen solution for 5 min at 22 °C. Sections were then counterstained with Mayer's haematoxylin for 5 min and mounted in non-aqueous medium (DPX, Sigma-Aldrich®). Mayer's haematoxylin was used on the same section for counterstaining IHC and identification of B-cell vacuoles. Detection of F-cells was based on modified Toluidine Blue protocol (Gurr 1962). Paraffin sections (one section per shrimp) were stained for 3 min in Toluidine Blue followed by 1 min in ThermoScientific™ Carifier 1 through an automated slide-stainer (Gemini AS, ThermoScientific™) and mounted in non-aqueous medium (DPX, Sigma-Aldrich®). Detection of lipid droplets

within the R-cells was based on Oil Red O staining. Therefore, frozen sections (one section per shrimp) were stained with Lillie and Ashburn's isopropanol Oil Red O staining (ORO) (Culling 1974) using an automated slide-stainer (Gemini AS, ThermoScientific™) and mounted in aqueous media (Aquatex®, VWR International®). All sections were label-coded and one experienced examiner observed slides under light microscope to evaluate the suitability of the sections for image analysis (BX53, Olympus®).

Table 2. List of stainings used for the development of computer assisted image analysis of the hepatopancreas in whiteleg shrimp (*Penaeus vannamei*).

Staining	APP
IHC with Mabs WSH8 counterstained with Mayer's haematoxylin	HIVB (Haemocyte Infiltration and Vacuole of B-cells)
modified Toluidine Blue protocol	F (F-cells)
Oil Red O	LD (Lipid Droplets within R-cells)

Note: Each APP was developed analyzing region of interests (ROI) of 13372 μm^2 for HIVB and F, and 1650 μm^2 for LD. APP = protocol for computer assisted image analysis; IHC = immunohistochemistry; Mabs = monoclonal antibodies.

Digital image acquisition

Slides were scanned using automated slide-scanner (Leica SCN400, Leica Microsystems®, Germany) producing digitized images (scn file format) in 20x magnification.

Image processing

The software Visiopharm (version VIS 6.0.0.1765 with Author™ module, Visiopharm®, Denmark) was used for image analysis. Author™ module allows developing customized APPs. For each section a region of interest (ROI; 13372 μm^2 for APP HIVB and F and 1650 μm^2 for APP F) was selected for image processing. An example of a representative ROI is shown in Figure 2. ROI was selected avoiding the borders of the HP (where distal ends of the tubules are present) and selecting the medial part of the cross section of the tubule.

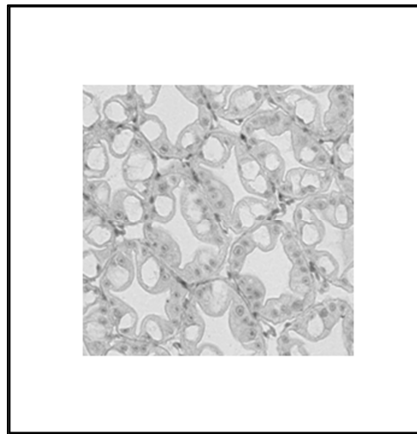


Figure 2. Region of interest (ROI) selected as representative area a cross section of the hepatopancreas (HP) of whiteleg shrimp (*Penaeus vannamei*) for the development of computer assisted image analysis protocol (APP).

The workflow for each APP was divided in four phases: 1) pre-processing, 2) image classification, 3) post-processing, and 4) calculations.

1) Pre-processing

The purpose of pre-processing is to enhance phenomena that can improve the subsequent image segmentation and/or to remove phenomena that will disturb the subsequent image segmentation. A combination of two color bands was used for each APP. Main filters used were Mean and Median (filter size 5 x 5).

2) Classification

During classification the image is segmented into multiple segments (sets of pixels) sharing common features in the selected color bands. APPs were developed using Linear Bayesian classification method and trained on representative sets of images.

3) Post-processing

In post-processing the image segmentation can be further refined based on morphological and contextual information. Main steps used were Change, Erode, Dilate, Open, Close, Fill holes and Separate objects.

4) Calculations

After post-processing, quantitative data of the morphological parameters were generated by the software.

APPs validation

Quantitative data generated using the proposed APPs (automated method) were compared to data generated with a semi-automated method. For semi-automated method, two trained observers (Ob1 and Ob2) used the same software (Visiopharm®, Denmark) to extract the same morphological parameters manually (without the developed APPs). Each operator manually drew labels of the different tissue types (tubule, lumen, F-cells, vacuoles of B-cells and lipid droplets within R-cells, and haemocytes) within the selected ROI. Then, calculations and ratios were automatically extracted by the software. For each APP, operators evaluated ten sections (one ROI per section) to measure time efficiency, accuracy, and reproducibility (inter- and intra-observer variability) (Silva *et al.* 2015). For efficiency, total computational time for data generation with automated and semi-automated methods were compared. To show the robustness of the proposed APPs, inter- and intra-observer variability between automated and semi-automated methods were compared. For intra-observer variability, operators evaluated the same sections in three consecutive day. For intra-observer variability, data generated on the same sections by the two observers were compared.

Statistical analysis

Data were tested and treated as parametric data. For accuracy and reproducibility, Pearson's correlation coefficient r (95% confidence interval) was used to measure the strength of association between automated and semi-automated methods and intra- and inter-observer variability (Galarraga *et al.* 2012; Mukaka 2012; Shi *et al.* 2012).

Results

In the present study, three APPs (HIVB, LD, and F) were developed to identify haemocytes and B-cell vacuoles, lipid droplets within R-cells, and F-cells. Morphological parameters assessed by each APP are reported in Table 3.

Table 3. Protocols (APPs) and morphological parameters for the development of computer assisted image analysis of the hepatopancreas in whiteleg shrimp (*Penaeus vannamei*).

APP	Morphological parameters assessed
HIVB (Haemocyte Infiltration and Vacuoles of B-cells)	HIA, VBA, TLA, and their ratios to TTA
F (F-cells)	FCA, TLA, and their ratios to TTA
LD (Lipid Droplets within R-cells)	LDA, TLA, , and their ratios to TTA

Note: FCA = F-cell area; LDA = total lipid area; HIA = haemocyte infiltration area; TLA = total lumen area; TTA = total tissue area; VBA = vacuole of B-cell area.

Figure 3 shows main steps for the development of HIVB. Haemocytes were stained with IHC using WHS8 and no background staining was observed (a). In the post-processing phase (d) 17 steps allowed identifying lumen (grey), tissue area (pink), B-cells vacuoles (light blue) and haemocytes (dark blue). Development of LD is shown in Figure 4. In the post-processing phase (d) 26 steps allowed identifying lumen (white), tissue area (blue), and lipid droplets (red). The workflow for F is reported in Figure 5. In the post-processing phase (d) 30 steps allowed identifying F-cells (dark blue), lumen (pink) and tissue area (light blue).

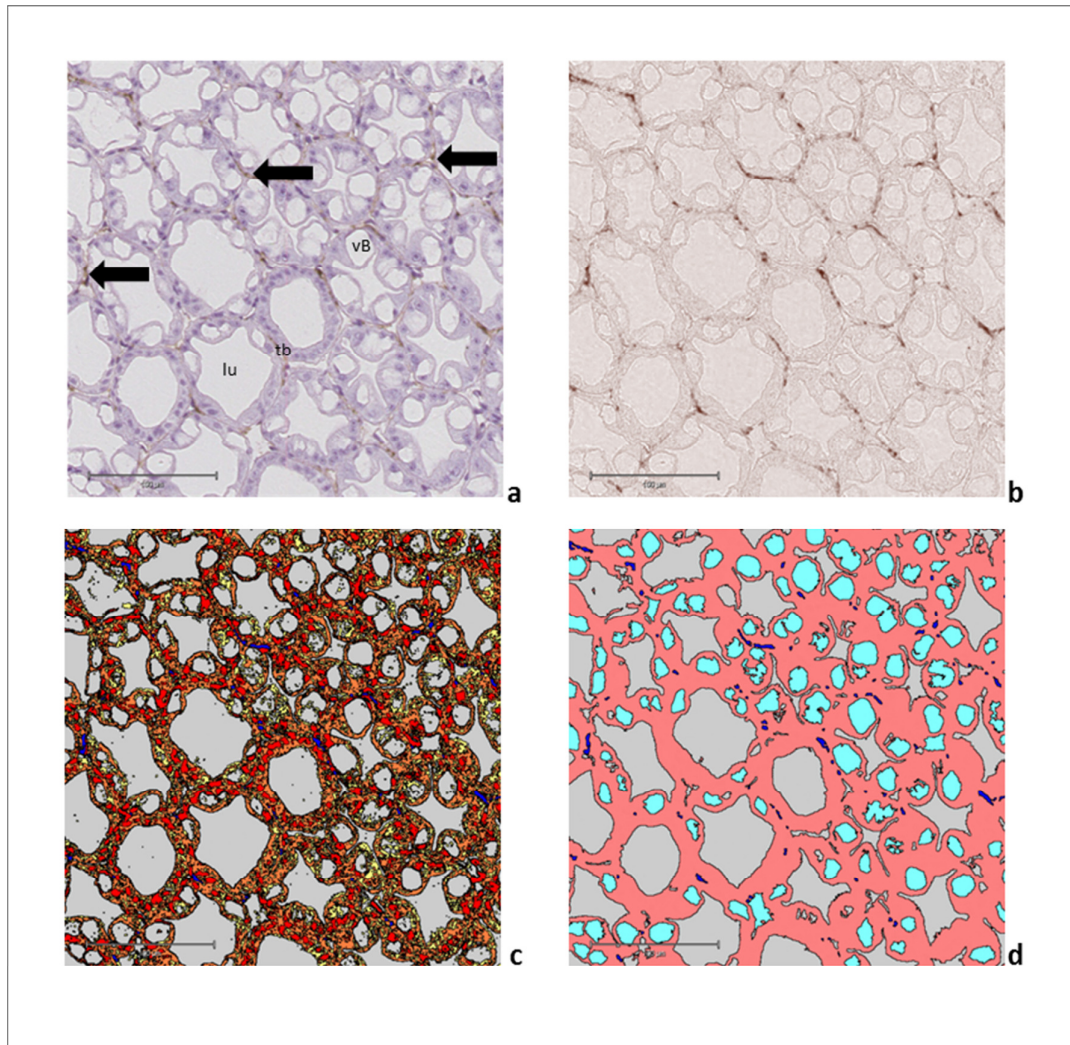


Figure 3. Development of computer assisted image analysis protocol (APP) for the detection of haemocytes and B-cell vacuoles in the hepatopancreas (HP) of whiteleg shrimp (*Penaeus vannamei*). Paraffin section (5 μm) of the HP stained with immunohistochemistry using monoclonal antibodies WSH8 counterstained with Mayer's haematoxylin (a). APP workflow (b,c,d): pre-processing (b), classification (c), post-processing (d). In d: total tissue area (pink), lumen area (grey), B-cell vacuoles (light blue), haemocytes (blue). lu = lumen; tb = hepatopancreatic tubule; vB= B-cell vacuole; black arrows = haemocytes. Scale bar = 100 μm.

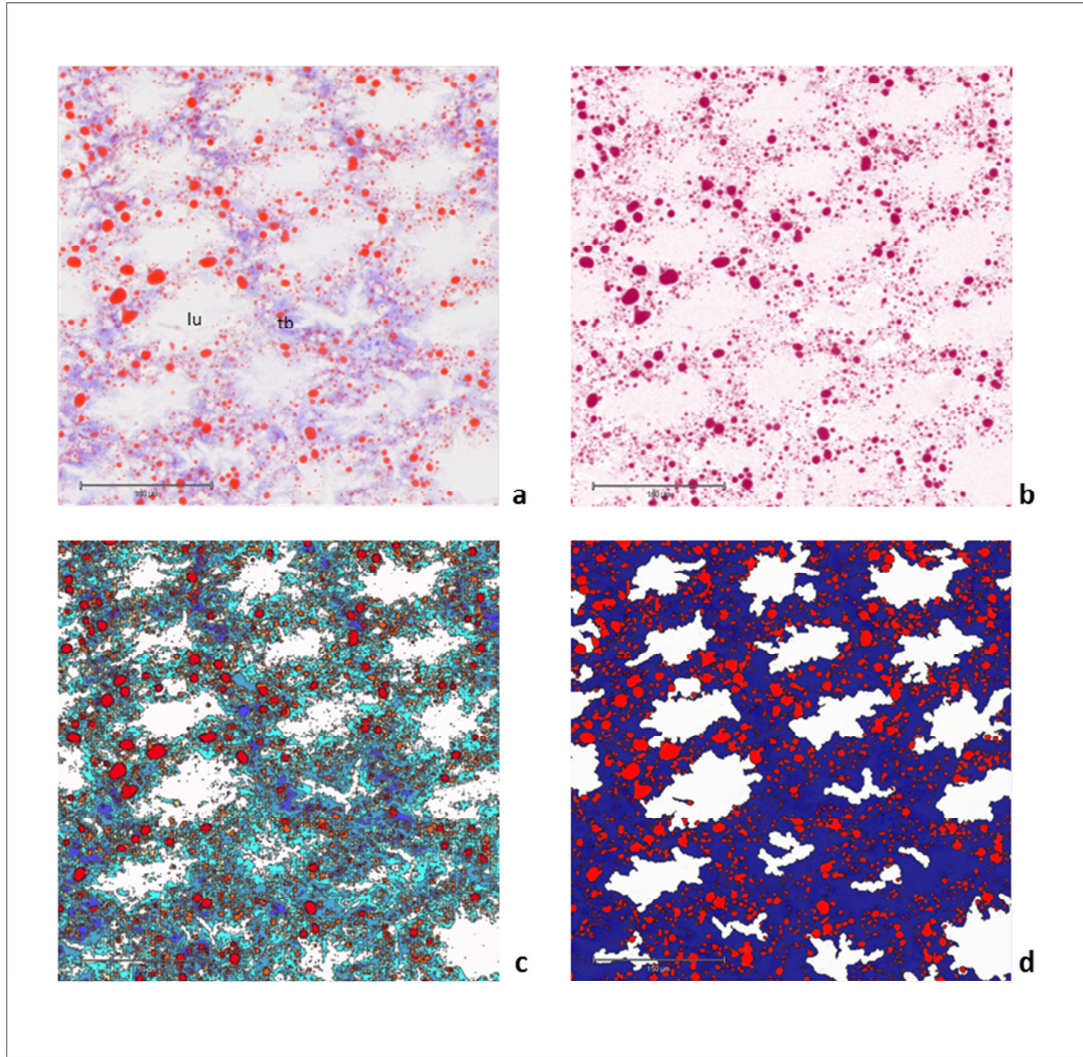


Figure 4. Development of computer assisted image analysis protocol (APP) for the detection of lipid droplets within R-cells in the hepatopancreas (HP) of whiteleg shrimp (*Penaeus vannamei*). Frozen section (16 μm) of the HP stained with Oil Red O (a). APP workflow (b,c,d): pre-processing (b), classification (c), post-processing (d). In d: total tissue area (blue), lumen area (white), lipid droplets (red). lu = lumen; tb = hepatopancreatic tubule. Scale bar = 150 μm .

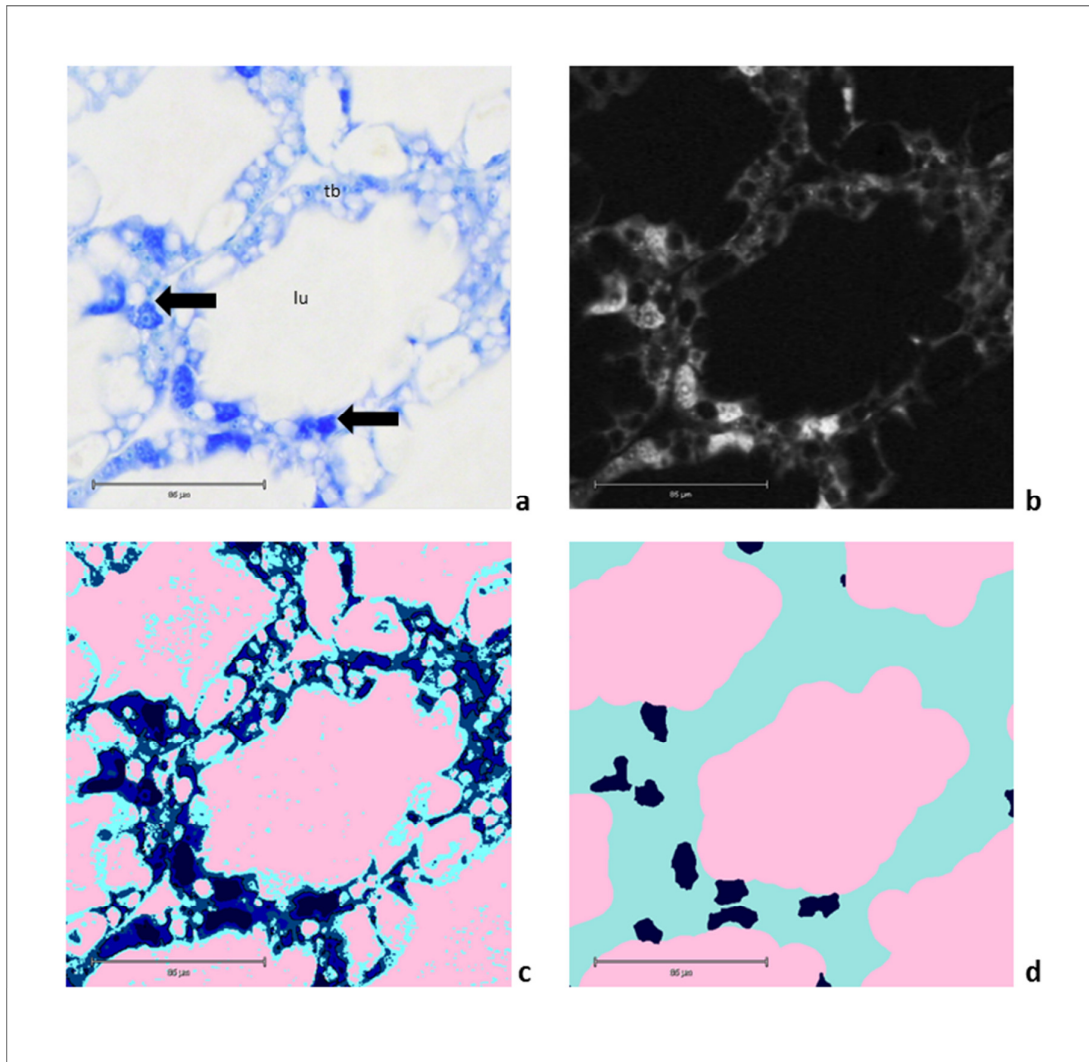


Figure 5 Development of computer assisted image analysis protocol (APP) for the detection of F-cells in the hepatopancreas (HP) of whiteleg shrimp (*Penaeus vannamei*). Paraffin section (5 μm) of the HP stained with modified Toluidine blue protocol (a). APP workflow (b,c,d): pre-processing (b), classification (c), post-processing (d). In d: total tissue area (light blue), lumen area (pink), F-cells (blue). lu = lumen; tb = hepatopancreatic tubule; arrows = F-cells. Scale bar = 85 μm .

APPs validation and statistical analysis

Transparency slider in the label drawing dialog was used to examine the results during each phase of image processing. Data for time efficiency are summarized in Table 4. Automated method was about 200 to 700 times faster than semi-automated method. In particular, APPS generated results in less than 1 s. Ob2 resulted to be always faster than Ob1. Accuracy is reported in Table 5. Pearson's correlation coefficient r (95% confidence interval) ranged from 0.91 to 0.99, depending on the morphological parameter assessed. Finally, inter and intra observer variability is reported in Table 6. Pearson's correlation coefficient r for intra-observer variability ranged from 0.98 to 0.99, while automated method gave always 1. Coefficient for inter-observer variability was 0.96 for the semi-automated method and 1 for the automated method.

Table 4. Comparison of time efficiency between automated and semi-automated methods for computer assisted image analysis of the hepatopancreas in whiteleg shrimp (*Penaeus vannamei*).

Morphological parameters assessed	Total average processing time
HIVB (HIA, VBA, TTA, TLA)	
Automated	0'0.5'' ± 00'' (always)
Semi-automated	5'53'' ± 43'' (Ob1) 5'06'' ± 53'' (Ob2)
F (FCA, TTA, TLA)	
Automated	0'0.5'' ± 00'' (always)
Semi-automated	2'05'' ± 22'' (Ob1) 1'53'' ± 35'' (Ob2)
LD (LDA, TTA, TLA)	
Automated	0'0.5'' ± 00'' (always)
Semi-automated	3'12'' ± 47'' (Ob1) 2'42'' ± 29'' (Ob2)

Note: for each protocol (HIVB, F, and LD), ten histological sections (one ROI per section) were analyzed by two operators (Ob1, Ob2). FCA = F-cell area; LDA = total lipid area; HIA = haemocyte infiltration area; ROI = region of interest; TTA = total tissue area; TLA = total lumen area; VBA = vacuole of B-cell area.

Table 5. Comparison of accuracy between automated and semi-automated methods for computer assisted image analysis of the hepatopancreas in whiteleg shrimp (*Penaeus vannamei*).

Morphological parameter evaluated	Pearson's coefficient (r)
Protocol HIVB	
HIA	0.92
VBA	0.91
TTA	0.95
TLA	0.95
Protocol F	
FCA	0.95
TTA	0.94
TLA	0.95
Protocol LD	
LDA	0.93
TTA	0.91
TLA	0.99

Note: for each protocol (HIVB, F, and LD), ten histological sections (one ROI per section) were analyzed by two operators (Ob1, Ob2). Pearson's correlation coefficient (r) is calculated with 95% confidence interval. FCA = F-cell area; LDA = total lipid area; HIA = haemocyte infiltration area; ROI = region of interest; TTA = total tissue area; TLA = total lumen area; VBA = vacuole of B-cell area.

Table 6. Reproducibility of automated and semi-automated methods for computer assisted image analysis of the hepatopancreas in whiteleg shrimp (*Penaeus vannamei*).

Method	Intra-observer variability	Inter observer variability
Automated	r = 1 (always)	r = 1 (always)
Semi-automated	r = 0.99 (Ob1) r = 0.98 (Ob2)	r = 0.96

Note: ten histological sections (one ROI per section) were analyzed by two operators (Ob1, Ob2). For inter-observer variability, sections were analyzed three times in three consecutive days. Pearson's correlation coefficient (r) is calculated with 95% confidence interval. ROI = region of interest.

Discussion

The goal of CAIA in histopathology is to increase the amount and quality of data derived from a specimen, providing quantitative measurements to assist the pathologist (Fuchs & Buhmann 2011; He *et al.* 2012; Miedema *et al.* 2012; Nativ *et al.* 2014). The basic principle of automated image analysis for histology is the use of a series of mathematical algorithms to process images, enabling the segmentation of picture elements into regions of interest based on their color, texture, and/or context (Webster & Dunstan 2014).

Although many image analysis software systems utilize similar image segmentation and image-processing concepts to their algorithms, a key differentiating factor of commercial software packages is the amount of supervision required, or allowed, by the user. It is possible to classify software in two categories: unsupervised and supervised. Unsupervised packages do not need extensive training of operators and rely on algorithms built into the software. Supervised packages, such as Visiopharm®, instead require upfront training in image analysis, but allow users to program specific algorithms and to develop unique analyses (Webster & Dunstan 2014). Berillis *et al.* (2013) have described an image processing method for the HP to determine the nutritional condition in lobsters: however the method was not fully automatized and required manual marking of tubules by drawing the contours. Moreover, the algorithm measured R-cells total area without quantifying lipid droplets. The present study describes a fully automated CAIA method for the study of the HP in whiteleg shrimp. Three APPs were developed and validated for detection and quantification of morphological parameters.

Morphometric parameters, such as HIA and ratio HIA:TTA, could be used in future studies for monitoring the health condition of the HP and improve the understanding of

the pathophysiological mechanisms of this organ. In the future, morphological parameters as FCA, VCA, LDA, TLA and their ratios to the TTA could support the study of the HP physiology comparing the effect of different diets and feeding regimes. The TISSUEalign™ module in Visiopharm® software allows automated high precision alignment of an unlimited amount of serial sections and it could be used to extract morphologic parameters from serial sections stained with different dyes. For automated analysis systems, each source of variability presents a significant obstacle (McCann *et al.* 2015). There are three main sources of variability in a histology-based diagnosis: biological, inter- and intra-observer, and technical variability. Fixation, staining and scanning are sources of technical variability (Kothari *et al.* 2013; McCann *et al.* 2015). For clinical application of CAIA, it is essential to minimize these sources of variability and validate APPs on multiple datasets (Kothari *et al.* 2013). In the present study, shrimp of the same intermoult stage were fixed with a standardized method developed for image analysis (Cervellione *et al.* 2016). Automated stainer and automated scanner were used to minimize technical variability. The APPs validation was done by analyzing data generated by two observers on ten sections (one ROI per section) using automated and semi-automated methods. Three parameters were assessed: efficiency, accuracy and reproducibility. The automated method was about 200 to 700 faster than the semi-automated method. Efficiency in time allows the proposed method to analyze big datasets in a short time.

The accuracy of image analysis methods greatly affects the robustness of downstream analysis (Kothari *et al.* 2013). Accuracy values for the proposed methods ranged from 0.91 to 0.99 and are comparable with those reported in literature (Sieren 2010;

Galarraga *et al.* 2012; Pajor *et al.* 2012; Shi *et al.* 2012; Wang *et al.* 2016). Correlation value for intra- and inter-observer variability in the automated method was always higher than in the semi-automated method. The proposed method is fully automated and reduces the intra- and inter-observer variability to zero, increasing workflow efficiency and reproducibility (Bueno *et al.* 2016). The exact parameters and assumptions can be used across every sample with no-inter-observer bias, which can significantly impact the reproducibility of data analysis (Inman *et al.* 2005; Diller & Kellar 2015). In the present study, CAIA was developed using shrimp with a mean body weight of 2 ± 1 g in C-intermoult stage: the same methodology should be validated in shrimp of different sizes and moulting stages. Development of immunohistochemistry methods and test of other stainings for targeting specific structures in the HP should also be investigated.

Development of immunohistochemistry, *in situ* hybridization methods and test of other stainings for targeting specific structures and pathogens should be also investigated.

To our best knowledge, the present study describes for the first time the use of CAIA in whiteleg shrimp. CAIA allows detection of initial histopathological changes useful for early diagnosis of diseases: for example, infiltration of haemocytes associated with lack of differentiation in the tubule epithelial cells have been described in the early stages of acute hepatopancreatic necrosis disease (AHPND). CAIA could also be used for detecting emerging diseases, as hepatopancreatic microsporidiosis caused by *Enterocytozoon hepatopenaei* (EHP), in combination with *in situ* hybridization method (Thitamadee *et al.* 2016). Furthermore, CAIA could be helpful in identifying histopathological changes of the HP in case of starvation, as reduction of the epithelial thickness, loss of the typical star-shaped lumen, reduction of B-cells and lipid droplets

within R-cells, observed during disease outbreaks and adverse environmental conditions (Vogt *et al.* 1985; Nakamura 1987; Lavilla-Pitogo *et al.* 1998; Ong & Johnston 2006; Leser *et al.* 2008; Calvo *et al.* 2011; Sacristán *et al.* 2016). In the future, the application of CAIA on routine health screening of shrimp farms might support the shrimp industry anticipating diagnosis, facilitating therapeutical and management solutions.

References

- Alday-Sanz, V. (2010) *The shrimp book*, Nottingham University Press, Loughborough.
- Arevalo, J., Cruz-Roa, A. & Gonzàles, F.A. (2014) Histopathology image representation for automatic analysis: a state-of-the-art review. *Revista Facultad de Medicina*, **22** (2), 79-91.
- Barker, P.L. & Gibson, R. (1977) Observation on feeding mechanism, structure of gut, and digestive physiology of european lobster *Homarus gammarus* (L) (Decapoda-Nephropidae). *Journal of Experimental Marine Biology and Ecology*, **26**, 297-324.
- Berillis, P., Simon, C., Mente, E., Sofos, F. & Karapanagiotidis, I.T. (2013) A novel image processing method to determine the nutritional condition of lobsters. *Micron*, **45**, 140-144.
- Bueno, G., Fernandez-Carrobles, M.M., Deniz, O. & Garcia-Rojo, M. 2016. New Trends of Emerging Technologies in Digital Pathology. *Pathobiology*, **83**, 61-69.
- Calvo, N.S., Stumpf, L., Pietrokovsky, S. & Greco, L.S.L. 2011. Early and late effects of feed restriction on survival, growth and hepatopancreas structure in juveniles of the red claw crayfish *Cherax quadricarinatus*. *Aquaculture*, **319**, 355-362.
- Cervellione, F., McGurk, C., Silva, P., Owen, M.A.G. & Van den Broeck, W. 2016. Optimization of fixation methods for image analysis of the hepatopancreas in whiteleg shrimp, *Penaeus vannamei* (Boone). *Journal of Fish Diseases*, doi 10.1111/jfd.12531.
- Chiodi Boudet, L.N., Polizzi, P., Romero, M.B., Robles, A., Marcovecchio, J.E. & Gerpe, M.S. (2015) Histopathological and biochemical evidence of hepatopancreatic toxicity caused by cadmium in white shrimp, *Palaemonetes argentinus*. *Ecotoxicology and Environmental Safety*, **113**, 231-240.
- Corteel M., Dantas-Lima J.J., Wille M., Alday-Sanz V., Pensaert M.B., Sorgeloos P. & Nauwynck H.J. (2009) Molt stage and cuticle damage influence white spot syndrome virus immersion infection in penaeid shrimp. *Veterinary Microbiology* **137**, 209-216.

- Cuartas, E.I., Diaz, A.C. & Petriella, A.M. (2002) Morphological and histological study of the hepatopancreas of shrimp *Pleoticus muelleri* (Bate) (Crustacea, Penaeoidea). *Revista de Investigacion y Desarrollo Pesquero*, **15**, 5-13.
- Culling, C.F.A. (eds.) (1974) Identification of lipids. In *Handbook of Histopathological and Histochemical Techniques*, pp. 360–361. Butterworths & Co. Ltd, London.
- Diaz, A.C., Sousa, L.G. & Petriella A.M. 2010. Functional Cytology of the Hepatopancreas of *Palaemonetes argentinus* (Crustacea, Decapoda, Caridea) Under Osmotic Stress. *Brazilian Archives of Biology and Technology*, **53**, 599-608.
- Diller, R.B. & Kellar, R.S. 2015. Validating whole slide digital morphometric analysis as a microscopy tool. *Microscopy and Microanalysis*, **21**, 249-255.
- Esteve, M. & Herrera, F.C. (2000) Hepatopancreatic alterations in *Litopenaeus vannamei* (Boone, 1939) (Crustacea : Decapoda : Penaeidae) experimentally infected with a *Vibrio alginolyticus* strain. *Journal of Invertebrate Pathology*, **76**, 1-5.
- Felgenhauer, B.E. (1992) Internal Anatomy of the Decapods: An Overview. In: *Microscopic Anatomy of Invertebrates*, pp. 45-75. Wiley-Liss, New York.
- Franceschini-Vicentini, I.B., Ribeiro, K., Papa, L.P., Marques, J., Vicentini, C.A. & Valenti, P. (2009) Histoarchitectural Features of the Hepatopancreas of the Amazon River Prawn *Macrobrachium amazonicum*. *International Journal of Morphology*, **27**, 121-128.
- Fuchs, T.J. & Buhmann, J.M. (2011) Computational pathology: challenges and promises for tissue analysis. *Computerized Medical Imaging and Graphics*, **35**, 515-530.
- Galarraga, M., Campión, J., Muñoz-Barrutia, A., Boqué, N., Moreno, H., Martínez, J.A., Milagro, F. & Ortiz-De-Solórzano, C. 2012. Adiposoft: automated software for the analysis of white adipose tissue cellularity in histological sections. *Journal of Lipid Research*, **53**, 2791-2796.
- Gibson, R. & Barker, P.L. (1979) The decapod hepatopancreas. *Oceanography and Marine Biology an Annual Review*, **17**, 285-346.
- Gurr, E. (eds.) (1962) *Stainings Animal Tissues, Practical and Theoretical*, pp. 442. Leonard Hills Books Ltd., London.
- He, L., Long, L.R., Antani, S. & Thoma, G.R. (2012) Histology image analysis for carcinoma detection and grading. *Computer Methods and Programs in Biomedicine*, **107**, 538-556.
- Higgins, C. 2015. Applications and challenges of digital pathology and whole slide imaging. *Biotechnic & Histochemistry*, **90**, 341-347.

Inman, C.F., Rees, L.E., Barker, E., Haverson, K., Stokes, C.R. & Bailey, M. 2005. Validation of computer-assisted, pixel-based analysis of multiple-colour immunofluorescence histology. *Journal of Immunological Methods*, **302**, 156-167.

Johnson, P.T. (1980) *Histology of the blue crab Callinectes sapidus. A model for the Decapoda*, Praeger Publishers, New York.

Johnson, S.K. (1995) *Handbook of Shrimp Diseases*, Texas A&M University, Texas.

Kothari, S., Phan, J.H., Stokes, T.H. & Wang, M.D. (2013) Pathology imaging informatics for quantitative analysis of whole-slide images. *Journal of the American Medical Informatics Association*, **20**, 1099-1108.

Laohabanjong, R., Tantikitti, C., Benjakul, S., Supamattaya, K. & Boonyaratpalin, M. (2009) Lipid oxidation in fish meal stored under different conditions on growth, feed efficiency and hepatopancreatic cells of black tiger shrimp (*Penaeus monodon*). *Aquaculture*, **286**, 283-289.

Lavilla-Pitogo, C.R., Leaño, E.M. & Paner, M.G. (1998) Mortalities of pond-cultured juvenile shrimp, *Penaeus monodon*, associated with dominance of luminescent vibrios in the rearing environment. *Aquaculture*, **164**, 337-349.

Leser, V., Drobne, D., Vilhar, B., Kladnik, A., Znidarsic, N. & Strus, J. (2008) Epithelial thickness and lipid droplets in the hepatopancreas of *Porcellio scaber* (Crustacea: Isopoda) in different physiological conditions. *Zoology*, **111**, 419-432.

Lightner D.V. (2015) Diseases of Crustaceans. In: *Manual of Diagnostic Tests for Aquatic Animals* (ed. by OIE), Section 2.2.0, pp. 1-10. World Organization of Animal Health, Paris.

Longo, M.V. & Diaz, A.O. (2015) Histological and Histochemical Study of the Hepatopancreas of Two Estuarine Crab Species, *Cyrtograpsus angulatus* and *Neohelice granulata* (Grapsoidea, Varunidae): Influence of Environmental Salinity. *Zoological Science*, **32**, 163-170.

Masson, I., Diaz, A. C. & Petriella, A. M. 2012. Effect of salinity changes on the midgut gland of *Artemesia longinaris* (Decapoda, Penaeidae). *Latin American Journal of Aquatic Research*, **40**, 358-366.

Mccann, M.T., Ozolek, J.A., Castro, C.A., Parvin, B. & Kovacevic, J. (2015) Automated histology analysis opportunities for signal processing. *Ieee Signal Processing Magazine*, **32**, 78-87.

McGallery, S.E. (2011) Shellfish diseases (viral, bacterial and fungal). In: *Fish Diseases and Disorders, volume 3*, (ed. by P.T.K. Woo & D.W. Bruno, 2nd edition), pp.809-810. CAB International, Wallingford.

Miedema, J., Marron, J.S., Niethammer, M., Borland, D., Woosley, J., Coposky, J., Wei, S., Reisner, H. & Thomas, N.E. (2012) Image and statistical analysis of melanocytic histology. *Histopathology*, **61**, 436-444.

Mukaka, M.M. 2012. A guide to appropriate use of Correlation coefficient in medical research. *Malawi Medical Journal : The Journal of Medical Association of Malawi*, **24**, 69-71.

Nakamura, K. (1987) Classification of diverticular cells of the midgut gland in the prawn *Penaeus japonicus*. *Memoirs of Faculty of Fisheries Kagoshima University*, **36**, 207-214.

Nativ, N.I., Chen, A.I., Yarmush, G., Henry, S.D., Lefkowitz, J.H., Klein, K.M., Maguire, T.J., Schloss, R., Guarrera, J.V., Berthiaume, F. & Yarmush, M.L. (2014) Automated image analysis method for detecting and quantifying macrovesicular steatosis in hematoxylin and eosin-stained histology images of human livers. *Liver Transplantation*, **20**, 228-236.

Odendaal, J.P. & Reinecke, A.J. (2003) Quantifying histopathological alterations in the hepatopancreas of the woodlouse *Porcellio laevis* (Isopoda) as a biomarker of cadmium exposure. *Ecotoxicology and Environmental Safety*, **56**, 319-325.

Odendaal, J.P. & Reinecke, A.J. (2007) Quantitative assessment of effects of zinc on the histological structure of the hepatopancreas of terrestrial isopods. *Archives of Environmental Contamination and Toxicology*, **53**, 359-364.

Ong, B.L. & Johnston, D. (2006) Influence of feeding on hepatopancreas structure and digestive enzyme activities in *Penaeus monodon*. *Journal of Shellfish Research*, **25**, 113-121.

Pajor, G., Alpar, D., Kajtar, B., Melegh, B., Somogyi, L., Kneif, M., Bollmann, D., Pajor, L. & Sule, N. 2012. Automated signal pattern evaluation of a bladder cancer specific multiprobe-fish assay applying a user-trainable workstation. *Microscopy Research and Technique*, **75**, 814-820.

Sacristán, H.J., Ansaldo, M., Franco-Tadic, L.M., Gimenez, A.V.F. & Greco, L.S.L. 2016. Long-term starvation and posterior feeding effects on biochemical and physiological responses of midgut gland of *Cherax quadricarinatus* juveniles (Parastacidae). *PloS one*, **11**, e0150854.

Sánchez-Paz, A., García-Carreño, F., Hernández-López, J., Muhlia-Almázan, A. & Yepiz-Plascencia, G. 2007. Effect of short-term starvation on hepatopancreas and plasma energy reserves of the Pacific white shrimp (*Litopenaeus vannamei*). *Journal of Experimental Marine Biology and Ecology*, **340**, 184-193.

- Shi, L., Liu, S., Wang, D., Wong, H.-L., Hunag, W.-H., Wang, Y.-X. J., Griffith, J. F., Leung, P.-C. & Ahuja, A. T. 2012. Computerized quantification of bone tissue and marrow in stained microscopic images. *Cytometry Part A*, **81A**, 916-921.
- Sieren, J. C., Weydert, J., Bell, A., De Young, B., Smith, A. R., Thiesse, J., Namati, E. & McLennan, G. 2010. An Automated Segmentation Approach for Highlighting the Histological Complexity of Human Lung Cancer. *Annals of Biomedical Engineering*, **38**, 3581-3591.
- Silva, P.F., McGurk, C., Thompson, K.D., Jayasuriya, N.S. & Bron, J.E. (2015a) Development of a quantitative semi-automated system for intestinal morphology assessment in Atlantic salmon, using image analysis. *Aquaculture*, **442**, 100-111.
- Sousa, L.G., Cuartas, E.I. & Petriella, A.M. (2005) Fine structural analysis of the epithelial cells in the hepatopancreas of *Palaemonetes argentinus* (Crustacea, Decapoda, Caridea) in intermoult. *Biocell*, **29**, 25-31.
- Tam, Q. & Avenant-Oldewage, A. 2009. The effect of starvation on the ultrastructure of the digestive cells of *Dolops ranarum* (Stuhlmann, 1891) (Crustacea: Branchiura). *Arthropod Structure & Development*, **38**, 391-399.
- Thitamadee, S., Prachumwat, A., Srisala, J., Jaroenlak, P., Salachan, P.V., Sritunyalucksana, K., Flegel, T.W. & Itsathitphaisarn, O. (2016) Review of current disease threats for cultivated penaeid shrimp in Asia. *Aquaculture*, **452**, 69-87.
- Van De Braak, C.B.T., Taverne, N., Botterblom, M.H.A., Van Der Knaap, W.P.W. & Rombout, J. (2000) Characterisation of different morphological features of black tiger shrimp (*Penaeus monodon*) haemocytes using monoclonal antibodies. *Fish & Shellfish Immunology*, **10**, 515-530.
- Vasagam, K.P.K., Balasubramanian, T. & Venkatesan, R. (2007) Apparent digestibility of differently processed grain legumes, cow pea and mung bean in black tiger shrimp, *Penaeus monodon* Fabricius and associated histological anomalies in hepatopancreas and midgut. *Animal Feed Science and Technology*, **132**, 250-266.
- Vogt, G., Storch, V., Quintio, E.T. & Pascual, F.P. (1985) Midgut gland as monitor organ for the nutritional value of diets in *Penaeus monodon* (Decapoda). *Aquaculture*, **48**, 1-12.
- Wang, P., Hu, X., Li, Y., Liu, Q. & Zhu, X. 2016. Automatic cell nuclei segmentation and classification of breast cancer histopathology images. *Signal Processing*, **122**, 1-13.
- Webster, J.D. & Dunstan, R.W. 2014. Whole-slide imaging and automated image analysis: considerations and opportunities in the practice of pathology. *Veterinary Pathology*, **51**, 211-223.

Chapter 3

**Effect of starvation and refeeding on the hepatopancreas in
whiteleg shrimp, *Penaeus vannamei* (Boone) using computer assisted image
analysis**

Fabio Cervellione¹, Charles McGurk¹, Tommy Berger Eriksen¹, Wim Van den Broeck²

¹Skretting Aquaculture Research Centre, Stavanger, Norway

²Department of Morphology, Ghent University, Ghent, Belgium

Journal of Fish Disease 2017, DOI:10.1111/jfd.12639

Abstract

Under normal farming conditions, shrimp can experience starvation periods attributable to disease outbreaks or adverse environmental conditions. Starvation leads to significant morphological changes in the hepatopancreas (HP), being the main organ for absorption and storage of nutrients. In literature, limited research has described the effect on the HP of periods of starvation followed by refeeding, and none in whiteleg shrimp (*Penaeus vannamei*) using computer-assisted image analysis (CAIA). The present study describes the effect of starvation and starvation followed by refeeding on the HP of whiteleg shrimp using CAIA. Visiopharm® software was used to quantify the following morphological parameters, measured as ratio to the total tissue area (TTA): total lumen area (TLA:TTA), haemocytic infiltration area in the intertubular spaces (HIA:TTA), B-cell vacuole area (VBA:TTA), lipid droplet area within R-cells (LDA:TTA), and F-cell area (FCA:TTA). Significant changes were measured for HIA:TTA and LDA:TTA during starvation (increase of HIA:TTA associated with decreased of LDA:TTA) and starvation followed by refeeding (decrease of HIA:TTA associated with increase of LDA:TTA). In the future, HIA:TTA and LDA:TTA have the potential to be used in a pre-emptive manner to monitor the health of the HP, facilitate early diagnosis of diseases and study the pathophysiology of the organ.

Key words: hepatopancreas, starvation, computer-assisted image analysis, whiteleg shrimp, *Penaeus vannamei*.

Introduction

Over the last 30 years the production of crustaceans, notably penaeid shrimp, has increased in aquaculture, with an average annual growth of approximately 14% per year since 1989 (Peeler 2012). This rapid growth largely reflects the dramatic increase in the production of the whiteleg shrimp (*Penaeus vannamei*). Due to this rapid intensification of shrimp production, farms have become increasingly affected by pathogenic diseases and stressful environmental challenges (Bondad-Reantaso *et al.* 2012). Farmed shrimp can experience starvation periods during disease outbreaks, adverse environmental conditions, and molting (Lavilla-Pitogo *et al.* 1998; Sacristán *et al.* 2016). The hepatopancreas (HP), being the principal organ for storage of nutrients (mainly lipids) which can be mobilized during non-feeding periods, plays a fundamental role during starvation (Sánchez-Paz *et al.* 2007; Sacristán *et al.* 2016). The HP is a large, bilobed organ that occupies most of the cephalotorax. It flanks the stomach and the anterior midgut, and each lobe is composed of many blind ending tubules (Gibson & Barker 1979). Each hepatopancreatic tubule is composed of four cell types: E-, F-, R- and B-cells (Nakamura 1987; Franceschini-Vicentini *et al.* 2009). The E-cells are undifferentiated cells located at the blind end of the tubules and develop into R-, F-, and B-cells (Brunet, Arnaud & Mazza 1994). The R-cells are the most abundant cell type in the HP and the primary site of uptake and storage of nutrients, resembling the absorptive cells of the vertebrate intestine (Barker and Gibson 1977; Ong & Johnston 2006). F-cells are responsible for the release of digestive enzymes for extracellular digestion, while B-cells are responsible for the intracellular digestion (Brunet *et al.* 1994). Starvation and refeeding affect the HP morphology (Sacristán *et al.* 2016). The main morphological

changes described by pathologists are disorganization of the tubular structure and reduction of the epithelial thickness, loss of the typical star-shaped lumen, reduction of the number of R-, F- and B-cells, reduction of lipid droplets within R-cells and hypertrophy of B-cells (Vogt *et al.* 1985; Nakamura 1987; Ong & Johnston 2006; Leser *et al.* 2008; Berillis, Simon, Mente, Sofos & Karapanagiotidis 2013; Sacristán *et al.* 2016). However, pathologists' quantification is generally time-consuming, mainly subjective and open to operator variations (He *et al.* 2012; Higgins 2015). This has motivated the development of computer assisted image analysis (CAIA) methods for producing unbiased, reproducible, and reliable data (Nativ *et al.* 2014). This methodology requires optimization of histological procedures for preparation of samples. In a previous study, our research group proposed standardized protocols for preparation of paraffin and frozen sections of the HP in whiteleg shrimp and developed three protocols for quantification of morphological parameters of the HP using CAIA (Cervellione *et al.* 2016a and b). To our best knowledge, CAIA has not been used in starvation and refeeding studies in whiteleg shrimp. Therefore the aim of the present study was to describe the effect of starvation on the HP morphology in whiteleg shrimp and whether or not these morphological changes are reversible over time, in controlled experimental conditions. A detailed description of the morphological changes was done using the previously developed CAIA method.

Materials and Methods

Shrimp and rearing conditions

Experiments were conducted in collaboration with IMAQUA, located at the Faculty of Veterinary Medicine (Ghent, Belgium). Specific pathogen-free whiteleg shrimp were imported from Shrimp Improvement Systems (Florida, USA). One hundred and twenty shrimp were housed individually in 50 L glass tanks divided by plastic separators in five compartments (one shrimp per compartment, five shrimp per tank, 8 tanks per treatment, and total of 24 tanks), each supplied with constant aeration and independent biological/mechanical filters. Water temperature was kept at 27 ± 1 °C, with a pH of 7.8 – 8.1 and salinity of 20 ± 1 g L⁻¹. The biological filters and regular water exchanges kept the total ammonium concentrations below 0.5 mg L⁻¹ and the total nitrites below 0.15 mg L⁻¹. The room was illuminated 12 h d⁻¹ by a dimmed luminescent light-tube. Shrimp were acclimatized for 14 d and fed a commercial diet at 5% of the body weight, distributed in 4 times/d.

Experimental design

Experimental design is summarized in Table 1. Shrimp of 2 ± 1 g were divided into three groups (40 shrimp each), receiving three treatments (one treatment per group) for 15 days: FE (fed), ST (starved), and REF (starved for 5 d and then re-fed for 10 d). Shrimp were sampled at day 0, 5, 10, and 15 (six shrimp per treatment and sampling point; three shrimp for paraffin sections, three shrimp for frozen sections) and selected for the C-intermolt stage (Corteel *et al.* 2009) before being transported to the Department of Morphology (Ghent University, Belgium) in aerated buckets. Shrimp were then euthanized as

described by Lightner (2015) for paraffin sections and euthanized in cold ice for frozen sections.

Table 1. Experimental design to study the effect of starvation and refeeding on the hepatopancreas in whiteleg shrimp (*Penaeus vannamei*) using computer assisted image analysis.

Group	Treatment
FE	Fed for 15 days
ST	Starved for 15 days
REF	Starved for 5 days and then refed for 10 d

Note: four sampling points (day 0, 5, 10, 15) and six shrimp per sampling point/group. Feeding regime was 5% of the body weight, distributed in 4 times/d.

Preparation of paraffin and frozen sections

Shrimp were processed for paraffin and frozen sections as described by Cervellione *et al.* (2016a). For paraffin sections, shrimp were individually weighed and fixed with Davidson's solution (30 mL 95% ethanol, 20 mL 37% formaldehyde, 10 mL glacial acetic acid, and 30 mL distilled water). After injection and lateral slitting of the cuticle from the sixth abdominal segment to the base of the rostrum, shrimp were immersed in Davidson's fixative (ratio of fixative to tissue volume of 10:1) for 48 h at 22 °C. The shrimp were then bisected transversally at the junction of the cephalothorax and abdomen, the cephalothorax bisected longitudinally on the mid-line, and both parts placed in tissue processing cassettes. Tissues were dehydrated in a graded series of alcohol baths (70%,

80%, 95%, and 100%) and cleared in xylene, using an automated tissue processor (Microm STP120D, ThermoScientific™). Then, the tissues were embedded in paraffin (melting point 54 – 56 °C, Paraclean Klinipath BV, VWR International®) using manual embedding station (Microm EC350, ThermoScientific™). Five µm thick longitudinal sections were cut with an automated microtome (Microm HM 360, ThermoScientific™), placed on APES (3-Aminopropyltriethoxysilane) coated glass slides, dried for 1 h at 56 °C and kept at 37 °C overnight. For frozen sections, shrimp were bisected transversally at the junction of the cephalothorax and the abdomen, and immediately anterior to the HP. Cephalothorax was frozen by immersion for 20 s in liquid nitrogen and storing in dry air. After freezing, all samples were kept at -80 °C. Samples were embedded in water-soluble media (Tissue-Tek® OCT, VWR International®) and 16 µm thick longitudinal sections cut, by use of an automated cryostat (Microm HM505E, ThermoScientific™) at -25 °C and placed on glass slides (HistoBond®+, Marienfeld). Then frozen sections were fixed for 10 s in 60% isopropanol at 22 °C. For each group and each sampling point, three stainings were used: immuno-histochemistry, modified toluidine blue staining (both on paraffin sections), and Oil red O staining (on frozen sections) (Table 2). Detection of haemocytes in the intertubular spaces was based on immunohistochemistry (IHC). WSH8 monoclonal antibodies (Mabs) were produced by the Wageningen Institute of Animal Science (Wageningen University, The Netherlands) using membrane lysates of tiger shrimp (*Penaeus monodon*, Fabricus 1798) haemocytes as immunogen (Van de Braak *et al.* 2000). Sections (one section per shrimp) were processed as described by Cervellione *et al.* (2016a). After deparaffination in xylene and rehydration in ethanol series, paraffin sections were subjected to heat-induced epitope retrieval using citrate solution in

microwave for 150 s at 750 W followed by 10 min at 160 W and stored for 30 min at 4 °C. Then sections were incubated for 5 min at 22 °C with Dako REAL™ Peroxidase-Blocking Solution followed by incubation with 30% rabbit serum blocking solution for 30 min at 22 °C. After incubation of the slides for 1h at 22 °C with the Mabs dilution (100x), peroxidase-conjugated reaction was carried out using Dako REAL™ EnVision™ Labelled Polymer HRP anti-mouse for 30 min at 22 °C, followed by DAB chromogen solution for 5 min at 22 °C. Sections were then counterstained with Mayer's haematoxylin for 5 min and mounted in non-aqueous medium (DPX, Sigma-Aldrich®). Mayer's haematoxylin was used on the same section for counterstaining IHC and identification of B-cell vacuoles.

Table 2. Stainings used for computer assisted image analysis of the hepatopancreas in whiteleg shrimp (*Penaeus vannamei*).

Staining	APP
IHC with Mabs WSH8 counterstained with Mayer's haematoxylin	HIVB (Haemocyte Infiltration and Vacuole of B-cells)
modified Toluidine Blue protocol	F (F-cells)
Oil Red O	LD (Lipid Droplets within R-cells)

Note: For each shrimp, four regions of interest (ROIs, 198611 μm^2 each) of the hepatopancreas were analyzed. APP = protocol for computer assisted image analysis; IHC = immunohistochemistry; Mabs = monoclonal antibodies.

For the identification of F-cells, paraffin sections (one section per shrimp) were stained for 3 min in Toluidine Blue followed by 1 min in ThermoScientific™ Carifier 1 through an automated slide-stainer (Gemini AS, ThermoScientific™) and mounted in non-aqueous medium (DPX, Sigma-Aldrich®). Detection of lipid droplets within the R-cells was based on Oil Red O staining. Therefore, frozen sections (one section per shrimp) were stained with Lillie and Ashburn's isopropanol Oil Red O staining (ORO) (Culling 1974) using an

automated slide-stainer (Gemini AS, ThermoScientific™) and mounted in aqueous media (Aquatex®, VWR International®). All sections were label-coded and one experienced examiner observed slides under light microscope to evaluate the suitability of the sections for image analysis (BX53, Olympus®).

Digital image acquisition

Slides were scanned using an automated slide-scanner (Leica SCN400, Leica Microsystems®, Germany) producing digitized images (scn file format) in 20x magnification.

Image processing

The software Visiopharm (version VIS 6.5.0.2303 with Author™ module, Visiopharm®, Denmark) was used for image analysis. In each hepatopancreas, four representative regions of interest (ROIs; 198611 μm^2 each) were randomly selected for image processing. An example of a representative ROI is shown in Figure 2. ROI was selected avoiding the borders of the HP (where distal ends of the tubules are present) and selecting the medial part of the cross section of the tubule.

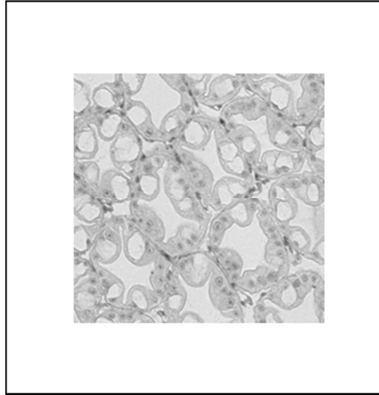


Figure 2. Region of interest (ROI) selected as representative area a cross section of the hepatopancreas (HP) of whiteleg shrimp (*Penaeus vannamei*) for the development of computer assisted image analysis protocol (APP).

Image analysis workflow and protocols (APPs) were used as described by Cervellione *et al.* (2016b). Three APPs (HIVB, LD, and F) were used to quantify total lumen area (TLA), haemocytic infiltration (HIA), B-cell vacuoles (VBA), lipid droplets within R-cells (LDA), and F-cells (FCA), and their ratios to total tissue area (TTA). Before data extraction, one experienced observer assessed the result of the post-processing using the transparency tool bar and applied manual corrections when needed. Description of morphometric parameters is summarized in Table 3.

Statistical analysis

Data extracted were tested and treated as parametric data and analyzed using GraphPad Prism® version 6 (GraphPad Software Inc., USA). One-way ANOVA was applied for testing equality of means among treatments. Dunnett's multi comparison test with mean ranks ($p = 0.05$) was used to compare sampling points within the treatment.

Table 3. Morphometric parameters used for measuring the effect of starvation and refeeding on the hepatopancreas of whiteleg shrimp (*Penaeus vannamei*) using computer assisted image analysis.

Morphometric parameter	Description
Total Tissue Area	Total area covered by tubular epithelium, composed by B-cells, F-cells and R-cells
Total Lumen Area (TLA)	Total area covered by lumen
TLA:TTA	Ratio of Total Lumen Area to Total Tissue Area, as measure of the variation of the tubular lumen, expressed as %
Haemocyte Infiltration Area (HIA)	Area of the haemocytes infiltrating the intertubular spaces of the HP
Morphometric parameter	Description
HIA:TTA	Ratio of Haemocyte Infiltration Area to Total Tissue A, as measure of the HP response to noxa, expressed as %
Vacuoles of B-cells Area (VBA)	Area of the tubule composed by vacuoles of B-cells
VBA:TTA	Ratio of Vacuoles of B-cells Area to Total Tissue Area, as measure of intra-cellular digestion of the HP, expressed as %
F-Cells Area (FCA)	Area of the tubule composed by F-cells
FCA:TTA	Ratio of F-Cells Area to Total Tissue Area, as measure of the enzymatic activity of the HP, expressed as %
Lipid Droplets Area (LDA)	Area of the tubule composed by lipid droplets within R-cells
LDA:TTA	Ratio of Lipid Droplets Area to Total Tissue Area, as measure of the lipid reserves in the HP, expressed as %

Note: HP = hepatopancreas. For each shrimp, four regions of interest (ROIs, 198611 μm^2 each) were analyzed.

Results

Morphometric parameters extracted were TLA:TTA (Fig. 2), HIA:TTA (Fig. 3), LDA:TTA (Fig. 4), VBA:TTA (Fig. 5) and FCA:TTA (Fig. 6).

For the fed group, variation of the TLA:TTA was not statistically significant. However, a slight increase was observed over time (from 33% to 45%). HIA:TTA and LDA:TTA did not vary significantly over time (HIA:TTA avg 0.1%; LDA:TTA avg 42.9%). Variation of the VBA:TTA and FCA:TTA was not statistically significant. However, for VBA:TTA a slight increase followed by decrease was observed (from 11.2% to 19.9% and down to 7.8%), while FCA:TTA slightly increased over time (from 9.7% to 14.1%).

For the starved group, variation of the TLA:TTA was not statistically significant. However, a slight decrease was observed over time (from 46% to 36%). HIA:TTA and LDA:TTA varied significantly during starvation, with an increase of HIA:TTA (from 0.1% to 1.4%), and a decrease of LDA:TTA (from 42.8% to 0%). VBA:TTA and FCA:TTA did not vary significantly over time. However, both parameters slightly decreased over time (VBA:TTA from 13.3% to 6.1%; FCA:TTA from 11.3% to 5.5%).

For the refeed group, variation of the TLA:TTA was not statistically significant. However, a slight increase was observed over time (from 44% to 61%). HIA:TTA and LDA:TTA varied significantly during refeeding, with a decrease of HIA:TTA (from 0.58% to 0.3%) and an increase of LDA:TTA (from 0% to 35.8%). VBA:TTA slightly decreased (from 14.2% to 9.6%) but non significantly. FCA:TTA decreased significantly after 5 days of refeeding (from 11.3% to 3.1%).

The application of CAIA on light microscopic images of the HP is shown in Fig. 7 (haemocytic infiltration) and Fig. 8 (lipid droplets). After 15 d of starvation it was possible to observe an increase in the number of haemocytes infiltrating the intertubular spaces associated with the complete depletion of lipid droplets within R-cells. Refeeding contributed instead to a reduction of the haemocytic infiltration associated with an increase of lipid droplets.

No mortality was observed during the experiment. In the starved group, a progressive reduction of the muscular texture was observed overtime during manipulation.

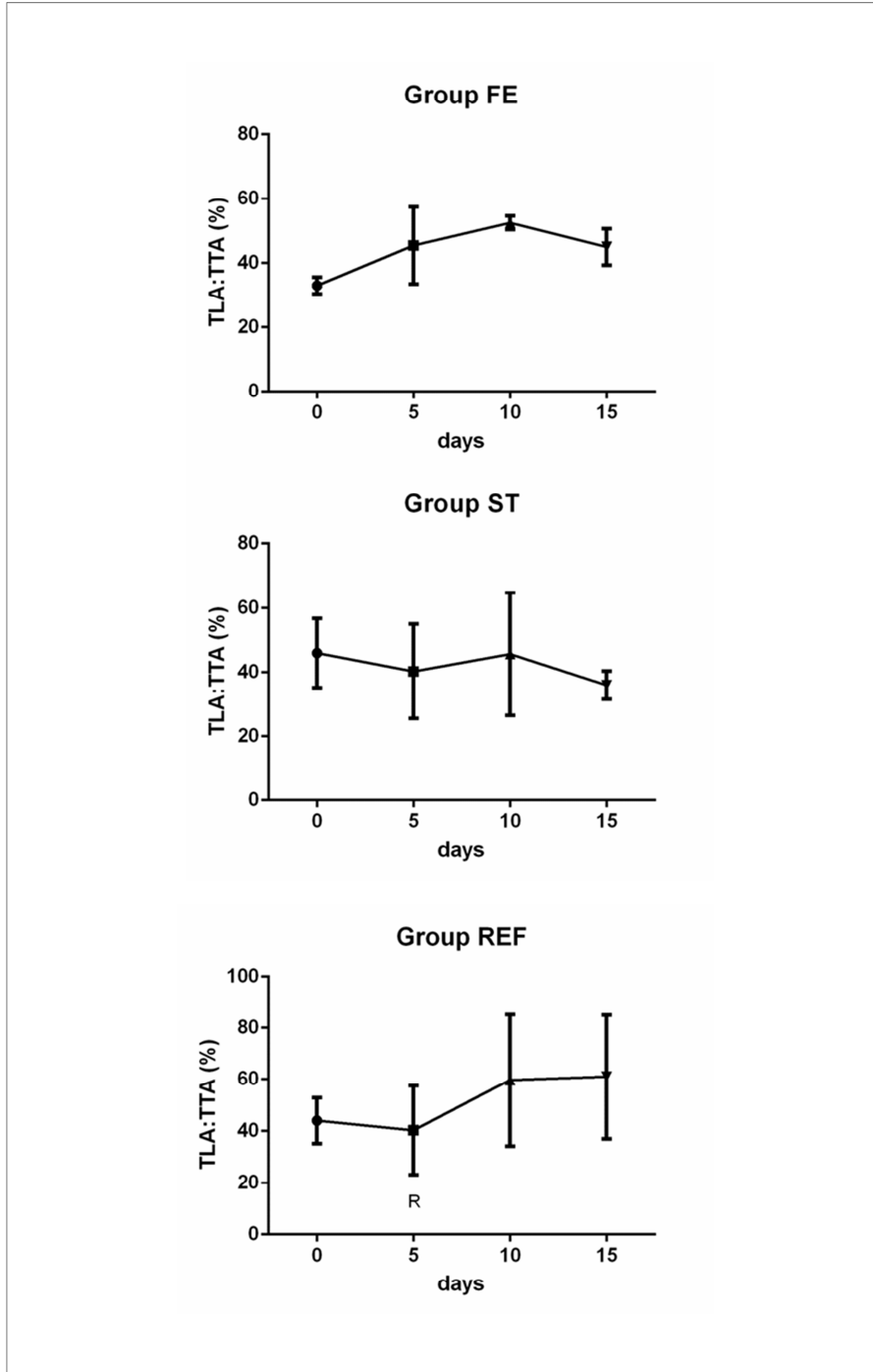


Fig 2. Effect of starvation and refeeding on the lumen area of the tubules of the hepatopancreas in whiteleg shrimp (*Penaeus vannamei*). Note: TL:TTA = ratio of Total Lumen Area to Total tissue Area (as %). FE = fed; ST = starved; REF = refed; R = start of refeeding after 5 days of starvation. Error bars indicate the standard deviation of the mean. Sample size for each point is n=5.

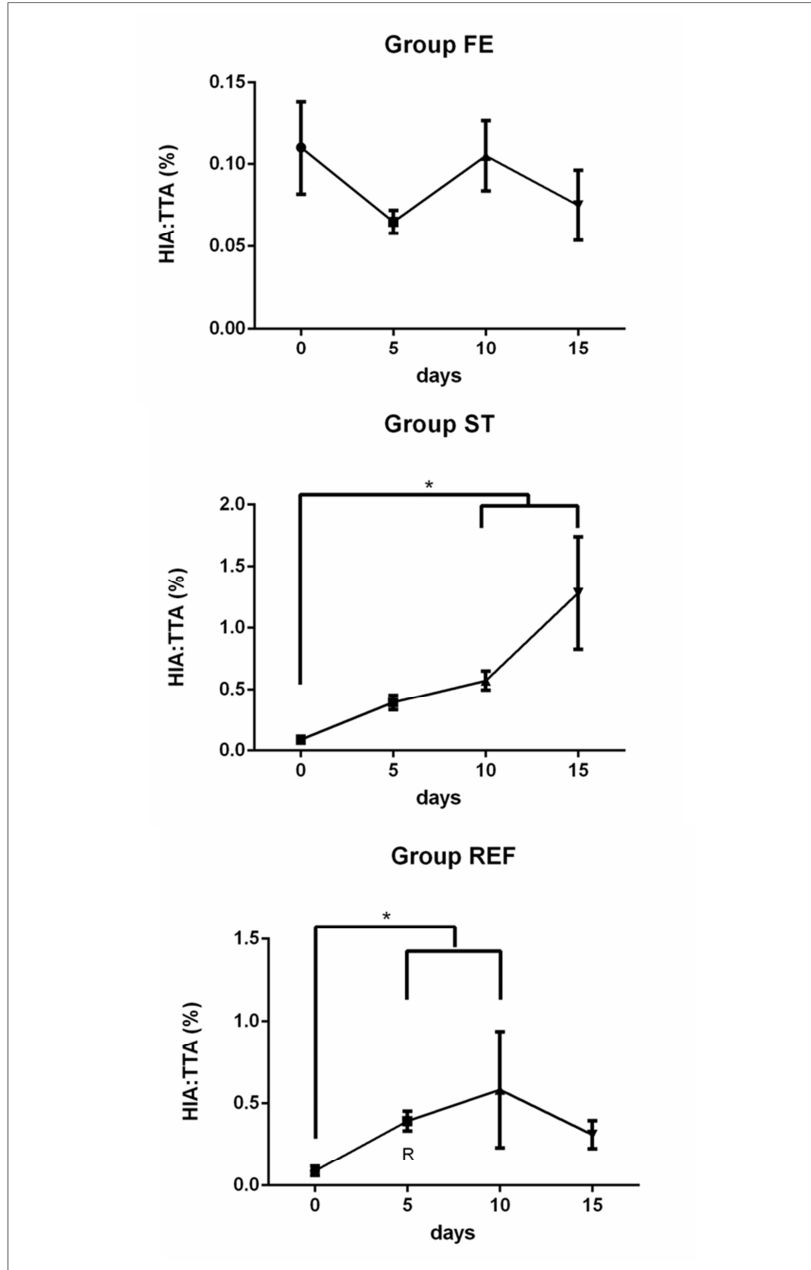


Fig 3. Effect of starvation and refeeding on the haemocytic infiltration in the intertubular spaces of the hepatopancreas in whiteleg shrimp (*Penaeus vannamei*). Note: HIA:TTA = ratio of Haemocytic Infiltration Area to Total Tissue Area (as %). FE = fed; ST = starved; REF = refed; R = start of refeeding after 5 days of starvation. One-way ANOVA with 95% confidence interval and multicomparison (* = $p < 0.05$). Error bars indicate the standard deviation of the mean. Sample size for each point is $n=5$.

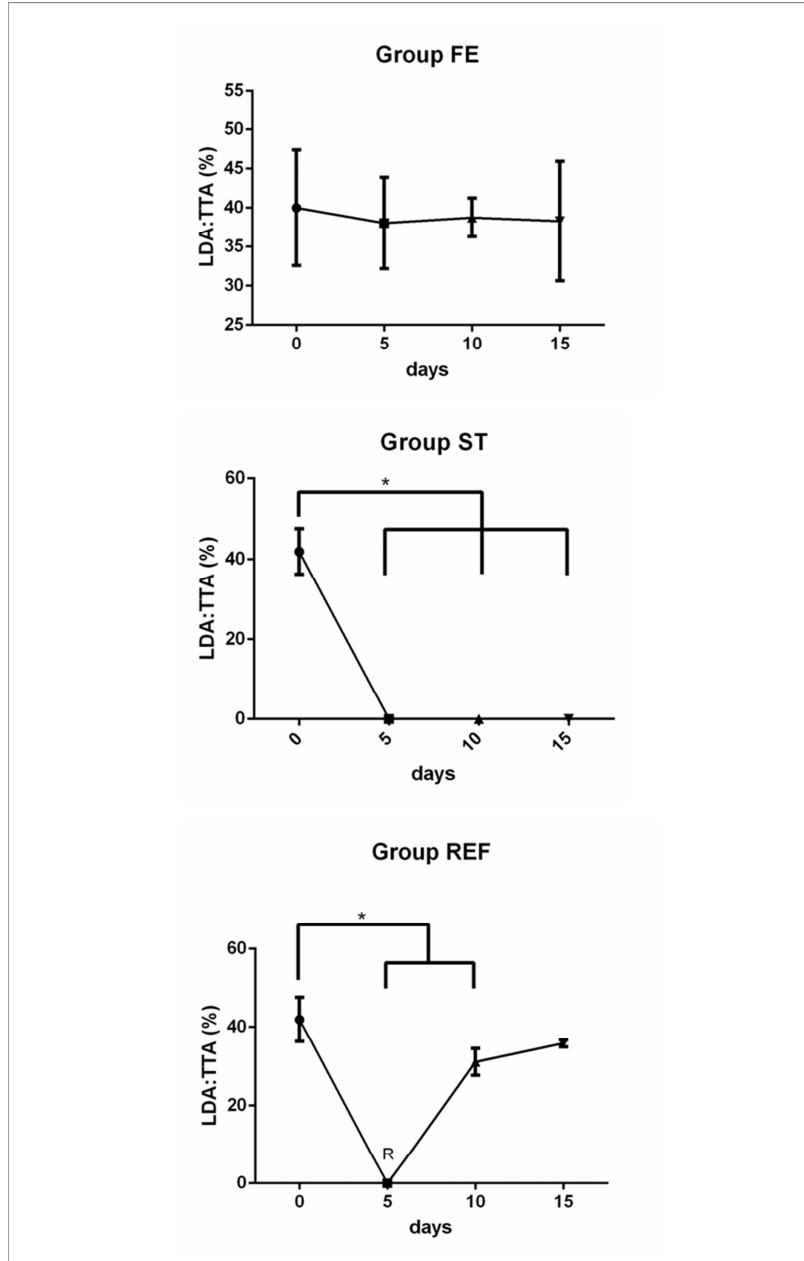


Fig 4. Effect of starvation and refeeding on the lipid droplets of the hepatopancreas in whiteleg shrimp (*Penaeus vannamei*). Note: LDA:TTA = ratio of Lipid Droplet Area to Total Tissue Area (as %). FE = fed; ST = starved; REF = refed; R = start of refeeding after 5 days of starvation. One-way ANOVA with 95% confidence interval and multicomparison ($* = p < 0.05$). Error bars indicate the standard deviation of the mean. Sample size for each point is $n=5$.

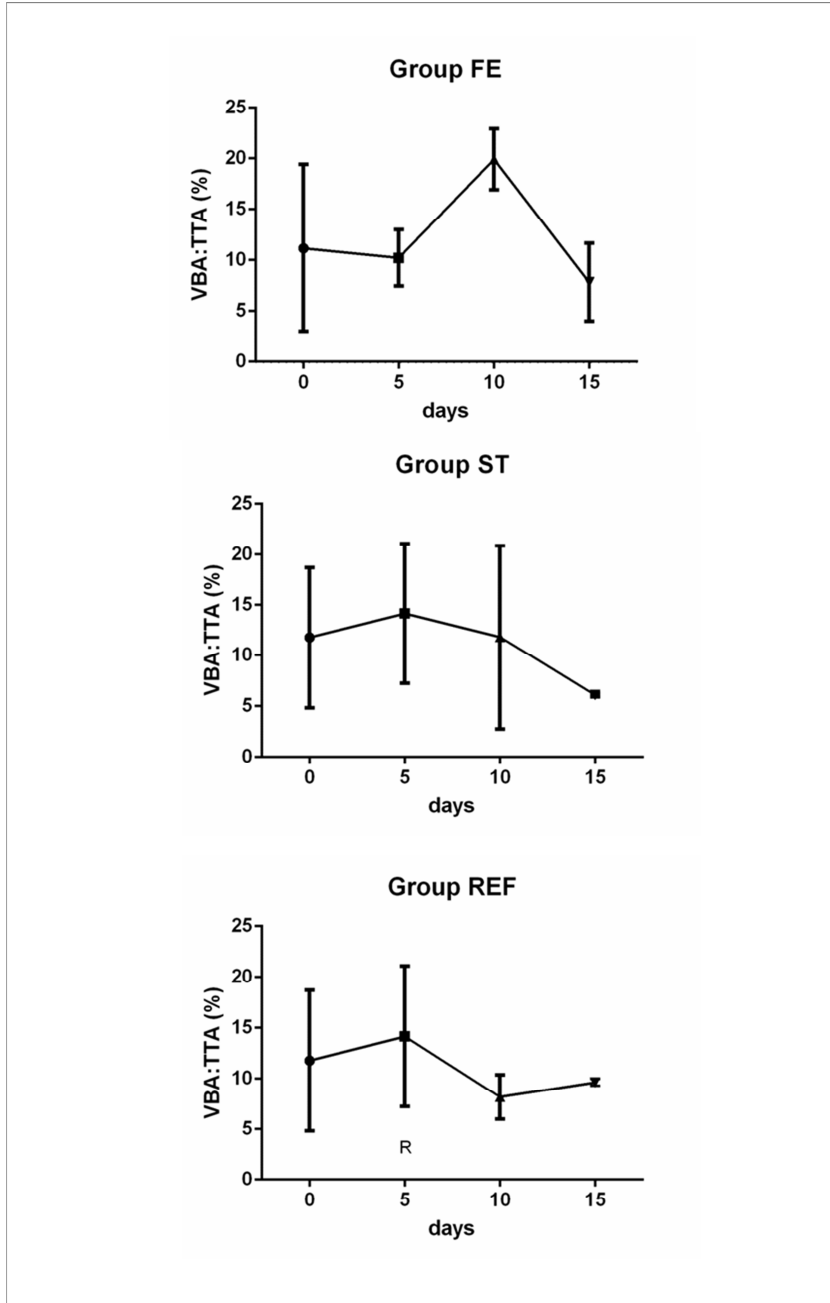


Fig 5. Effect of starvation and refeeding on B-cell vacuoles of the hepatopancreas in whiteleg shrimp (*Penaeus vannamei*). Note: VBA:TTA = ratio of Vacuole of B-cells Area to Total tissue Area (as %). FE = fed; ST = starved; REF = refed; R = start of refeeding after 5 days of starvation. Error bars indicate the standard deviation of the mean. Sample size for each point is n=5.

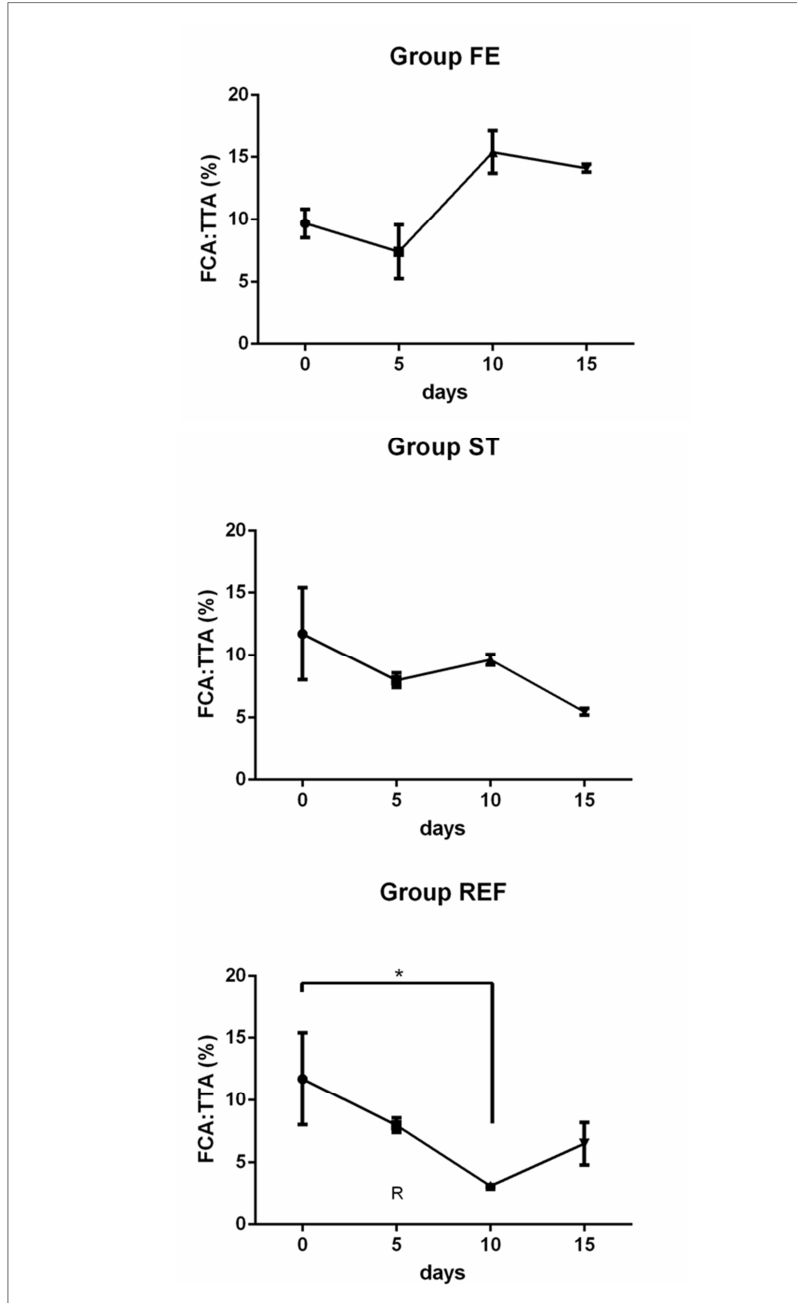


Fig 6. Effect of starvation and refeeding on F-cells of the hepatopancreas in whiteleg shrimp (*Penaeus vannamei*). Note: LDA:FCA = ratio of F-Cell Area to Total tissue Area (as %). Group FE = fed group; Group ST = starved; Group REF = refed; R = start of refeeding after 5 days of starvation. One-way ANOVA with 95% confidence interval and multicomparison (* = $p < 0.05$). Error bars indicate the standard deviation of the mean. Sample size for each point is $n=5$.

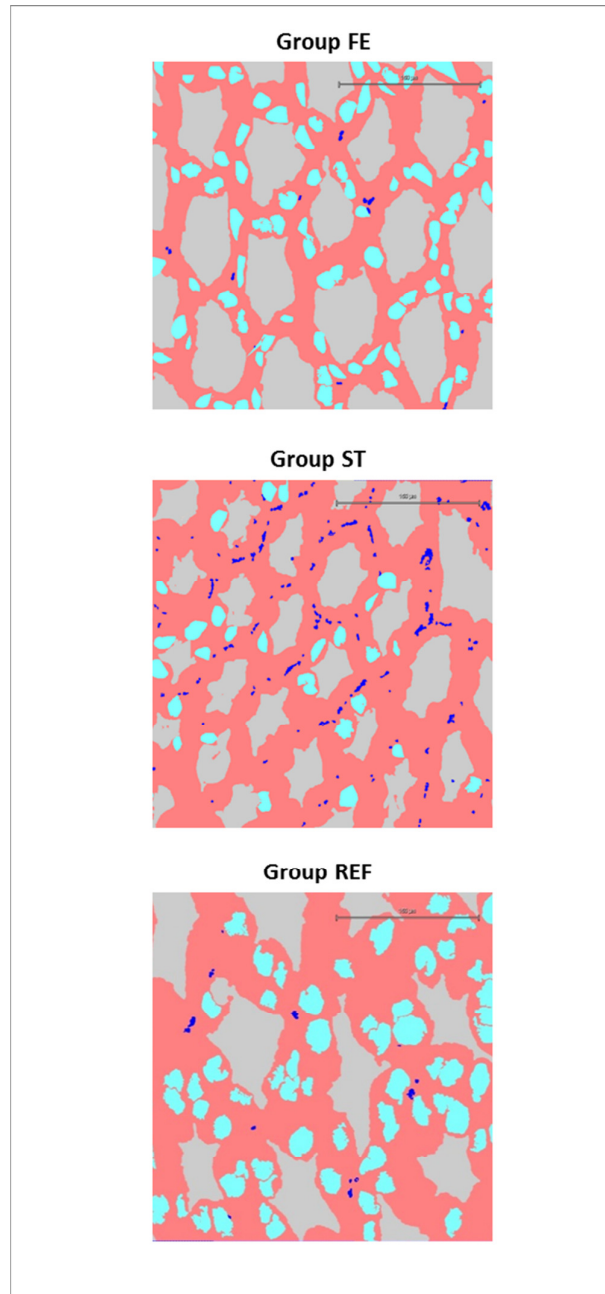


Fig 7. Effect of feeding, starvation and refeeding on the haemocytic infiltration in the intertubular spaces of the hepatopancreas in whiteleg shrimp (*Penaeus vannamei*) using computer assisted image analysis. FE, fed for 15 days; ST, starved for 15 days; REF, starved for 5 days and re-fed for 10 days. Total Tissue Area (pink), Total Lumen Area (grey), B-cell Vacuoles Area (light blue), Haemocytic Infiltration Area (blue). Scale bar = 150 μ m.

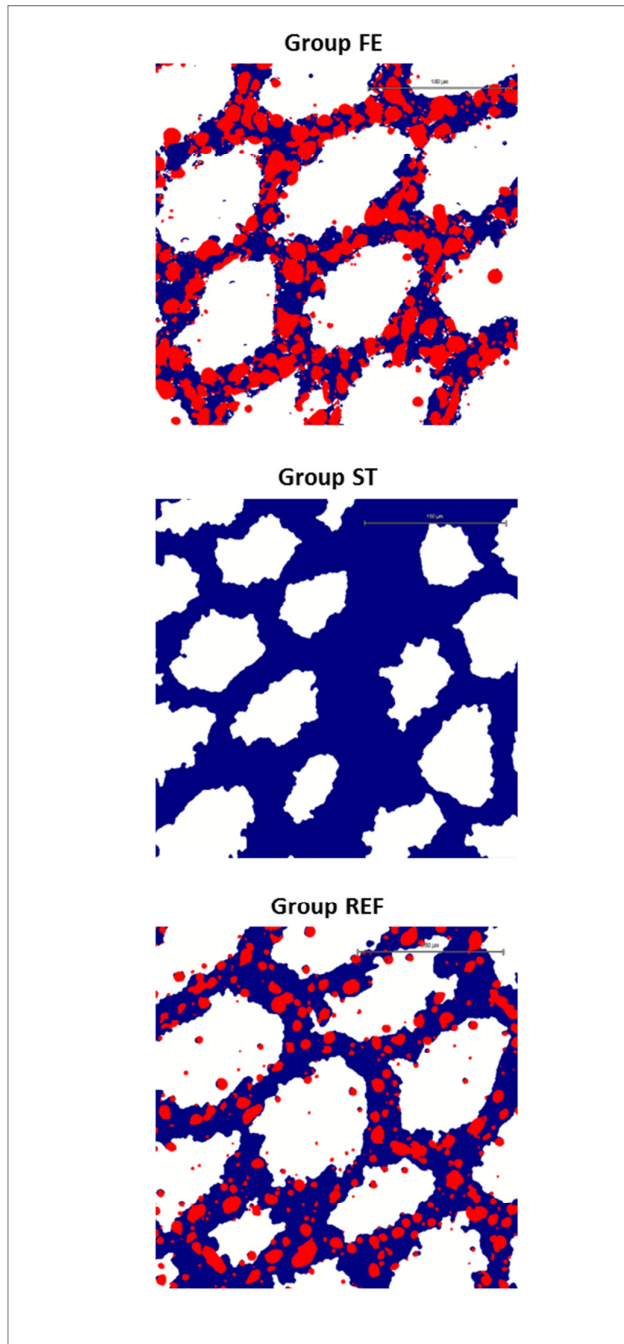


Fig 8. Effect of feeding, starvation and refeeding on the lipid droplets of the hepatopancreas in whiteleg shrimp (*Penaeus vannamei*) using computer assisted image analysis. FE, fed for 15 days; ST, starved for 15 days; REF, starved for 5 days and re-fed for 10 days. Total tissue area (blue), Total Lumen Area (white), Lipid Droplets Area (red). Scale bar = 150 μ m.

Discussion

Moulting and development stage are influenced by starvation. Five days of starvation corresponds to the approximate time that juvenile shrimp starve during the moulting cycle: shrimp feed actively during C-intermoult stage and stop eating during stage E (ecdysis) and stage A-B (post-moult) (Nakamura 1987; Sanchez-Paz *et al.* 2006). During starvation, lipid droplets stored within R-cells are used as initial energy source, while for longer periods protein is used as main energy source (Nakamura 1987). In the present study, although not statistically significant TLA:TTA slightly increase during feeding and refeeding while slightly decreased during starvation. A systematic interpretable change was not observed by our research group: future studies should repeat the same experimental design to better understand which effect starvation and refeeding has on the lumen area of the tubules. Nakamura (1987) described with subjective appraisal an increase of the lumen area in adults of kuruma shrimp (*Penaeus japonicus*) after 30 d of starvation. Future studies should verify if longer starvation periods can affect TLA and TTA in whiteleg shrimp.

In the decapod HP, haemocytic infiltration has been reported as initial response of the immune system to tissue damage (traumatic or due to infection), starvation, toxicity and environmental stress (Johnson 1980; McGallery 2011; Chiodi Boudet *et al.* 2015; Longo & Diaz 2015). Tissue damage stimulates the degranulation of granular and semigranular haemocytes. The release of the prophenoloxidase system and other plasma factors from the stored granules promotes phagocytosis by hyaline cells or encapsulation by semigranular cells (Johansson *et al.* 2000).

In the present study, starvation induced the activation of the inflammatory pathway, stimulating the migration of haemocytes to the intertubular spaces of the HP. Refeeding had a progressive reduction of the haemocytic infiltration leading to the partial recovery of the organ within 10 d. HIA:TTA has the potential to be used in the future in a very early state to monitor the health of the HP, facilitate early diagnosis of diseases and study the pathophysiology of the organ. Future studies should also investigate if the HP has the potential to recover completely after more prolonged refeeding periods and if recovery is possible after more prolonged starvation periods.

VBA:TTA and FCA:TTA did not vary significantly during the starvation and refeeding periods, with the exception of FCA:TTA in the Refed group. From previous studies, it is not clear what the impact of starvation on the B- and F-cells is (Ong & Johnston 2006; Calvo *et al.* 2011; Berillis *et al.* 2013; Sacristán *et al.* 2016). In the present study, our research group did not see a systematic interpretable change for VBA:TTA and FCA:TTA. It is important to notice that B- and F-cell distribution is not uniform in the tubule. B-cells are mainly located in proximal zone of the tubule, while F-cells are located in the proximal and medial zones of the tubule (Sousa *et al.* 2015). Consequently, the variability of the plane of section could have partially influenced the results. Furthermore, longer period of starvation could be necessary to modify the B- and F-cell population in whiteleg shrimp, but this should be linked to cell turnover as well. However, information about cell turnover of B- and F-cells is scarce in the available literature (Vogt 2008; Gherardi *et al.* 2010). Physiological cell turnover plays a crucial role in maintaining normal tissue function and architecture and it can be up- or down-regulated by external factors (Medh & Thompson

2000). Future studies should investigate if starvation and refeeding can modulate the physiological cell turnover of the different cell type composing the HP.

The importance of the HP for lipid storage was first described in 1893 and depletion of lipid droplets during starvation and their recovery during refeeding has been observed using subjective appraisal (Cuénot 1893; Barker & Gibson 1977; Vogt *et al.* 1985; Sacristán *et al.* 2016). In the present study, data show that juvenile shrimp deplete lipid droplets within 5 d of starvation at 27 ± 1 °C and salinity of 20 ± 1 g L⁻¹. LDA:TTA is a very clear indicator of starvation: CAIA method has already been validated and has the potential to be utilized as measure of starvation and to understand the dynamics of starvation. Future studies are required to quantify the LDA depletion profile over time at different temperatures, salinities, shrimp size and molting stage. After the complete depletion of lipid droplets, shrimp start to utilize proteins as energy source (Nakamura 1987). In the present study, “soft” muscular texture was observed in the Starved group during manipulation. This softness increased progressively over time and it could be attributed to the utilization of the muscular protein as energy source.

To our best knowledge, the present study describes for the first time the effect of starvation and refeeding on the HP in whiteleg shrimp using CAIA. For the first time, F-cells, B-cells, lipid droplets and haemocytic infiltration are calculated objectively as % of the TTA. CAIA has the potential to be use in the future to evaluate the effect of diets and feeding regimes on the HP, and to study the HP affected by diseases, facilitating the anticipation of diagnosis.

References

- Barker, P.L. & Gibson, R. (1977) Observation on feeding mechanism, structure of gut, and digestive physiology of european lobster *Homarus gammarus* (L) (Decapoda-Nephropidae). *Journal of Experimental Marine Biology and Ecology*, **26**, 297-324.
- Berillis, P., Simon, C., Mente, E., Sofos, F. & Karapanagiotidis, I.T. (2013) A novel image processing method to determine the nutritional condition of lobsters. *Micron*, **45**, 140-144.
- Bondad-Reantaso, M.G., Subasinghe, R.P., Josupeit, H., Cai, J.N. & Zhou, X.W. (2012) The role of crustacean fisheries and aquaculture in global food security: Past, present and future. *Journal of Invertebrate Pathology*, **110**, 158-165.
- Brunet, M., Arnaud, J. & Mazza, J. (1994) Gut structure and digestive cellular processes in marine crustacea. *Oceanography and Marine Biology: An Annual Review*, **32**, 335-367.
- Calvo, N.S., Stumpf, L., Pietrokovsky, S. & Greco, L.S.L. (2011) Early and late effects of feed restriction on survival, growth and hepatopancreas structure in juveniles of the red claw crayfish *Cherax quadricarinatus*. *Aquaculture*, **319**, 355-362.
- Cervellione, F., McGurk, C., Berger Eriksen, T. & Van den Broeck, W. (2016b) Use of computer-assisted image analysis for semi-quantitative histology of the hepatopancreas in whiteleg shrimp, *Penaeus vannamei* (Boone). *Journal of Fish Diseases*, doi 10.1111/jfd.12599.
- Cervellione, F., McGurk, C., Silva, P., Owen, M.A.G. & Van den Broeck, W. (2016a) Optimization of fixation methods for image analysis of the hepatopancreas in whiteleg shrimp, *Penaeus vannamei* (Boone). *Journal of Fish Diseases*, doi 10.1111/jfd.12531.
- Chiodi Boudet, L.N., Polizzi, P., Romero, M.B., Robles, A., Marcovecchio, J.E. & Gerpe, M.S. (2015) Histopathological and biochemical evidence of hepatopancreatic toxicity caused by cadmium in white shrimp, *Palaemonetes argentinus*. *Ecotoxicology and Environmental Safety*, **113**, 231-240.
- Corteel M., Dantas-Lima J.J., Wille M., Alday-Sanz V., Pensaert M.B., Sorgeloos P. & Nauwynck H.J. (2009) Molt stage and cuticle damage influence white spot syndrome virus immersion infection in penaeid shrimp. *Veterinary Microbiology* **137**, 209-216.
- Cuénot, L. (1893) Études physiologiques sur les crustacés décapodes. *Archives de Biologie*, **13**, 245-303.
- Culling C.F.A. (1974) Identification of Lipids. In: *Handbook of Histopathological and Histochemical Techniques*, pp. 360-361. Butterworths & Co. Ltd, London.
- Franceschini-Vicentini, I.B., Ribeiro, K., Papa, L.P., Marques, J., Vicentini, C.A. & Valenti, P. (2009) Histoarchitectural Features of the Hepatopancreas of the Amazon River Prawn *Macrobrachium amazonicum*. *International Journal of Morphology*, **27**, 121-128.

- Gherardi, F., Souty-Grosset, C., Vogt, G., Diéguez-Uribeondo, J. & Crandall, K.A. (2010). Infraorder Astacidea Latreille, 1802 P.P.: the freshwater crayfish. In: *The Crustacea, volume 9A (67)* (ed. by F.R. Schram & J.C. con Vaupel Klein), pp. 269-423. Brill, Boston.
- Gibson, R. & Barker, P.L. (1979) The decapod hepatopancreas. *Oceanography and Marine Biology an Annual Review*, **17**, 285-346.
- He, L., Long, L.R., Antani, S. & Thoma, G.R. (2012) Histology image analysis for carcinoma detection and grading. *Computer Methods and Programs in Biomedicine*, **107**, 538-556.
- Higgins, C. 2015. Applications and challenges of digital pathology and whole slide imaging. *Biotechnic & Histochemistry*, **90**, 341-347.
- Johnson, P.T. (1980) Histology of the blue crab *Callinectes sapidus*. *A model for the Decapoda*, Praeger Publishers, New York.
- Lavilla-Pitogo, C.R., Leaño, E.M. & Paner, M.G. (1998) Mortalities of pond-cultured juvenile shrimp, *Penaeus monodon*, associated with dominance of luminescent vibrios in the rearing environment. *Aquaculture*, **164**, 337-349.
- Leser, V., Drobne, D., Vilhar, B., Kladnik, A., Znidarsic, N. & Strus, J. (2008) Epithelial thickness and lipid droplets in the hepatopancreas of *Porcellio scaber* (Crustacea: Isopoda) in different physiological conditions. *Zoology*, **111**, 419-432.
- Lightner D.V. (2015) Diseases of Crustaceans. In: *Manual of Diagnostic Tests for Aquatic Animals* (ed. by OIE), Section 2.2.0, pp. 1-10. World Organization of Animal Health, Paris.
- Longo, M.V. & Diaz, A.O. (2015) Histological and Histochemical Study of the Hepatopancreas of Two Estuarine Crab Species, *Cyrtograpsus angulatus* and *Neohelice granulata* (Grapsoidea, Varunidae): Influence of Environmental Salinity. *Zoological Science*, **32**, 163-170.
- Medh, R.D. & Thompson, E.B. (2000) Hormonal regulation of physiological cell turnover and apoptosis. *Cell and Tissue Research*, **301**, 101-124.
- Nakamura, K. (1987) Classification of diverticular cells of the midgut gland in the prawn *Penaeus japonicus*. *Memoirs of Faculty of Fisheries Kagoshima University*, **36**, 207-214.
- Nativ, N.I., Chen, A.I., Yarmush, G., Henry, S.D., Lefkowitz, J.H., Klein, K.M., Maguire, T.J., Schloss, R., Guarrera, J.V., Berthiaume, F. & Yarmush, M.L. (2014) Automated image analysis method for detecting and quantifying macrovesicular steatosis in hematoxylin and eosin-stained histology images of human livers. *Liver Transplantation*, **20**, 228-236.

Ong, B.L. & Johnston, D. (2006) Influence of feeding on hepatopancreas structure and digestive enzyme activities in *Penaeus monodon*. *Journal of Shellfish Research*, **25**, 113-121.

Peeler, E.J. (2012) Costs and benefits of freedom from shrimp diseases in the European Union. *Journal of Invertebrate Pathology*, **110**, 188-195.

Sacristán, H.J., Ansaldo, M., Franco-Tadic, L.M., Gimenez, A.V.F. & Greco, L.S.L. (2016) Long-Term Starvation and Posterior Feeding Effects on Biochemical and Physiological Responses of Midgut Gland of *Cherax quadricarinatus* Juveniles (Parastacidae). *PloS one*, **11**, e0150854.

Sanchez-Paz, A., Garcia-Carreño, F., Muhlia-Almazan, A., Peregrino-Uriarte, A.B., Hernandez-Lopez, J. & Yepiz-Plascencia, G. (2006) Usage of energy reserves in crustaceans during starvation: Status and future directions. *Insect Biochemistry and Molecular Biology*, **36**, 241-249.

Sánchez-Paz, A., García-Carreño, F., Hernández-López, J., Muhlia-Almazán, A. & Yepiz-Plascencia, G. (2007) Effect of short-term starvation on hepatopancreas and plasma energy reserves of the Pacific white shrimp (*Litopenaeus vannamei*). *Journal of Experimental Marine Biology and Ecology*, **340**, 184-193.

Sousa, L.G., Cuartas, E.I. & Petriella, A.M. (2005) Fine structural analysis of the epithelial cells in the hepatopancreas of *Palaemonetes argentinus* (Crustacea, Decapoda, Caridea) in intermoult. *Biocell*, **29**, 25-31.

Van De Braak, C.B.T., Taverne, N., Botterblom, M.H.A., Van Der Knaap, W.P.W. & Rombout, J. (2000) Characterisation of different morphological features of black tiger shrimp (*Penaeus monodon*) haemocytes using monoclonal antibodies. *Fish & Shellfish Immunology*, **10**, 515-530.

Vogt, G., Storch, V., Quintio, E.T. & Pascual, F.P. (1985) Midgut gland as monitor organ for the nutritional value of diets in *Penaeus monodon* (Decapoda). *Aquaculture*, **48**, 1-12.

Vogt, G. (2008) How to minimize formation and growth of tumors: potential benefits of decapod crustaceans for cancer research. *International Journal of Cancer*, **123**, 2727-2734.

Chapter 4

Effect of starvation and refeeding computer on the ultrastructure of the hepatopancreas in whiteleg shrimp, *Penaeus vannamei* (Boone) using transmission electron microscopy

Fabio Cervellione¹, Charles McGurk¹, Wim Van den Broeck²

¹Skretting Aquaculture Research Centre, Stavanger, Norway

²Department of Morphology, Ghent University, Ghent, Belgium

Submitted to Journal of Crustacean Biology

Abstract

Shrimp can experience starvation periods attributable to disease outbreaks or adverse environmental conditions in modern farming. The hepatopancreas (HP), being the principal organ for storage of nutrients which can be mobilized during non-feeding periods, plays a fundamental role during starvation. Limited research has described the effect of periods of starvation followed by refeeding on the ultrastructure of the HP, and none of them in whiteleg shrimp (*Penaeus vannamei*). Therefore, the present study describes the ultrastructural changes in the HP of whiteleg shrimp occurring during starvation and refeeding. Starvation induced a progressive increase of cellular immunity (haemocytic infiltration, both hyaline and granular/semigranular haemocytes), signs of potential necrosis (swelling of organelles and cytolysis), and autophagy (formation of phagophores, autophagosomes, multivesicular and residual bodies). The complete depletion of lipid droplets and a few signs of apoptosis (chromatin condensation and nuclear fragmentation) were also observed during starvation. Refeeding did not result in a complete recovery the HP. The present findings indicate the capacity of the HP to recover when refed for 10 days after 5 days of starvation. Longer starvation periods severely affect the HP, causing potential economic losses to the famers.

Keywords: hepatopancreas, whiteleg shrimp, starvation, ultrastructure.

Introduction

In crustaceans, the primary role of the HP is the synthesis and secretion of digestive enzymes, digestion and uptake of nutrients, and detoxification (Laohabanjong *et al.* 2009). The HP is composed of many blindly ending tubules, and each tubule can be subdivided into a distal, medial and proximal zone relative to the distance from the midgut (Nakamura 1987; Felgenhauer 1992; Franceschini-Vicentini *et al.* 2009). Since the classification of Hirsch and Jacobs (1928), it is possible to distinguish four basic cell types composing the tubular epithelium: E-, F-, R- and B-cells (Nakamura 1987; Gibson & Barker 1979; Franceschini-Vicentini *et al.* 2009). E-cells, or embryonic cells, are located at the blind end of the tubule. E-cells differentiate and give origin to the other cell type of the tubule, namely F-, R-, and B-cells. E-cell cytoplasm has a nucleus located centrally or basally, many free ribosomes, and mitochondria concentrated mainly in the apical part. The rough endoplasmic reticulum (RER) and Golgi complex are poorly developed, whereas the smooth endoplasmic reticulum (SER) is well-developed. F-cells, or fibrillar cells, are responsible for enzyme production and are located at the medial and proximal zones of the tubule. Their cytoplasm contains abundant both free and membrane-bound ribosomes (long and narrow shape), scattered mitochondria, dilated Golgi cisternae, and a well-developed SER. The RER surrounds the nucleus and occupies most of the cytoplasm, giving it a fibrillar appearance (Stanier, Woodhouse & Griffin 1968; Muskó 1988; Sousa *et al.* 2005). R-cells, or reabsorptive cells, are the most abundant cell type in the tubule. These cells are responsible for absorption and storage of nutrients. Their cytoplasm has a well-developed RER, a Golgi complex with dilated cisternae, mitochondria and lipid droplets. Apically, R-cells resemble vertebrate intestinal epithelial

cells with a well-developed brush boarder (Muskó 1988; Hemambika & Paulraj 1996). B-cells, or blister cells, are more frequent at the proximal zone of the tubule at different stages of their life cycle. These cells are responsible for intracellular digestion. Their cytoplasm is characterized by a large supranuclear vacuole originating by coalescence of small vacuoles (Sousa *et al.* 2005). They contain many free ribosomes, a Golgi complex with flattened elongated cisternae and a poorly developed RER (Muskó 1988).

In multicellular organisms, the normal life span of a cell may vary between a few days and several years, depending on the cell type (Medh & Thomson 2000). Cell death can occur as a natural process or can be activated by cellular stress or inflammation, as toxic metals, pathogens, and starvation. Morphological and ultrastructural features of cell death allow to characterize and quantify early and late cytopathological changes occurring in cells undergoing degeneration (Tinari *et al.* 2008). In crustaceans, three types of morphological features indicating cell death have been described in literature so far: necrosis, apoptosis, and autophagy (Sonakowska *et al.* 2016). Necrosis is a type of cell death that is not programmed but rather accidental. Cellular swelling, breakdown of cell organelles and denaturation of cytoplasmic proteins are characteristic of necrosis. In contrast to apoptosis, necrosis is characterized by an inflammation of surrounding tissues due to the release of intracellular enzymes contained in lysosomes after cell membrane rupture. Apoptosis is a regulated, energy-dependent and programmed form of cell death that occurs in normal as well as in pathologically altered tissues (Ziegler & Groscurth 2004; Tinari *et al.* 2008). Chromatin condensation and nuclear fragmentation, membrane preservation, blebbing of the plasma membrane and formation of apoptotic bodies are observed during apoptosis (Van Cruchten & Van Den Broeck 2002). Apoptosis occurs

without associated inflammation due to the containment of the cellular constituents by an intact membrane and the subsequent engulfment of apoptotic bodies. Finally, autophagy is a catabolic, tight regulated process participating in organelle turnover, playing an essential role in the maintenance of cellular homeostasis and allowing cells to survive periods of starvation (Ziegler & Groscurth 2004; Tinari *et al.* 2008; Larsoon & Masucci 2016). Phagophores, autophagosomes, multivesicular bodies (MVBs), autolysosomes and residual bodies are characteristic of autophagy (Tsujiimoto & Shimizu 2005; Tinari *et al.* 2008). If not well-controlled and regulated, autophagy can cause cell death. Farmed shrimp can experience starvation periods during disease outbreaks, adverse environmental conditions, and molting (Lavilla-Pitogo, Leño & Paner 1998; Sacristán *et al.* 2016). The HP, being the principal organ for storage of nutrients which can be mobilized during non-feeding periods, plays a fundamental role during starvation (Sánchez-Paz *et al.* 2007; Sacristán *et al.* 2016). Few authors have described the effect of starvation on the ultrastructure of the HP in crustaceans and, to our best knowledge, none of them in whiteleg shrimp (*Penaeus vannamei*) (Storch & Anger 1983; Elendt & Storch 1990; Storch, Juario & Pascual 1984; Tam & Avenant-Oldewage 2009; Yoshida *et al.* 2009; Sonakowska *et al.* 2016). Our research group recently published a study on the effect of starvation and refeeding on light microscopic level using computer-assisted image analysis (Cervellione *et al.* 2017a). Significant changes were measured for haemocytic infiltration in the intertubular spaces and content of lipid droplets within R-cells during starvation (increase of haemocytic infiltration associated with decreased of lipid droplets) and starvation followed by refeeding (decrease of haemocytic infiltration associated with increase of lipid droplets). No interpretable changes were observed for B-

and F-cells. Therefore, the aim of the present study was to describe the effect of starvation and refeeding on the ultrastructure of the HP in whiteleg shrimp on electron microscopic level.

Materials and Methods

Shrimp and rearing conditions

Experiments were conducted in collaboration with IMAQUA, located at the Faculty of Veterinary Medicine (Ghent, Belgium). Specific pathogen-free whiteleg shrimp were imported from Shrimp Improvement Systems (Florida, USA). Sixty shrimp were housed individually in 50 L glass tanks divided by plastic separators in five compartments (one shrimp per compartment, five shrimp per tank), each supplied with constant aeration and independent biological/mechanical filters. Water temperature was kept at 27 ± 1 °C, with a pH of 7.8 – 8.1 and salinity of 20 ± 1 g L⁻¹. The biological filters and regular water exchanges kept the total ammonium concentrations below 0.5 mg L⁻¹ and the total nitrites below 0.15 mg L⁻¹. The room was illuminated 12 h d⁻¹ by a dimmed luminescent light-tube. Shrimp were acclimatized for 14 days (d) and fed a commercial diet at 5% of the body weight, distributed 4 times/d.

Experimental design

Experimental design is summarized in Table 1. Shrimp of 2 ± 1 g were divided into three groups (20 shrimp each), receiving three treatments (one treatment per group) for 15 d: fed, starved, and refeed (starved for 5 d and then refeed for 10 d). Shrimp were sampled at d 0, 5, 10, and 15 (three shrimp per treatment and sampling point) and selected for the C-

intermoult stage (Corteel *et al.* 2009) before being transported to the Department of Morphology (Ghent University, Belgium) in aerated buckets and euthanized in cold ice.

Table 1. Experimental design to study the effect of starvation and refeeding on the ultrastructure of the hepatopancreas (perigastric organ) in whiteleg shrimp (*Penaeus vannamei*) using transmission electron microscopy.

Group	Treatment
FE	Fed for 15 days
ST	Starved for 15 days
REF	Starved for 5 days and then refed for 10 d

Note: four sampling points (day 0, 5, 10, 15) and six shrimp per sampling point/group. Feeding regime was 5% of the body weight, distributed in 4 times/d.

Preparation of ultra-thin sections

After dissecting the HP, samples of four mm³ were cut and fixed with 2% paraformaldehyde and 2.5% glutaraldehyde in 0.1 M cacodylate buffer (pH 7.2 at 4 °C). After six hours, samples were further cut in blocks of one mm³ and put in the same but fresh fixative overnight. Samples were then washed in 0.1 M cacodylate buffer at 22 °C (four times, 15 min each), postfixed in 1% osmium tetroxide for 90 min and washed in distilled water (three times, 15 min each). Samples were then dehydrated in a graded series of alcohols (10%, 30%, 50%, 70%, 94%, absolute alcohol with CuSO₄, 10 min each) and acetone (four times, 10 min each) using an automated tissue processor (EM TP, Leica©). Samples were embedded in epoxy resin using epoxy embedding kit (EMbed 812 Resin Kit, EMS©) and left at 60 °C for 72 hours. One µm semi-thin sections were cut with an automated ultramicrotome (EM UC6, Leica©), stained with toluidine blue, and observed under light microscope (BX53, Olympus©). Then ninety nm ultra-thin sections

(two sections per shrimp) were cut with diamond knife (DiAtome 45°, EMS©) using the same ultramicrotome and placed on coated copper grids (Formvar, EMS©). Sections were then stained with 1% uranylacetate for 25 min followed by lead citrate for 10 min, and examined with transmission electron microscope (JEM-1400Plus, JEOL USA Inc.).

Selection of morphometric parameters for electron microscopy

Ultrastructural changes of the HP, such as depletion of lipid droplets, swelling of the mitochondria and reduction in the number of cristae, infolding and increased thickness of the basal lamina, fragmentation and dilation of the cisternae of RER, nuclear fragmentation and chromatin condensation, have been described by different authors in case of starvation and refeeding in crustacean (Storch & Anger 1983; Papathanassiou & King 1984; Storch *et al.* 1984; Yoshida *et al.* 2009; Tam & Avenant-Oldewage 2009; Sonakowska *et al.* 2016). In the present study, morphological features as potential signs of cell death (necrosis, apoptosis and autophagy) and activation of the cellular immunity (haemocytic infiltration) were used to describe the effect of starvation and refeeding on the HP in whiteleg shrimp (Table 2). For necrosis, morphological features considered were swelling and breakdown of cell organelles (mitochondria, RER and Golgi complex), and partial or complete cytolysis (observed as electron-lucent area) that can be caused by denaturation of cytoplasmic proteins. For apoptosis, morphological features considered were chromatin condensation and nuclear fragmentation, membrane preservation, blebbing of the plasma membrane and formation of apoptotic bodies. For autophagy, morphological features considered were the presence of phagophores, autophagosomes, multivesicular bodies, autolysosomes and residual bodies. Finally, haemocytic infiltration in the intertubular spaces was considered as initial response of cellular immunity, as

described in literature in case of tissue damage, starvation, toxicity and environmental stress (Johnson 1980; Chiodi Boudet *et al.* 2015; Longo & Diaz 2015). Three morphologically different classes of haemocytes have been described: hyaline, semigranular and granular. Pathogen recognition stimulates the degranulation of granular and semigranular cells. The release of the prophenoloxidase system and other plasma factors from the storage granules promotes phagocytosis by hyaline cells or encapsulation by semigranular cells (Cerenius *et al.* 2010; Dantas Lima 2013; Musthaq & Kwang 2014).

Table 2. Morphological features selected to study the effect of starvation and refeeding on the ultrastructure of hepatopancreas (perigastric organ) in whiteleg shrimp (*Penaeus vannamei*) using transmission electron microscopy.

Morphological features	Cellular process potentially linked to
swelling and breakdown of cell organelles (mitochondria, RER and Golgi complex), cytolysis	Necrosis
Chromatin condensation and nuclear fragmentation, membrane preservation, blebbing of the plasma membrane and formation of apoptotic bodies	Apoptosis
Presence of phagophores, autophagosomes, multivesicular bodies, autolysosomes and residual bodies	Autophagy
Infiltration of haemocytes in the intertubular spaces	Cellular immunity

Results

The present study was performed on 36 shrimp (three groups, four time points, three shrimp per group, and two sections per shrimp). Ultrastructural changes were observed mainly in R- and F-cells during starvation and starvation followed by refeeding. No changes were observed in B-cells. In the fed group, no signs of cell death (necrosis, apoptosis, and autophagy) were observed (Figure 1). Brush boarder was well-developed and uniform (about 1000nm in height), basal lamina was intact and not infolded. Mitochondria showed a normal shape, RER was well developed both in R- and F-cells. Lipid droplets were abundantly dispersed within R-cells and a few haemocytes were present in the intertubular spaces (Figure 1). In the starved group, morphological features indicating potential necrosis and autophagy (Figure 2 for necrosis, and Figure 3 for autophagy) and haemocytic infiltration (Figure 4) were observed during food deprivation, increasingly overtime. Haemocytes (granular/semigranluar and hyaline) infiltrating the intertubular spaces and swelling of mitochondria increased progressively during 15 d of starvation. Haemocytes adhering to the tubular epithelium showed an electron-dense area with microfilament structure in the region proximal to the basal lamina. After five days of starvation, complete depletion of lipid droplets, mild infolding of the basal lamina, swelling of mitochondria and increase of haemocytic infiltration were observed. No signs of autophagy or dilatation of RER and Golgi complex cisternae were shown within the tubular epithelium. RER developed a concentric shape occasionally in R-cells. After ten days of starvation, the brush boarder lost integrity and uniformity, appearing damaged and reduced in height. Basal lamina had multiple infoldings and swollen mitochondria showed a few altered and disrupted cristae. Furthermore, more frequent signs of

autophagy (phagophores, autophagosomes, and MVBs) were present within the cytoplasm. Only few nuclei showed signs of chromatin condensation and nuclear fragmentation. Haemocytic infiltration increased considerably. After 15 days of starvation, ultrastructural changes increased compared to previous sampling point. Diffused cytolysis, swelling of mitochondria, dilation of the cisternae of SER, RER and Golgi complex, haemocytic infiltration and signs of autophagy were observed. Basal lamina was considerably infolded but not increased in thickness. In the refed group, signs of partial restitution of the HP were observed during refeeding. After five days of refeeding, a reduction of mitochondria swelling was observed. Authophagosomes and MVBs, dilatation of the cisternae of RER and Golgi complex, and infolding of the basal lamina were still present. After ten days of refeeding, brush boarder appeared well-developed and uniform (same length of the fed group, approximately 1 μ m), and basal lamina did not show sign of infolding. No signs of necrosis or apoptosis were observed. Lipid droplets within R-cells increased and haemocytic infiltration decreased over the refeeding period.

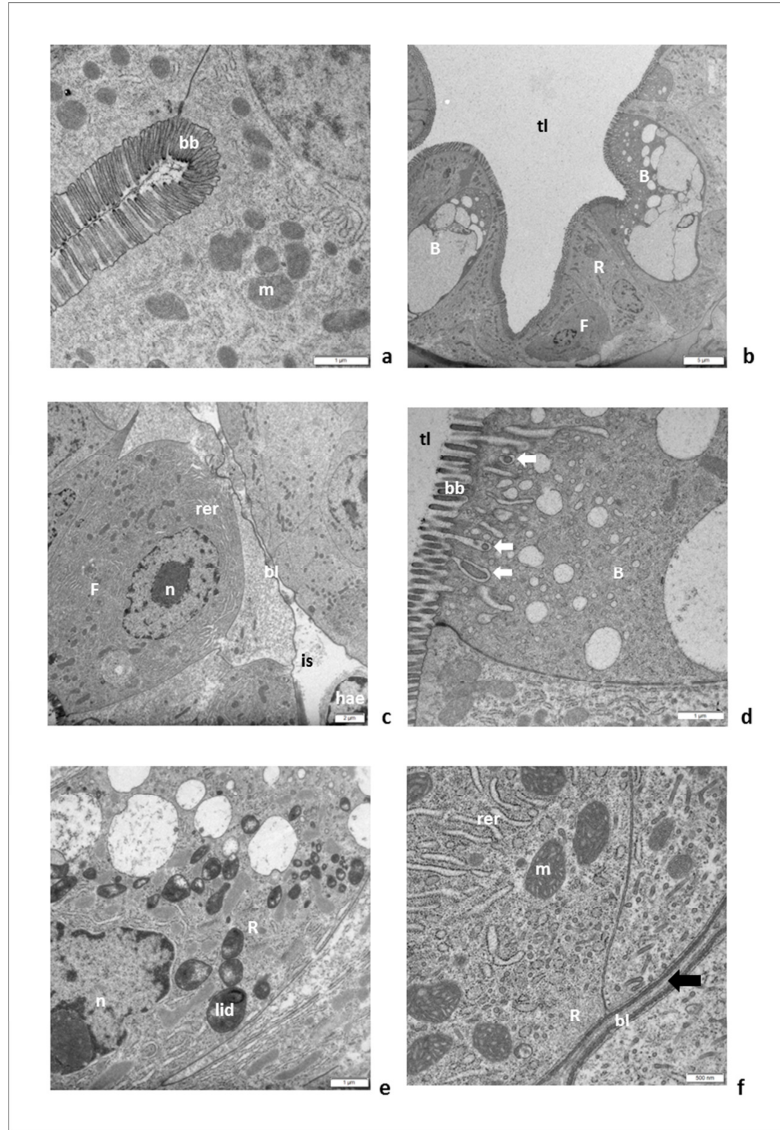


Fig 1. Normal ultrastructure of the hepatopancreas (perigastric organ) in whiteleg shrimp (*Penaeus vannamei*) at electron microscopic level. (a) well-developed brush boarder and mitochondria; (b) B-, F- and R-cells; (c) F-cells, well-developed rough endoplasmic reticulum; (d) B-cell, white arrows show endocytosis of extracellular particles; (e) R-cell, lipid droplets; (f) R-cell showing a well-developed rough endoplasmic reticulum and normal size mitochondria, black arrow indicates the intertubular space. bb = brush boarder; bl = basal lamina; hae = haemocyte; is = intertubular space; lid = lipid droplet; m = mitochondria; n = nucleus; rer = rough endoplasmic reticulum; tl = tubular lumen; B = B-cell; F = F-cell; R = R-cell. Scale bar = (a, d, e) 1 μ m, (b) 5 μ m, (c) 2 μ m, (f) 500 nm.

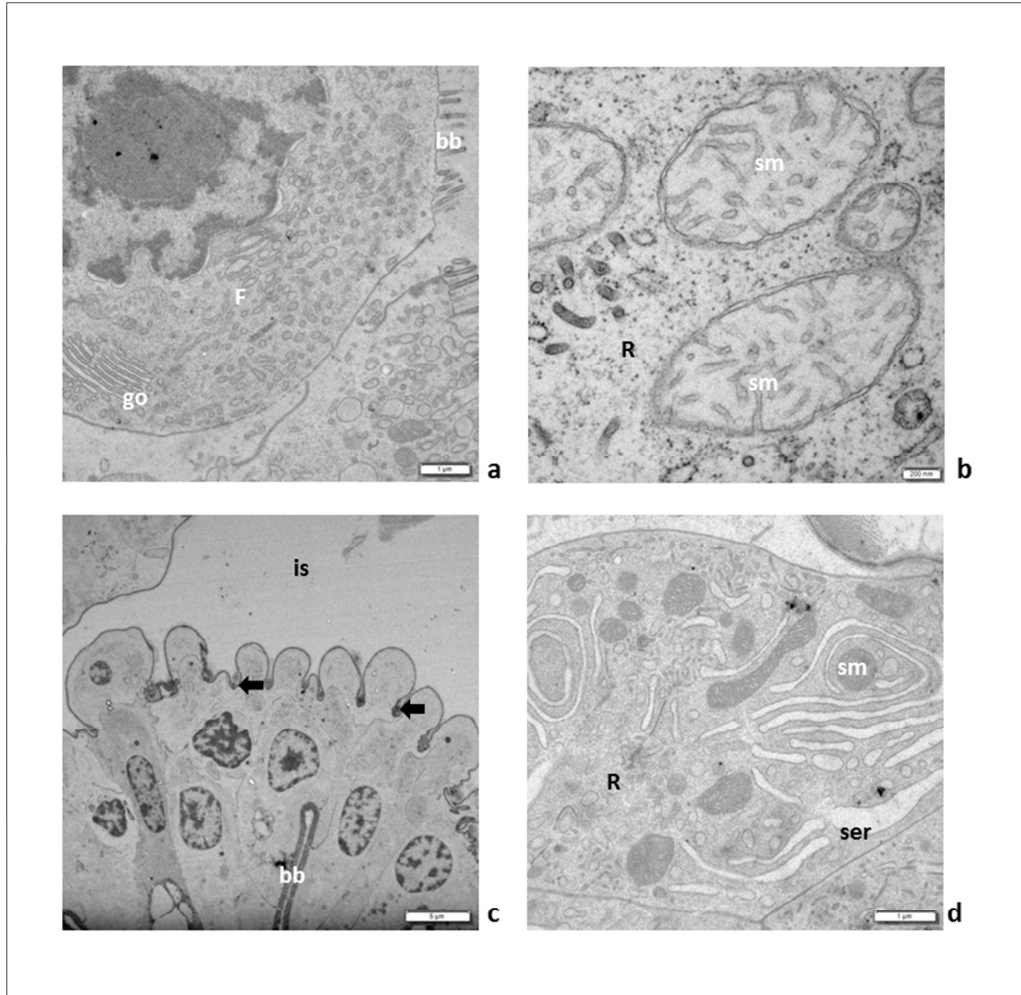


Fig 2. Effect of starvation on the ultrastructure of the hepatopancreas (perigastric organ) in whiteleg shrimp (*Penaeus vannamei*) at electron microscopic level showing potential signs of necrosis. (a) F-cell, disruption of the brush boarder, swelling of the Golgi cisternae; (b) R-cell, swelling of the mitochondria associated with few altered and disrupted cristae; (c) infolding of the basal lamina (black arrows); (d) R-cell, dilatation of the cisternae of the smooth endoplasmic reticulum. bb = brush boarder; bl = basal lamina; go = Golgi complex; is = intertubular space; ph = phagophore; sm = swollen mitochondria; ser = smooth endoplasmic reticulum; F = F-cell; R = R-cell. Scale bar = (a, d) 1 μ m, (b) 200nm, (c) 5 μ m.

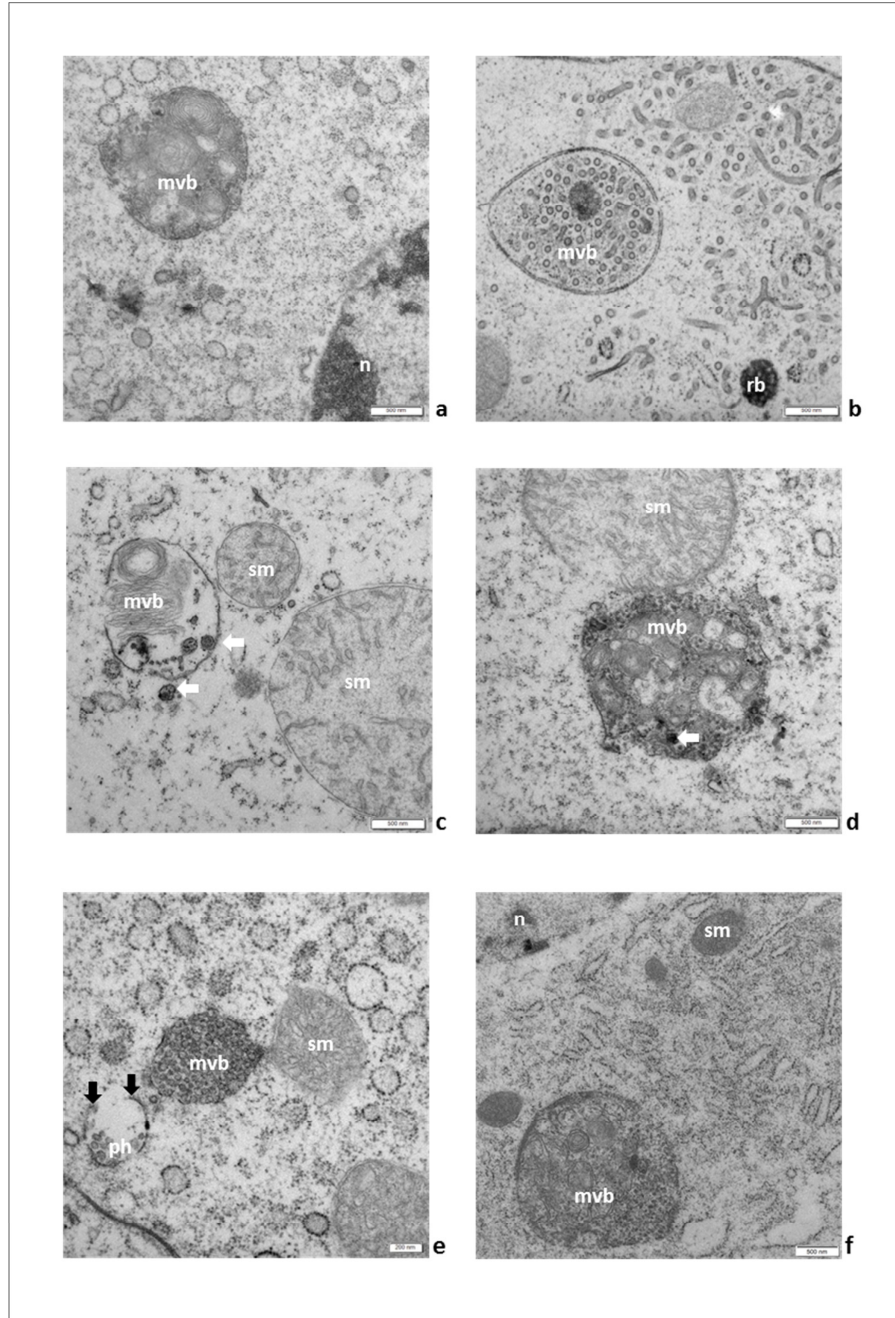


Fig 3. Effect of starvation on the ultrastructure of the hepatopancreas (perigastric organ) in whiteleg shrimp (*Penaeus vannamei*) at electron microscopic level showing signs of autophagy. (a) Multivesicular bodies present in the cell cytoplasm, containing degraded organelles. (b) residual body; (c) white arrows indicate lysosomes; (e) black arrows indicate the formation of the autophagosome. mvb = multivesicular body; n = nucleus; sm = swollen mitochondria; ph = phagophore; rs = residual body. Scale bar = (a, b, c, d, f) 500 nm, (e) 200 nm.

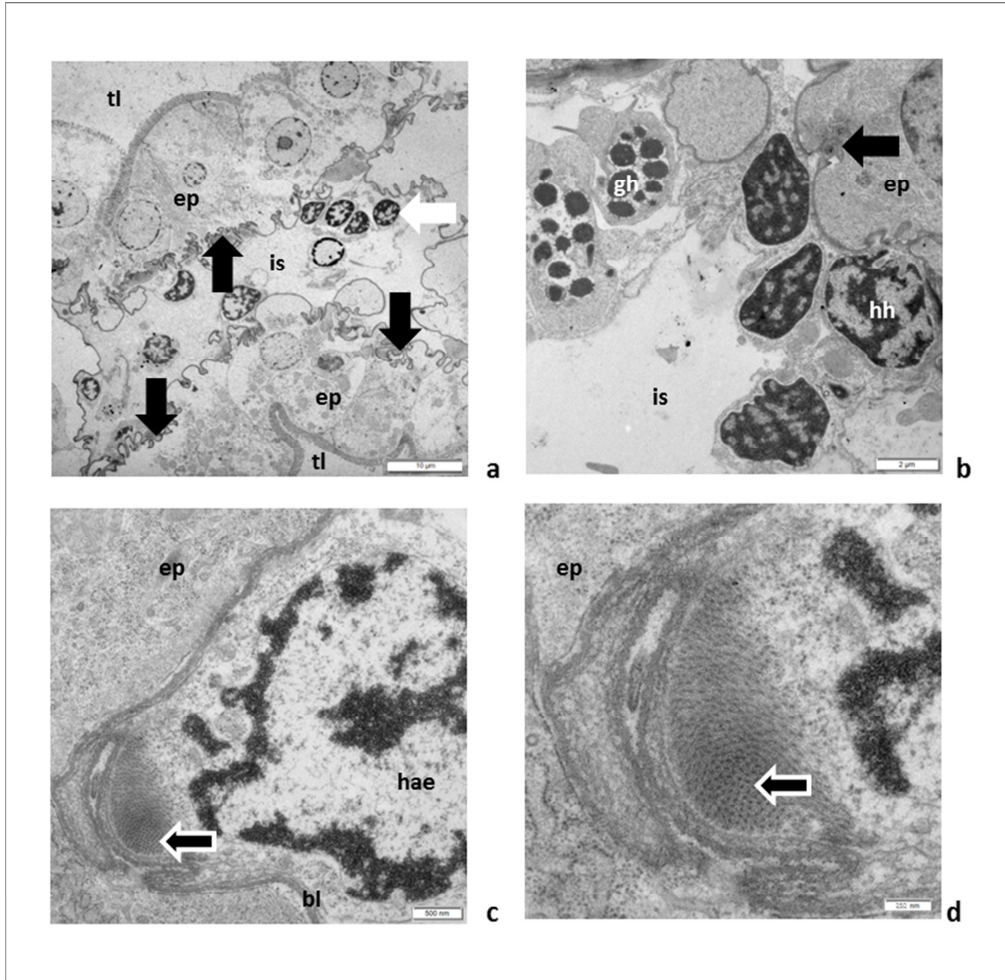


Fig 4. Effect of starvation on the ultrastructure of the hepatopancreas (perigastric organ) in whiteleg shrimp (*Penaeus vannamei*) at electron microscopic level showing haemocytic infiltration in the intertubular spaces. (a) high number of haemocytes (white arrow) infiltrating the intertubular spaces, infolding of the basal membrane of the tubular epithelium (black arrow) (b) granular/semigranular and hyaline haemocytes (arrow indicates the infolding of the basal lamina); (c) haemocyte adhering to the tubular epithelium showing an electron-dense area (white/black arrow) in the region proximal to the basal lamina (white and black arrow); (d) high magnification of (c) showing the microfilament structure of the electron-dense area (white/black arrow); of the haemocyte. bl = basal lamina; ep= tubular epithelium; gh = granular/semigranular haemocyte; hae = haemocyte; hh = hyaline haemocyte; is = intertubular space. Scale bar = (a) 10 1 μ m, (b) 2 μ m, (c) 500 nm, (d) 250 nm.

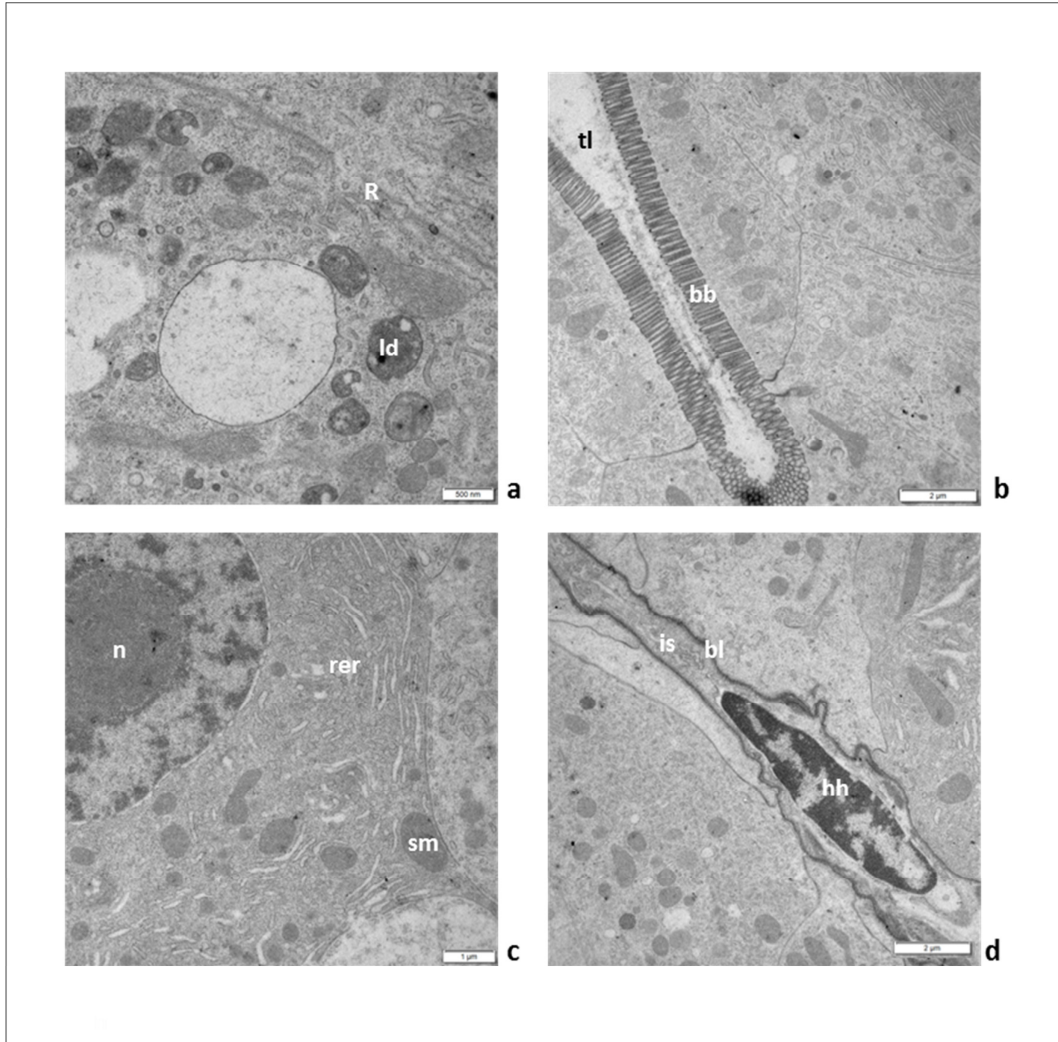


Fig 5. Effect of starvation followed by refeeding on the ultrastructure of the hepatopancreas (perigastric organ) in whiteleg shrimp (*Penaeus vannamei*) at electron microscopic level. (a) R-cell, lipid droplets; (b) integrity and uniformity of the brush boarder; (c) dilation of the cisternae of the rough endoplasmic reticulum; (d) hyaline haemocyte infiltrating the intertubular space. bb = brush boarder; bl = basal lamina; ld = lipid droplets; hh = hyaline haemocyte; is = intertubular space; n = nucleus; sm = swollen mitochondria; n = nucleus; rer = rough endoplasmic reticulum; R = R-cell. Scale bar = (a) 500nm, (b, d) 2 μ m, (c) 1 μ m.

Discussion

During starvation, ultrastructural changes can be observed in the digestive system of crustaceans, particularly in the HP (Storch & Anger 1983; Papathanassiou & King 1984; Storch *et al.* 1984; Yoshida *et al.* 2009; Tam & Avenant-Oldewage 2009; Sonakowska *et al.* 2016) The capacity of crustaceans to survive transitory periods of starvation and to subsequently recover depends on physiological and behavioral marks, especially on their capacity of storing and mobilizing energy in the HP (Calvo *et al.* 2012). In the present study, morphological features as potential signs of cell death (necrosis, apoptosis and autophagy) and cellular immunity (haemocytic infiltration) were observed during starvation and refeeding in the HP of whiteleg shrimp. Starvation induced a progressive increase of cellular immunity (haemocytic infiltration, both hyaline and granular/semigranular haemocytes), determining potential signs of necrosis (swelling of organelles and cytolysis), and autophagy (formation of phagophores, autophagosomes, MVBs and residual bodies). Lipid droplets were completely depleted after five days of starvation. The depletion of lipid droplets and increase in haemocytic infiltration observed during food deprivation followed by the partial restitution of lipid droplets and reduction of the haemocytic infiltration during refeeding are supported by our previous light microscopic study describing the effect of starvation and refeeding using computer-assisted image analysis (Cervellione *et al.* 2017a).

Haemocytes adhering to the tubular epithelium showed an electron-dense area, composed by microfilaments, in the region proximal to the basal lamina. These microfilaments might be formed by the assembling of actin subunits for the formation of pseudopodia. In leukocytes, the formation of pseudopodia is described as a cellular

response to chemotactic factors for promoting migration, adhesion and phagocytosis (Moazzam *et al.* 1997). Further ultrastructural studies are requested to better understand this process in decapods. Disruption of the brush boarder was only observed after ten days of starvation indicating that five days of starvation do not compromise the absorptive capacity of the epithelial cells. Regarding apoptosis, no blebbing and formation of apoptotic bodies were observed. Infolding of the basal lamina can be caused by the shrinkage of the cells during necrosis, however during necrosis swelling of the cell is expected rather than shrinkage. Future studies should what causes the infolding of the basal lamina. Nuclear fragmentation and chromatin segmentation were rarely observed, suggesting that apoptosis plays a minor role during short term starvation. Future studies should investigate the role of apoptosis when shrimp are starved for longer periods. Signs of necrosis were frequently observed during starvation and refeeding. Swelling of mitochondria (observed after five days of starvation) and alteration and disorganization of the mitochondrial cristae (observed after ten days of starvation) were observed during starvation and refeeding. Mitochondria are the sites of respiration, and generate chemical energy in the form of adenosine triphosphate (ATP) by metabolizing sugars, fats, and other chemical fuels with the assistance of molecular oxygen. Damage of mitochondria can lead to ATP depletion, and furthermore ion deregulation and altered mitochondrial permeability contribute to both apoptotic and necrotic death (Nieminen 2003). Refeeding for ten days did not result in a complete recovery of the cell organelles, as described in other crustaceans and in teleost and mammalian hepatocytes (Pokrovskii *et al.* 1976; Storch & Anger 1983). Future studies should evaluate if complete recovery is possible after more prolonged refeeding periods. As reported by Elendt & Storch (1990), when

shrimp are fixed right after molting, the uptake of water leads to a short change of the intracellular osmotic value that can result in swollen mitochondria even in well-fed shrimp. Our research group strongly recommends to sample shrimp in C-intermolt stage for both light and electron microscopic studies to minimize this event.

The term autophagy (from the Greek *autos* for “self”, and *phago* for “digestion”) was first coined by Christian de Duve in 1963, and was largely based on the observed degradation of mitochondria and other intra-cellular structures within lysosomes of rat liver perfused with the pancreatic hormone glucagone (Glick *et al.* 2010). Since then, many researchers have been studying the machinery of autophagy, culminating with the 2016 Nobel Prize awarded to Dr. Ohsumi for his discoveries of mechanisms for autophagy. Autophagy is a complex process involving degradation of cellular components to maintain organelles and protein homeostasis in response to stress-induced damage as well as starvation. It operates engulfing non-functional cellular components into double-membrane vesicles and delivering them to the lysosome for degradation. By this mechanism, autophagy mediates the digestion and recycling of non-essential parts of the cell for macromolecular synthesis and energy production when external nutrient supply is limited. Deficiency in the clearing and restoring function of autophagy leads to cell death (Suwansa-Ard *et al.* 2016; Antonioli *et al.* 2017). A few studies have shown the presence of autophagy within cells of the midgut in crustaceans by using electron microscopy (Suwansa *et al.* 2016). In the present study, autophagy was one of the most frequent physiological process observed during starvation and refeeding. The presence of autophagosomes, multivesicular bodies (MVBs), and autolysosomes increased over time during starvation, reflects the organism switching over to a forced endogenous alimentation. MVBs are

specialized subsets of endosomes that contain membrane-bound intraluminal vesicles, formed by budding into the lumen of the MVBs. Their content can be degraded, via fusion with lysosomes, or released in the extracellular space, via fusion with the plasma membrane. In the present study, electron microscopy was conducted on cross sections of the HP and did not investigate the effect of starvation and refeeding on embryonic E-cells, located at the blind end of the tubule. Future studies should evaluate if food deprivation and refeeding have an impact on the ultrastructure of E-cells.

Depending on the species, the reestablishment of the ultrastructure of R-cell is not possible after a prolonged period of food deprivation. After this period, known as point of no return (PNR), animals are unable to recover from the effect of prolonged starvation (Storch & Anger 1983). Future studies should also investigate if the HP has the potential to recover completely after more prolonged refeeding periods and if subsequent recovery is possible (identification of PNR).

To our best knowledge, the present study describes for the first time the ultrastructural changes occurring in the HP of whiteleg shrimp during starvation and refeeding. Autophagy, followed by necrosis and a few signs of apoptosis, were the most frequent cell death mechanisms observed. The present findings should contribute in the future to better understand the impact of starvation on the HP and shrimp health and describe the different cell death types occurring in crustaceans during disease outbreaks and adverse environmental conditions.

References

- Antonioli, M., Di Rienzo, M., Piacentini, M. & Fimia, G.M. (2017) Emerging Mechanisms in Initiating and Terminating Autophagy. *Trends Biochem Sci*, **42**, 28-41.
- Calvo, N.S., Tropea, C., Anger, K.A. & Greco, L.L. (2012) Starvation resistance in juvenile freshwater crayfish. *Aquatic Biology*, **16**, 287-297.
- Cerenius, L., Jiravanichpaisal, P., Liu, H. & Söderhäll, I. (2010) Crustacean immunity. In: *Invertebrate Immunity* (ed. by K. Söderhäll), pp. 239-259. Springer Science, New York.
- Cervellione, F., McGurk, C., Berger Eriksen, T. & Van den Broeck, W. (2017a) Effect of starvation and refeeding on the hepatopancreas in whiteleg shrimp, *Penaeus vannamei* (Boone). *Journal of Fish Diseases*, doi 10.1111/jfd.12639.
- Chiodi Boudet, L.N., Polizzi, P., Romero, M.B., Robles, A., Marcovecchio, J.E. & Gerpe, M.S. (2015) Histopathological and biochemical evidence of hepatopancreatic toxicity caused by cadmium in white shrimp, *Palaemonetes argentinus*. *Ecotoxicology and Environmental Safety*, **113**, 231-240.
- Corteel M., Dantas-Lima J.J., Wille M., Alday-Sanz V., Pensaert M.B., Sorgeloos P. & Nauwynck H.J. (2009) Molt stage and cuticle damage influence white spot syndrome virus immersion infection in penaeid shrimp. *Veterinary Microbiology* **137**, 209-216.
- Dantas Lima, J. (2013). Development of Techniques to Culture Shrimp Haemocytes and Purify White Spot Syndrome Virus (WSSV) in Order to Study WSSV-Haemocyte Interactions. PhD thesis, Ghent University.
- Elendt, B.-P. & Storch, V. (1990) Starvation-Induced Alterations of the Ultrastructure of the Midgut of *Daphnia Magna* Straus, 1820 (Cladocera). *Journal of Crustacean Biology*, **10**, 79-86.
- Felgenhauer, B.E. (1992) Internal Anatomy of the Decapods: An Overview. In: *Microscopic Anatomy of Invertebrates*, pp. 45-75. Wiley-Liss.
- Franceschini-Vicentini, I.B., Ribeiro, K., Papa, L.P., Marques, J., Vicentini, C.A. & Valenti, P. (2009) Histoarchitectural Features of the Hepatopancreas of the Amazon River Prawn *Macrobrachium amazonicum*. *International Journal of Morphology*, **27**, 121-128.
- Gibson, R. & Barker, P.L. (1979) The decapod hepatopancreas. *Oceanography and Marine Biology an Annual Review*, **17**, 285-346.
- Glick, D., Barth, S. & Macleod, K.F. (2010) Autophagy: cellular and molecular mechanisms. *Journal of Pathology*, **221**, 3-12.

Hemambika, M. & Paulraj, R. (1996) An Ultrastructural Study of the Hepatopancreas of Indian White Prawn *Penaeus indicus* H. Milne Edwards. In: *The Fourth Indian Fisheries Forum Proceedings*, pp. 291-294.

Hirsch, G.C. & Jacobs, W. (1928) Der Arbeitrhythmus der Mitteldarmdrüse von *Astacus leptodactylus*. *Zeitschrift für vergleichende Physiologie*, **8**, 102-144.

Johnson, P.T. (1980) *Histology of the blue crab Callinectes sapidus. A model for the Decapoda*, Praeger Publishers, New York.

Laohabanjong, R., Tantikitti, C., Benjakul, S., Supamattaya, K. & Boonyaratpalin, M. (2009) Lipid oxidation in fish meal stored under different conditions on growth, feed efficiency and hepatopancreatic cells of black tiger shrimp (*Penaeus monodon*). *Aquaculture*, **286**, 283-289.

Larsson, N.G. & Masucci, M.G. (2016) Scientific background, Discoveries of Mechanisms for autophagy. *Nobelförsamlingen, the Nobel Assembly at Karolinska Institutet*, 1-7. Karolinska Institute, Solna, Sweden.

Lavilla-Pitogo, C.R., Leñaño, E.M. & Paner, M.G. (1998) Mortalities of pond-cultured juvenile shrimp, *Penaeus monodon*, associated with dominance of luminescent vibrios in the rearing environment. *Aquaculture*, **164**, 337-349.

Lightner D.V. (2015) Diseases of Crustaceans. In: *Manual of Diagnostic Tests for Aquatic Animals* (ed. by OIE), Section 2.2.0, pp. 1-10. World Organization of Animal Health, Paris.

Longo, M.V. & Diaz, A.O. (2015) Histological and Histochemical Study of the Hepatopancreas of Two Estuarine Crab Species, *Cyrtograpsus angulatus* and *Neohelice granulata* (Grapsodea, Varunidae): Influence of Environmental Salinity. *Zoological Science*, **32**, 163-170.

Medh, R.D. & Thompson, E.B. (2000) Hormonal regulation of physiological cell turnover and apoptosis. *Cell and Tissue Research*, **301**, 101-124.

Moazzam, F., Delano, F.A., Zweifach, B.W., Schmid, S., Xf & Nbein, G.W. (1997) The Leukocyte Response to Fluid Stress. *Proceedings of the National Academy of Sciences of the United States of America*, **94**, 5338-5343.

Musthaq, S.K.S. & Kwang, J. (2014) Evolution of specific immunity in shrimp - A vaccination perspective against white spot syndrome virus. *Developmental and Comparative Immunology*, **46**, 279-290.

Muskó, I.B. (1988) Ultrastructure of the Midgut Gland of *Gammarus roeselii* Gervais (Amphipoda, Gammaridea). *Crustaceana*, **54**, 207-217.

- Nakamura, K. (1987) Classification of diverticular cells of the midgut gland in the prawn *Penaeus japonicus*. *Memoirs of Faculty of Fisheries Kagoshima University*, **36**, 207-214.
- Nieminen, A.-L. (2003) Apoptosis and necrosis in health and disease: Role of mitochondria. In: *International Review of Cytology*, pp. 29-55. Academic Press.
- Papathanassiou, E. & King, P.E. (1984) Effects of starvation on the fine structure of the hepatopancreas in the common prawn *Palaemon serratus* (Pennant). *Comparative Biochemistry and Physiology a-Molecular & Integrative Physiology*, **77**, 243–249.
- Pokrovskii, A.A., Tashev, T.A., Krystev, L.P., Tutel'ian, V.A. & Kravchenko, L.V. (1976) Ultrastructural changes in the subcellular membranes of hepatocytes during the early periods of starvation. *Voprosy Pitaniia*, 26-31.
- Sacristán, H.J., Ansaldo, M., Franco-Tadic, L.M., Gimenez, A.V.F. & Greco, L.S.L. (2016) Long-Term Starvation and Posterior Feeding Effects on Biochemical and Physiological Responses of Midgut Gland of *Cherax quadricarinatus* Juveniles (Parastacidae). *PLoS one*, **11**, e0150854.
- Sánchez-Paz, A., García-Carreño, F., Hernández-López, J., Muhlia-Almazán, A. & Yepiz-Plascencia, G. (2007) Effect of short-term starvation on hepatopancreas and plasma energy reserves of the Pacific white shrimp (*Litopenaeus vannamei*). *Journal of Experimental Marine Biology and Ecology*, **340**, 184-193.
- Sonakowska, L., Włodarczyk, A., Wilczek, G., Wilczek, P., Student, S. & Rost-Roszkowska, M.M. (2016) Cell Death in the Epithelia of the Intestine and Hepatopancreas in *Neocaridina heteropoda* (Crustacea, Malacostraca). *PLoS one*, **11**, e0147582.
- Sousa, L.G., Cuartas, E.I. & Petriella, A.M. (2005) Fine structural analysis of the epithelial cells in the hepatopancreas of *Palaemonetes argentinus* (Crustacea, Decapoda, Caridea) in intermoult. *Biocell*, **29**, 25-31.
- Stanier, J.E., Woodhouse, M.A. & Griffin, R.L. (1968) The Fine Structure of the Hepatopancreas of *Carcinus maenas* (L.) (Decapoda Brachyura). *Crustaceana*, **14**, 56-66.
- Storch, V. & Anger, K. (1983) Influence of starvation and feeding on the hepatopancreas of larval *Hyas araneus* (Decapoda, Majidae). *Helgoländer Meeresuntersuchungen*, **36**, 67-75.
- Storch, V., Juario, J.V. & Pascual, F.P. (1984) Early effects of nutritional stress on the liver of milkfish, *Chanos chanos* (Forsskal), and on the hepatopancreas of the tiger prawn, *Penaeus monodon* (Fabricius). *Aquaculture*, **36**, 229-236.
- Suwansa-Ard, S., Kankuan, W., Thongbuakaew, T., Saetan, J., Kornthong, N., Kruangkum, T., Khornchatri, K., Cummins, S.F., Isidoro, C. & Sobhon, P. (2016)

Transcriptomic analysis of the autophagy machinery in crustaceans. *BMC Genomics*, **17**, 587.

Tam, Q. & Avenant-Oldewage, A. (2009) The effect of starvation on the ultrastructure of the digestive cells of *Dolops ranarum* (Stuhlmann, 1891) (Crustacea: Branchiura). *Arthropod Structure & Development*, **38**, 391-399.

Tinari, A., Giammarioli, A.M., Manganelli, V., Ciarlo, L. & Malorni, W. (2008) Analyzing morphological and ultrastructural features in cell death. *Methods in Enzymology*, **442**, 1-26.

Tsujimoto, Y. & Shimizu, S. (2005) Another way to die: autophagic programmed cell death. *Cell Death Differentiation*, **12 Suppl 2**, 1528-1534.

Van Cruchten, S. & Van Den Broeck, W. (2002) Morphological and biochemical aspects of apoptosis, oncosis and necrosis. *Anatomie Histologie Embryologie*, **31**, 214-223.

Yoshida, T., Kawagushi, S., Meyer, B., Virtue, P., Penschow, J. & Nash, G. (2009) Structural changes in the digestive glands of larval Antarctic krill (*Euphausia superba*) during starvation. *Polar Biology*, **32**, 503-507.

Ziegler, U. & Groscurth, P. (2004) Morphological features of cell death. *News Physiol Sci*, **19**, 124-128.

Chapter 5

“Perigastric organ”: a replacement name for the “hepatopancreas” in Decapoda

Fabio Cervellione¹, Charles McGurk¹ and Wim Van den Broeck²

¹Skretting Aquaculture Research Centre, Stavanger, Norway

²Department of Morphology, Ghent University, Ghent, Belgium

Journal of Crustacean Biology 2017, DOI: 10.1093/jcbiol/rux020

Abstract

Since its first description in 1848, many names have been given to the key organ of the gastro-intestinal tract of Decapoda, which have caused much confusion. Even the most commonly accepted name, “hepatopancreas”, is inappropriate because this organ inherently differs from the liver and pancreas of vertebrates. We briefly discuss the embryology, gross anatomy, histology, and physiology of the “hepatopancreas”. The names “perigastric organ” and “perigaster” (from the Greek *peri-* for “around” and “enclosing”, and *gaster* for “stomach”) are proposed as a replacement of “hepatopancreas”. This new name considers the topography of the organ without referring to its anatomy and physiology.

Key Words: perigaster, terminology.

Authors have been referring to the “hepatopancreas” of crustaceans using different names: “midgut gland”, “gastric gland”, “digestive gland”, “hepatic gland”, “pancreatic gland”, “racemose gland”, “pancreas”, “liver”, “liver diverticulum”, “midgut diverticulum”, “branched midgut caeca”, “branched diverticula”, “hepatopancreatic caeca”, “intestinal caecum”, “hepatic caecum”, “lateral caecum”, “pyloric caecum”, “midgut organ”, “digestive organ”, “digestive diverticula”, “gland diverticulum”, and “caeca anteriores” (Van Weel 1974; Gibson & Barker 1979; McLaughlin 1980; Bliss 1983; McLaughlin 1983; Cornelius 1985; Herreid & Full 1988). Scientists continue to use these various names, often interchangeably (Cornelius 1985), even if it adds to the confusion. The greatest degree of complexity of this organ among crustaceans is seen in Decapoda, and it is in this group that research began, attracting the interest of scientists for over 150 years (Gibson & Barker 1979). As a result, most of the terminology appearing in the literature has been coined by decapod researchers, and secondarily applied to non-decapod crustaceans.

Siebold (1848, 1874) first named the organ *die leber* (the liver) and described it in the Order Siphonostoma of Decapoda. Felix Hoppe-Seyler demonstrated in 1877 that the organ was involved in food digestion (see Gibson & Barker 1979). Huxley (1880) retained the name liver, linking the secretory functions of the organ with digestion in the European crayfish (*Astacus fluviatilis* Linnaeus, 1758).

Guieyesse (1906) named the organ the *organ entérique* and indicated it served five functions: the absorption of nutrients, secretion of digestive enzymes, storage of metabolic reserves, breakdown of toxic substances, and elimination of waste products (Gibson & Barker 1979; Sánchez-Paz *et al.* 2007). The most accepted name since 1960 has been the “hepatopancreas.” Van Weel (1974) and Phillips *et al.* (1977) argued that this organ

did not function as the homologous liver or pancreas in mammals and, therefore, “hepatopancreas” was both inappropriate and inaccurate when applied to any of the evaginations of the crustacean midgut. Consequently, they suggested the use of “midgut gland” (Van Weel 1974). Gibson and Barker (1979) nevertheless concluded that “hepatopancreas” was an appropriate name. McLaughlin (1980) described the organ in Decapoda using “digestive gland,” “hepatic cecum/ceca,” and “hepatopancreas.” Bliss (1983) and McLaughlin (1983) recommended to refer the ventral, glandular, digestive diverticula of all crustaceans as “midgut glands.” Dall & Moriarty (1983) argued for the use of “digestive gland,” based primarily on functionality, supporting the inappropriateness of the name “hepatopancreas.” Davie *et al.* (2015) more recently referred to the terminology of Dall & Moriarty (1983).

The use of “hepatopancreas” still remains controversial (Warburg 2012). “Hepatopancreas” is used in some fish species when the exocrine pancreas forms islets of tissue dispersed in the liver. This exocrine pancreatic tissue is formed around the portal vein, and it penetrates deeply into the liver parenchyma during ontogenesis, separated from the rest of the liver by a thin layer of connective tissue (Seyrafi *et al.* 2009; Nejedli & Gajger 2013). The use of the same name for the putative analog invertebrate structure has resulted in some confusion (Dall & Moriarty 1983; Cornelius 1985). The name “hepatopancreas” is not appropriate, because this organ differs from the vertebrate liver and pancreas (Table 1) (Vonk 1960; Warburg 2012; Röszer 2014). It thus seems important to review these names and propose the most appropriate alternative.

Table 1. Schematic comparison of the main characteristics of the “hepatopancreas” in vertebrates and invertebrates (Decapoda).

	Vertebrates	Invertebrates (Decapoda)
Embryological origin	foregut endoderm	midgut endoderm
Tissue type		
Exocrine pancreas	yes	no
Endocrine pancreas	yes	no
Hepatocytes	yes	no
Haemopoietic tissue	yes	no
Functional units		
Acinar and lobular structure	yes	no
Tubular structure	no	yes
Physiology		
Production of bile salts and bile pigments	yes	no
Production of serum and blood-clotting protein	yes	no
Ability to regulate sugar levels in the “blood”	yes	no
Absorption of nutrients	no	yes
Storage of nutrients and minerals	yes	yes
Detoxification	yes	yes

The digestive tract of decapods is divided into three regions: fore-, mid-, and hindgut (McLaughlin 1980; Dall & Moriarty 1983; Ceccaldi 1989; Ceccaldi 1997; Davie *et al.* 2015). The midgut starts in the cephalothorax at its junction with the pyloric sac of the stomach and ends in a coiled tube, the posterior midgut caecum, at the anterior half of the sixth abdominal segment (Ceccaldi 1989; McGaw & Curtis 2013). The midgut is composed of the intestine and many evaginations, namely the “hepatopancreas” and the anterior and posterior midgut caeca (McLaughlin 1983). The intestine is lined by a simple columnar epithelium surrounded by circular and longitudinal muscular fibres. It has a limited absorptive function and mainly produces a mucous substance which forms the peritrophic

membrane that coats the non-digested products from the stomach, aiding the movement of food towards the hindgut (McLaughlin 1983; Ceccaldi 1989; Davie *et al.* 2015).

The midgut caeca are two blind ending extensions of the midgut, and histologically differ from the intestine in lacking longitudinal muscular fibres and in possessing considerably infolded walls. They play a role in ion and water regulation (Barker & Gibson 1977; Ceccaldi 1989). The "hepatopancreas" forms a large, compact, paired mass that occupies most of the cephalothorax, flanking the stomach and anterior midgut. It reaches its greatest degree of complexity in Decapoda. Each half of the organ is composed of two or three lobes and the entire structure is surrounded by a capsule of connective tissue (Gibson & Barker 1979; Davie *et al.* 2015). Each lobe is connected to the intestine through the corresponding principal duct (Esteve & Herrera 2000; Vasagam *et al.* 2007). Fine circular and longitudinal muscular fibres are found around each duct. The fibres allow for peristaltic and longitudinal contractions, facilitating the movement of liquids through the organ. The hepatopancreas is well supplied with hemolymph as the hepatic arteries pass into the lobes of the hepatopancreas, where they subdivide among ducts and tubules (Herreid & Full 1988; Ceccaldi 1989).

Each lobe is composed by many blind ending tubules, lined by a simple columnar epithelium made up of four basic cell types (E-, F-, R- and B-cells) (Nakamura 1987; Franceschini-Vicentini *et al.* 2009; Martin & Hose 2010; Davie *et al.* 2015). The E-cells, or embryonic cells, are small cuboidal cells located at the blind end of the tubule and give rise to the three other cell types. F-cells, or fibrillar cells, are cylindrical/prismatic cells located among R- and B-cells, and synthesize enzyme for extracellular digestion (Barker & Gibson 1977; Felgenhauer 1992; Sousa *et al.* 2005; Franceschini-Vicentini *et al.* 2009). B-cells, or

blister cells, are large primary secretory cells producing digestive enzymes in the hepatopancreas and are responsible for intracellular digestion, concentrating the absorbed materials in the large vacuole and secreting the vacuolar content into the tubular lumen at the end of the digestive process for reabsorption by R-cells (Barker & Gibson 1977; Gibson & Barker 1979; Felgenhauer 1992; Franceschini-Vicentini *et al.* 2009). The R-cells, or reabsorption cells, are the most numerous cell types in the hepatopancreas. These tall and cylindrical columnar cells are characterized by a large number of irregularly-shaped storage vesicles (primarily lipids) in their cytoplasm. These cells function in food absorption, storage of lipid droplets, glycogen and mineral deposits and resemble the absorptive cells of the vertebrate intestine (Herreid & Full 1988; Felgenhauer, 1992; Sousa *et al.* 2005; Franceschini-Vicentini *et al.* 2009; Davie *et al.* 2015).

The embryological origin of the digestive system is different in vertebrates and invertebrates. In vertebrates, the foregut, midgut, and hindgut derive from the endoderm, and liver and pancreas arise from the ventral foregut endoderm (Zorn 2008). In crustaceans, the foregut and hindgut derive from the ectoderm, whereas the midgut is from the endoderm and the “hepatopancreas” arises from the anterior midgut endoderm (Felgenhauer 1992). The histological structure of the hepatopancreas is completely different from that of a vertebrate liver and pancreas. Moreover, most of the functions present in vertebrates are not described in Decapoda, such as secretion of bile salts, bile pigments and endocrine substances, liver-derived serum proteins or blood-clotting components, and ability to regulate the “blood” sugar level (Cornelius 1985). Furthermore, there are some processes occurring in decapods that are not found in liver and pancreas,

such as the reabsorption of extracellular digested food (Van Weel 1974). It is evident that the name "hepatopancreas" is an inappropriate one when used for decapods.

Is the "hepatopancreas" an organ or a gland? A gland is an organ derived from epithelial tissue, specialized to secrete or excrete materials not related to their ordinary metabolic needs: glands do not absorb or store nutrients. The name "gland" is too restrictive because it considers only the secretory function of the hepatopancreas, excluding its absorption and storage functions. The name "organ," a collection of tissues joined into a structural unit to serve common function, is more appropriate, being less specific than gland. The names "digestive organ" and "midgut organ" are also physiologically incorrect. "Digestive organ" is too broad and only descriptive, and it can refer to any of the organs of the digestive system. Moreover, this name does not describe the nutrient storage function of the organ. The name "midgut organ" is also inappropriate because the midgut is an organ itself and it can also refer to the midgut caeca.

The physiological role of the "hepatopancreas" as a nutrient absorptive organ has been suggested for at least 75 years and this organ in fact functions as a true intestine (Burgents *et al.* 2004). As a result, Van Weel (1974) coined the name "intestinohepatopancreas" for "hepatopancreas." The hepatopancreas is clearly a complex organ that incorporates many functions. These functions cannot be described using a single name, nor combining names of organs present in vertebrates with similar (but not identical) functions, such as liver, pancreas, and intestine. The hepatopancreas of vertebrates can be considered as an amalgamation of two organs (liver and pancreas) having different structures and functions. The hepatopancreas of decapods is a single organ with uniform structure serving different functions.

Therefore, in replacement of “hepatopancreas,” we suggest to name the structure after its precise location. We propose to call it the “perigastric organ” (PO), from *perigaster* (from the Greek *peri-*, for “around” or “enclosing,” and *gaster* for “stomach”). This organ occupies most of the cephalothorax, and surrounds and flanks the posterior part of the stomach. The name defines its location without reference to its physiological functions. The PO is a complex three-dimensional structure that consists of epithelial elements arranged in repetitive microscopic functional units. The functional unit of the PO is the tubule, lined by a simple columnar epithelium made up of four basic cell types (E-, F-, R- and B-cells). The PO serves five functions: the production and secretion of enzymes, intracellular digestion, absorption of nutrients, storage of metabolic reserves and minerals, and breakdown of toxic substances.

Other vertebrate organs have been named based on their position, such as “hypothalamus” (from the Greek *ipo-* for “under” and *thalamus*), “parathyroid” (from the Greek *para-* for “near” and *thyroid*), and suprarenal gland (from the Latin *supra* for “above” and *renes* for “kidney”).

There is great heterogeneity in the structure and function of accessory digestive organs in Mollusca and Crustacea. These glands perform analogous functions and differ in location, structure, and complexity (Cornelius, 1985). Future studies should review if the terminology in use in these taxa is appropriate.

When an improper name is frequently used, it becomes generally accepted and as such it appears in publications, especially textbooks. It is then difficult to have it replaced by more accurate ones (Van Weel, 1974). The name “hepatopancreas” is widely used, but this organ differs fundamentally from those of the liver, pancreas, and hepatopancreas

described in vertebrates. The proposed name "perigastric organ" and its equivalent "perigaster" would aid in standardizing the terminology of this key organ, minimizing confusion and misunderstanding between scientists.

References

- Barker, P.L. & Gibson, R. (1977) Observation on feeding mechanism, structure of gut, and digestive physiology of european lobster *Homarus gammarus* (L) (Decapoda-Nephropidae). *Journal of Experimental Marine Biology and Ecology*, **26**: 297–324.
- Bliss, D.E. (1983) General preface. In: *The Biology of Crustacea: systematics, the fossil record and biogeography*, **Vol. 1**, (ed. D.E. Bliss), pp. xiii–xiv. Academic Press, New York.
- Burgents, J.E., Burnett, K.G. & Burnett, L.E. (2004) Disease resistance of Pacific white shrimp, *Litopenaeus vannamei*, following the dietary administration of a yeast culture food supplement. *Aquaculture*, **231**: 1–8.
- Ceccaldi, H.J. (1989) Anatomy and physiology of digestive tract of crustacean decapods reared in aquaculture. Advances in tropical aquaculture, Tahiti, Feb. 20 - March 4, 1989, AQUACOP, IFREMER. Actes de Colloque, **Vol. 9**, pp. 243–259.
- Ceccaldi, H.J. (1997) Anatomy and physiology of the digestive gland. In: *Crustacean nutrition* (eds. L.R. D'Abramo, D.E. Conklin & D.M. Akiyama), pp. 261–291. Advances in World Aquaculture, **Vol. 6**. World Aquaculture Society, Baton Rouge, LA.
- Cornelius, C.E. (1985) Hepatic ontogenesis. *Hepatology*, **5**: 1213–1221.
- Dall, W. & Moriarty, D.J.W. (1983) Functional aspects of nutrition and digestion. In: *The Biology of Crustacea: internal anatomy and physiological regulation*, **Vol. 5** (ed. D.E. Bliss), pp. 215–261. Academic Press, New York.
- Davie, P.J.F., Guinot, D. & Ng, P.K.L. (2015) Anatomy and Functional Morphology of Brachyura. In: *Treatise on Zoology - Anatomy, Taxonomy, Biology. The Crustacea* (eds. P. Castro, P.J.F. Davie, D. Guinot, F. R. Schram & J. C. von Vaupel Klein), **9C-I**, pp. 11–163. Brill, Boston.
- Esteve, M. & Herrera, F.C. (2000) Hepatopancreatic alterations in *Litopenaeus vannamei* (Boone, 1939) (Crustacea: Decapoda: Penaeidae) experimentally infected with a *Vibrio alginolyticus* strain. *Journal of Invertebrate Pathology*, **76**: 1–5.
- Felgenhauer, B.E. (1992). Internal anatomy of the decapods: an overview. In: *Microscopic anatomy of invertebrates* (eds. F.W. Harrison & A.G. Humes), **10**: pp. 45–75. Wiley-Liss, New York.

Franceschini-Vicentini, I.B., Ribeiro, K., Papa, L.P., Marques, J., Vicentini, C.A. & Valenti, P. (2009) Histoarchitectural features of the hepatopancreas of the Amazon river prawn *Macrobrachium amazonicum*. *International Journal of Morphology*, **27**: 121–128.

Gibson, R. & Barker, P.L. (1979) The decapod hepatopancreas. *Oceanography and Marine Biology: an Annual Review*, **17**: 285–346.

Guieyese, A. (1906) Étude du système digestif de la langouste. *Bulletin de la Société Philomatique*, série 9, **6**: 117–128.

Herreid, C.F., & Full, R.J. (1988) Energetic and locomotion. In: *Biology of the land crabs* (eds. W.W Burggren & B.R. McMahon), pp. 341–345. Cambridge University Press, Cambridge, UK.

Hoppe-Seyler, F. (1877) Ueber Unterschiede in chemischen Bau und Verdauung höherer und niederer Tiere. *Pflügers Archiv – European Journal of Physiology*, **14**: 395–400.

Huxley, T.H. (1880) *The crayfish*. Appleton, New York.

Martin, G.G & Hose, J.E. (2010) Functional anatomy of penaeid shrimp. In: *The shrimp book* (ed. V. Alday-Sanz), pp. 47–72. Nottingham University Press, Loughborough, UK.

McGaw, I.J. & Curtis, D.L. (2013) A review of gastric processing in decapod crustaceans. *Journal of Comparative Physiology B*, **183**: 443–465.

McLaughlin, P.A. (1980) *Comparative morphology of Recent Crustacea*. W.H Freeman, San Francisco.

McLaughlin, P.A. (1983) Internal anatomy. In: *The biology of Crustacea: internal anatomy and physiological regulation*, **Vol. 5** (ed. D.E. Bliss), pp. 1–41. Academic Press, New York.

Nakamura, K. (1987) Classification of diverticular cells of the midgut gland in the prawn *Penaeus japonicus*. *Memoirs of Faculty of Fisheries Kagoshima University*, **36**: 207–214.

Nejedli, S. & Gajger, I.T. (2013) Hepatopancreas in some sea fish from different species and the structure of the liver in teleost fish, common pandora, *Pagellus erythrinus* (Linnaeus, 1758) and whiting, *Merlangius merlangus euxinus* (Nordmann, 1840). *Veterinarski Archiv*, **83**: 441–452.

Phillips, J.W., McKinney, R.J.W., Hird, F.J.R. & Macmillan, D.L. (1977) Lactic acid formation in crustaceans and the liver function of the midgut gland questioned. *Comparative Biochemistry and Physiology B*, **56**: 427–433.

Rőszer, T. (2014) The invertebrate midintestinal gland ("hepatopancreas") is an evolutionary forerunner in the integration of immunity and metabolism. *Cell and Tissue Research*, **358**: 685–695.

Sánchez-Paz, A., García-Carreño, F., Hernández-López, J., Muhlia-Almazán, A. & Yepiz-Plascencia, G. (2007) Effect of short-term starvation on hepatopancreas and plasma energy reserves of the Pacific white shrimp (*Litopenaeus vannamei*). *Journal of Experimental Marine Biology and Ecology*, **340**: 184–193.

Seyrafi, R., Najafi, G., Rahmati-Holasoo, H., Hajimohammadi, B. & Shamsadin, A.S. (2009) Histological study of hepatopancreas in iridescent shark catfish (*Pangasius hypophthalmus*). *Journal of Animal and Veterinary Advances*, **8**: 1305–1307.

Siebold, C.TH. (1848) *Lehrbuch der vergleichenden Anatomie der Wirbellosen Thiere*. Veir, Berlin.

Siebold, C.TH. (1874) *Anatomy of the Invertebrata*. James Campbell, Boston.

Sousa, L.G., Cuartas, E.I. & Petriella, A.M. (2005) Fine structural analysis of the epithelial cells in the hepatopancreas of *Palaemonetes argentinus* (Crustacea, Decapoda, Caridea) in intermoult. *Biocell*, **29**: 25–31.

Van Weel, P.B. (1974) Hepatopancreas? *Comparative Biochemistry and Physiology A*, **47**: 1–9.

Vasagam, K.P.K., Balasubramanian, T. & Venkatesan, R. (2007) Apparent digestibility of differently processed grain legumes, cow pea and mung bean in black tiger shrimp, *Penaeus monodon* Fabricius and associated histological anomalies in hepatopancreas and midgut. *Animal Feed Science and Technology*, **132**: 250–266.

Vonk, H.J. (1960) Digestion and metabolism. In: *The physiology of the Crustacea*, **Vol. 1** (ed. T.H. Waterman), pp. 291–311. Academic Press, New York.

Warburg, M.R. (2012) Reviewing the structure and function of the scorpion's hepatopancreas. *Arthropods*, **1**: 79–93.

Zorn, A.M. (2008) Liver development. In: *Stembook* (ed. L. Girard), pp. 1–26. The Stem Cell Research Community, StemB.

General discussion

The final goal of the present PhD was to develop a semi-quantitative histological method to monitor health in whiteleg shrimp using computer-assisted image analysis (CAIA) on microscopical sections. To monitor health, we focused on the hepatopancreas (HP), being the principal organ of the digestive tract and vulnerable to pathophysiological changes. The HP is site of synthesis and secretion of digestive enzymes, digestion and nutrients absorption, reserve storage, and detoxification (Laohabanjong *et al.* 2011).

Optimization of fixation methods for paraffin sections

The purpose of fixation is to preserve cells and tissue components in a “life-like state” by preventing autolysis and putrefaction. Inadequate fixation cannot be remedied at any later stage, and the finished section can only be as good as its primary fixation (Hopwood 2002). No matter how much care is subsequently taken in tissue processing, sectioning and staining, the morphological and histochemical information obtainable from the specimen will be compromised if fixation is not adequate. During fixation and the steps that follow, there are substantial changes to the composition and appearance of cell and tissue components. It is important to realize that fixatives produce a number of changes to the tissues, including shrinkage, swelling and hardening of various components. However, standardization of fixation and tissue processing can lead to consistent chemical and physical characteristics in tissue sections which allow patterns to be observed, morphological and chemical changes to be noted and comparisons to be made (Leica Biosystem 2017). Fixation of tissues can be achieved by chemical or physical means.

Physical methods include heating, micro-waving and cryo-preservation. Chemical fixation is achieved instead by immersion, injection or perfusion of the specimen in a chemical fixative solution. Chemical fixative solutions can contain a single fixative agent (dissolved in a solvent such as water, alcohol, or buffer solution) or several different fixing agents in combination (Kiernan 2008). Different fixing agents are used to compensate negative effects of one solution by the addition of another. In Davidson's fixative, for example swelling caused by acetic acid is present to counter the shrinkage caused by ethanol.

As inadequate or improper fixation makes histological sections unsuitable to be further processed for CAIA, the initial objective of this PhD was to develop a standardized operating protocol for sample collection and fixation. The rapid autolysis of the HP occurs immediately after death (Bell & Lightner 1988). Autolysis results in tissue digestion by intracellular enzymes released by rupture of organelle membranes, and bacterial decomposition or putrefaction brought by microorganisms which may already present in the specimen. Loss and diffusion of soluble substances must be avoided as far as possible by precipitation or coagulation of these components or by cross-linking them to other insoluble structural components. Through comparison of different fixatives (Davidson, Bouin, formaldehyde, Carnoy and Zinc salt based fixatives) and techniques (immersion and injection), it was ascertained that Davidson's fixative injected directly into the organ resulted in the best fixation quality. In our experience, for juvenile and adult shrimp immersion in the fixative was shown to be insufficient. The HP lobes are surrounded by a capsule of connective tissue that slows down the penetration rate of the fixative within the organ. During injection, artefacts are created at each injection point, modifying the normal morphology and architecture of the organ. Therefore, multiple injections into the HP are

not recommended. We suggest one single injection lateral to the HP in the right or left lobe using a small needle (26/28 Gauge). However, even when fixative is injected once, a certain degree of artefacts cannot be completely avoided. The increase of the volume injected from the previously recommended 10% (Bell and Lightner's protocol) to our recommendation of 30% of the body weight improved the fixation of the organ. Ten percent is not sufficient to preserve the morphology and tissue architecture of the entire organ: the HP is often fixed only in the outermost layers resulting in the detachment of the tubules from the basal membranes in the innermost layers and consequently the alteration of the normal tubular architecture, causing the specimen to be unsuitable for CAIA. Shrimp should be fixed immediately after sampling in both laboratory and field conditions. It is crucial to fix the shrimp while still alive, immediately after sedation in cold ice. Delays of few seconds in the injection can determine improper fixation. If ice is not available on a farming site, we recommend refrigerating the fixative, to minimize the time occurring between injection and death of the animal and to slow down the enzymatic activity of the organ. The use of this protocol for paraffin sections can be used in both laboratory and field conditions, and facilitates the preparation of consistently samples for sectioning, staining and subsequent automated analysis.

Optimization of fixation methods for frozen sections

Chemical fixation and paraffin wax continue to be the most popular procedure for histological analysis. However, alcohol-soluble tissue lipids are extracted during the dehydration process, and if lipids have to be demonstrated paraffin sections are not adequate (Bancroft & Marylin 2002). In the past, some alternatives were proposed to

overcome lipid extraction, including plastic embedding (Van Goor *et al.* 1986) and fixation of lipids in formaldehyde-fixed samples (Tracy & Walia 2002). We tested both methodologies (data not shown) but we found them to be time-consuming and not successful. However, this alternative approach could be worthy of further investigation and future studies should evaluate more thoroughly the potential of plastic embedding for the preserving lipids in the HP. In general, plastic embedding preserves morphology better than frozen sections. Cryosectioning is the standard method for lipid preservation in histology (Hopwood 2002). We focused then on the optimization of frozen sections. We optimized Oil Red O staining for identifying neutral lipids and fatty acids. This is a simple staining that can be used for both fresh smears and frozen sections. Cryo-sectioning adversely affects morphology of the sections, because crystal formation disrupts the cells, and freezing rate is critical to control ice crystal formation and thus cell disruption. The methodology proposed for frozen sections requires snap freezing in liquid nitrogen followed by storing samples in cold ice. Because of these substances, this methodology can only be implemented in specialist laboratories with little feasibility of application on farming sites. To overcome these limitations, in a recent experiment (data not shown) we test Oil Red O staining on fresh smears of the HP for preservation of lipid droplets (Figure 1).

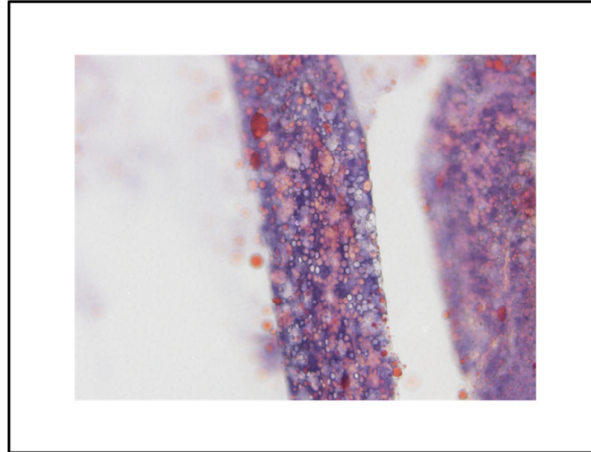


Fig.1 Oil Red O staining on fresh smears of the hepatopancreas of whiteleg shrimp (*Penaeus vannamei*).

This methodology is fast (requires about 20 minutes), straightforward and can be adopted in field conditions. Fresh smears are fixed with heat, stained with Oil Red O and counterstained with haematoxylin and eosin. In the future, protocols for fresh smears should be further optimized and validated on both well-fed and starved shrimp. The comparison between fresh smears and CAIA on frozen sections could permit the development of scoring tables containing images that can be used in the field to evaluate the lipid droplet content in the HP. Because of the linear relationship between nutritional status and lipid droplet content, these tables could allow farmers to assess if shrimp are well-fed and adapt consequently the feeding regime.

Optimization of staining protocols for image analysis

CAIA refers to the field of using computer algorithms to extract quantitative information from digital images of sections (Kårnsnäs 2014). During image classification/segmentation, the image is portioned into multiple segments, each of which corresponds to a group of

pixels that share common visual characteristics (colour, intensity, etc). Maximization of staining uniformity and minimization of staining variability are then fundamental for accuracy and reproducibility of image processing protocols (Kothari *et al.* 2013; McCann *et al.* 2015). Manual staining cannot guarantee staining uniformity and automated stainers are crucial for staining sections. However, staining intensity can also vary from batch to batch when an automated stainer is used, greatly affecting the whole image analysis process. Classical automated stainers contain different stations (boxes filled with reagents) arranged in a circle or a line. Batches of slides (usually around 20 per cycle) are stained by consecutive programmed movement of holders. If reagents within boxes are not substituted after each batch, staining uniformity is not guaranteed. Even the use of the same consumables provided by different suppliers can result in different staining intensities. Recently, automated stainers, such as the Ventana BenchMark (Ventana Medical Systems, Roche Ltd) adopted a different system, where reagents are dropped directly on the single section, similar to automatic stainers for IHC. These newer machines are recommended for maximal staining uniformity (He *et al.* 2012; Miedema *et al.* 2012; Nativ *et al.* 2014).

We recommend storing some control paraffin blocks to check the impact of different consumables on the developed image analysis protocols. The comparison between the quantitative data generated with different consumables allows validating or adapting the existing protocols or the need to develop new ones.

Ideally for image analysis of the HP, stainings should be selective for each of the cell types comprising the tubular epithelium (F-, B-, E- and R-cells).

Development of immunohistochemistry (IHC), *in situ* hybridization methods and testing of other stainings for targeting specific structures and pathogens should be investigated for future development of image analysis of the HP.

Role of computer-assisted image analysis (CAIA)

In crustaceans, routine histological assessments are core to diagnostic laboratories (Lightner & Redman 1998). However, classic diagnostic methods have some limitations in both human and veterinary medicine. The analysis of tissue sections depends on the experience and expertise of histopathologists, it is time consuming and subjective. To overcome these limitations, CAIA has been developing fast in the last years in human medicine. CAIA does not replace the pathologist, but increases the amount and quality of data derived from a histological specimen, providing quantitative measurements to assist the pathologist in the slide interpretation (Fuchs & Buhmann 2011; He *et al.* 2012; Miedema *et al.* 2012; Nativ *et al.* 2014). CAIA is fast, objective and is suitable for high throughput data. Visiopharm® software is currently mainly used for cancer diagnostic in human medicine and specific protocols (called APPs) are already available in the market for the detection of specific cell structures/markers. In the Skretting Aquaculture Research Centre, CAIA has been used in the past seven years for semi-quantitative histology on skin, gills and intestine of different farmed fish species for morphological studies and pathogen detection.

Visiopharm® offers APPs “ready to use” for specific staining and IHC. However, the methodology is quite expensive, both for the software and the hardware. It also demands intensive training of the operator for familiarizing with the software and time for the development of customized image analysis protocols. It is not recommended for every

histology laboratories but only for reference centres, where operators can use it on a daily basis. Moreover, APPs have to be validated carefully before implementation to avoid generation of false data. Image segmentation/classification is the most crucial step during the image analysis workflow and mistakes during this step cannot be easily corrected during post-processing.

Selection of morphological parameters for computer assisted image analysis (CAIA)

Three image analysis protocols were developed and validated for the quantification of morphological parameters of the HP. Ratio of Haemocyte Infiltration Area to Total Tissue Area (HIA:TTA, or inflammatory index) and ratio of Lipid Droplet Area to Total Tissue Area (LDA:TTA, or nutritional index) have the potential to be used in the future respectively for detecting early inflammatory stages and evaluate the nutritional status of shrimp.

Ratio of Vacuoles B-cells Area and F-Cell Area to Total Tissue Area (VBA:TTA and FCA:TTA) have the potential to be used for monitoring the intracellular digestion and enzyme production in the HP. However, because of some difficulties in the development of protocols for detecting these structures (VBA measures only the vacuole area and Toluidine Blue for FCA was not counterstained), we recommend in the future to develop specific IHC stainings for both B- and F-cells. IHC could be developed by laser capture dissection or centrifugal elutriation of the different cell types and production of monoclonal antibodies targeting enzymes present in the cells (Vogt *et al.* 1989; Emmert-Buck *et al.* 1996; Espina *et al.* 2007)

For all the morphological parameters, ratios were indicated as % of TTA. Total Tissue Area (TTA) has some limitations, representing not only the total area covered by tubular

epithelium (B-, F- and R-cells), but also including the intertubular space. The intertubular space is the space where haemolymph circulates within the HP. It is in fact extremely difficult to train the software to recognize automatically the connective tissue with haematoxylin and eosin staining. Masson Trichrome staining could help in the identification of connective tissue, but it would require the development of a separate image analysis protocol. It is difficult for the software to distinguish the intertubular space from the lumen when the latter is reduced. It is possible for the operator to correct the post-processing manually but we recommend keeping the protocols as much automated as possible to minimise operator bias. We preferred to optimise the protocol HIVB for both detection of haemocytes using IHC and haematoxylin and eosin for vacuoles of B-cell. Total Lumen Area (TLA) represented the area covered by tubular lumen.

All these morphological parameters can only be interpreted within properly controlled trials. There are no standard reference values that have been established for any of these indices yet. The ratio TLA:TTA indicated the variation of tubular lumen, tubular epithelium thickness and intertubular space. Atrophy of the tubular epithelium determines a reduction of TTA and subsequently increase of TLA, determining an increase of TLA:TTA. Hypertrophy of the tubular epithelium determines an increase of TTA and subsequently decrease of TLA, determining a reduction of TLA:TTA. At the same time, during inflammation an increase of the intertubular space due to the migration of haemocytes and production of connective tissue can increase TTA value even if the tubular epithelium is reduced in thickness. These potential cases are speculative and future studies should verify if the presented scenarios are correct or not.

To overcome the limitation of the morphological parameter TTA, we recommend in the future calculating TTA by subtracting the lumen area to the tubular epithelium (Figure 2). The tubular epithelium could be identified developing IHC targeting the basal lamina of the tubule. By doing this the intertubular space will not be counted as part of TTA.

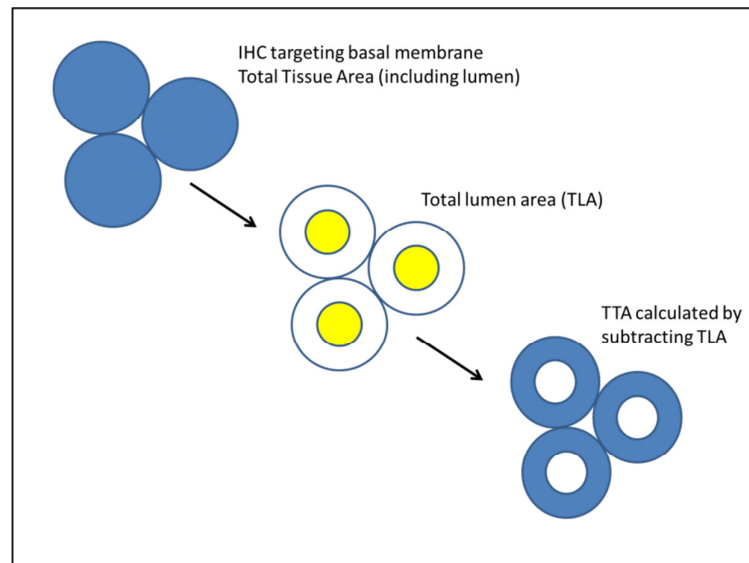


Fig.2 Schematic drawing for the potential development of image analysis protocols for the calculation of the total tissue area (TTA) of the hepatopancreas of whiteleg shrimp (*Penaeus vannamei*) by immunohistochemistry targeting the basal lamina of the tubule.

Effect of starvation and refeeding on the HP morphology using computer assisted image analysis on light microscopy

Shrimp experience starvation periods during moulting, disease outbreaks and adverse environmental conditions (Lavilla-Pitogo *et al.* 1998; Sacristán *et al.* 2016). In the present PhD, CAIA was used to study the effect of starvation and starvation followed by refeeding on the HP morphology and evaluate whether or not these morphological changes were

reversible over time. Shrimp can partially recover when starved for five days and subsequently refed for ten days.

Longer periods of refeeding might be necessary for a complete restitution of the lipid droplets within R-cells and a reduction of the haemocytic infiltration in the intertubular spaces of the HP. Data extracted using CAIA on light microscopy indicated that F-cells and B-cells did not react to the different feeding regimes. F-cells and B-cells are responsible respectively for enzyme production and intracellular digestion. However, on electron microscopic level, R- and F-cells reacted to the different feeding regimes, while B-cells were not apparently affected. We elaborated three hypothesis to interpret the lack of variation of VBA and FBA during starvation. One, starvation could not have an influence on F- and B-cells. Two, the decrease in number of cells is compensated by the increase in area due to the swelling of the cell caused by reversible tissue damage. Three, the decrease in the area is compensated by the increase of cell number. Further research is needed to calculate the mitotic index of B and F-cells and to develop image analysis protocols cable to quantify the number of cells. For F-cells, the combination of nuclear staining and toluidine blue could allow to quantify the number of cells by counting the nuclei surrounded by FCA. For B-cells, VBA does not quantify the area of the cell but the vacuole area. The same approach then is not feasible and the nucleus is not centrally located in the B-cell. Development of IHC for B-cell should allow in the future to quantify the total area and number of B-cells. Moreover, CAIA should also investigate if starvation and refeeding affect the E-cell population, by developing specific IHC and image analysis protocols for the embryonic cells.

Effect of starvation and refeeding on the HP morphology using electron microscopy

Transmission electron microscopy was used to study the ultrastructural changes in the HP caused by starvation and refeeding and correlate them to the light microscopic findings. Ultrastructural changes were observed in R- and F-cells, while B-cells were not apparently affected by food deprivation. Signs indicating potential autophagy and necrosis were the main ultrastructural changes observed during starvation and refeeding, while apoptosis was rarely observed.

Electron microscopic findings supported the light microscopic results, indicating that starvation is mainly characterized by lipid depletion, haemocytic infiltration and degenerative processes typical of cell death. Electron microscopy could be also used in the future to measure the area of the different cell types of the tubule to better understand the influence of starvation and refeeding on the cell population.

Transmission electron microscopy has the potential to be used in the future to further clarify the degenerative cell processes occurring during disease outbreaks or more prolonged starvation periods.

Terminology for the hepatopancreas

At present, the HP in crustaceans has been named using different terms, creating confusions between researchers. The HP is not a liver, pancreas or a combination of both organs. It is an organ, with a peculiar structure that is not comparable with any organ in vertebrates. We reviewed the terms adopted in the past considering the gross anatomy, histology and physiology of the organ and concluded that the term “hepatopancreas” was not appropriate when applied to this organ in the Decapoda. We decided then to propose

the new name of *perigaster* (or perigastic organ) considering primarily the topography of the organ, following the convention of certain other organs in human and veterinary anatomy. Future studies should evaluate if the appropriateness of the name “hepatopancreas” in the other crustacean groups.

Conclusions and future perspectives

The optimization of fixation stainings methods permitted the development of CAIA on light microscopic sections for monitoring morphological parameters of the HP in whiteleg shrimp. CAIA showed great potential for its efficiency, accuracy and reproducibility. However, more research has to be conducted for improving the image analysis protocols for overcoming the limitations of the current developed method. The main finding of this PhD can be considered as a starting base to implement image analysis in the shrimp histology labs for diagnosis purposes and to start collecting reference values of the developed morphological parameters to be used for screening health in crustaceans. The same principles applied for the HP can be used in the future for implementing CAIA in different organs in various crustacean species.

Based on the findings described on this PhD, future research should consider in the future:

- ✓ to use of laser capture microdissection or centrifugal elutriation for isolating different cell types of the HP for the development of antibodies allowing to stain selectively F-, B, R, and E-cells in immunohistochemistry;
- ✓ to develop “ready to use” image analysis protocols for immunohistochemistry and identification of new morphological parameters in the HP and gastro-intestinal tract to monitor health;
- ✓ to collect reference values of the developed morphological parameters to be used for screening health in crustaceans;
- ✓ to study the effect of long term starvation on the HP with CAIA and electron microscopy (identify point of no return);
- ✓ to apply quantitative measurement for cell death with electron microscopy.

References

- Bell T.A. & Lightner D.V. (1988) *A handbook of normal penaeid shrimp histology*, pp. 2-6. The World Aquaculture Society, Baton Rouge.
- Emmert-Buck, M.R., Bonner, R.F., Smith, P.D., Chuaqui, R.F., Zhuang, Z., Goldstein, S.R., Weiss, R.A. & Liotta, L.A. (1996) Laser capture microdissection. *Science*, **274**, 998-1001.
- Espina, V., Heiby, M., Pierobon, M. & Liotta, L.A. (2007) Laser capture microdissection technology. *Expert Review of Molecular Diagnostics*, **7**, 647-657.
- Fuchs, T.J. & Buhmann, J.M. (2011) Computational pathology: challenges and promises for tissue analysis. *Computerized Medical Imaging and Graphics*, **35**, 515-530.
- He, L., Long, L.R., Antani, S. & Thoma, G.R. (2012) Histology image analysis for carcinoma detection and grading. *Computer Methods and Programs in Biomedicine*, **107**, 538-556.
- Hopwood D. (2002) Fixation and fixatives. In: *Theory and practice of histological techniques* (ed. by J. D. Bancroft & GM. Gamble), pp. 67-68. Elsevier Health Publications, Edinburgh.
- Kårsnäs A. (2014) Image analysis methods and tools for digital histopathology applications relevant to breast cancer diagnosis. *Digital Comprehensive Summaries of Uppsala Dissertations from the Faculty of Science and Technology* 1128, pp. 129. Uppsala.
- Kothari, S., Phan, J.H., Stokes, T.H. & Wang, M.D. (2013) Pathology imaging informatics for quantitative analysis of whole-slide images. *Journal of the American Medical Informatics Association*, **20**, 1099-1108.
- Lavilla-Pitogo, C.R., Leño, E.M. & Paner, M.G. (1998) Mortalities of pond-cultured juvenile shrimp, *Penaeus monodon*, associated with dominance of luminescent vibrios in the rearing environment. *Aquaculture*, **164**, 337-349.
- Mccann, M.T., Ozolek, J.A., Castro, C.A., Parvin, B. & Kovacevic, J. (2015) Automated Histology Analysis Opportunities for signal processing. *Ieee Signal Processing Magazine*, **32**, 78-87.
- Miedema, J., Marron, J.S., Niethammer, M., Borland, D., Woosley, J., Cposky, J., Wei, S., Reisner, H. & Thomas, N.E. (2012) Image and statistical analysis of melanocytic histology. *Histopathology*, **61**, 436-444.
- Nativ, N.I., Chen, A.I., Yarmush, G., Henry, S.D., Lefkowitz, J.H., Klein, K.M., Maguire, T.J., Schloss, R., Guarrera, J.V., Berthiaume, F. & Yarmush, M.L. (2014) Automated

image analysis method for detecting and quantifying macrovesicular steatosis in hematoxylin and eosin-stained histology images of human livers. *Liver Transplantation*, **20**, 228-236.

Sacristán, H.J., Ansaldo, M., Franco-Tadic, L.M., Gimenez, A.V.F. & Greco, L.S.L. (2016) Long-Term Starvation and Posterior Feeding Effects on Biochemical and Physiological Responses of Midgut Gland of *Cherax quadricarinatus* Juveniles (Parastacidae). *PLoS one*, **11**, e0150854.

Tracy R.E. & Walia P. (2002) A method to fix lipids for staining fat embolism in paraffin sections. *Histopathology* **41**, 75-79.

Van Goor H., Gerrits P.O. & Grond J. (1986) The application of lipid-soluble stains in plastic-embedded sections. *Histochemistry* **85**, 251-253.

Vogt, G., Stocker, W., Storch, V. & Zwilling, R. (1989) Biosynthesis of *Astacus* protease, a digestive enzyme for crayfish. *Histochemistry*, **91**, 373-381.

Summary - Samenvatting

Summary

The aquaculture of penaeid shrimp has grown from its experimental beginnings roughly three decades ago into a major industry. Almost from the start, diseases and adverse environmental conditions were recognized as threats to the shrimp industry, causing serious economic losses. Clinical examination of penaeid shrimp largely relies upon histological analysis, which is subjective and time consuming. Computer-assisted image analysis (CAIA) is instead faster, objective and suitable for routine screening; however it requires standardized protocols.

In the General introduction, we described the anatomy, histology and physiology of the gastro-intestinal tract of whiteleg shrimp (*Penaeus vannamei*), focusing mainly on the hepatopancreas (HP), being responsible for digestion, absorption and storage of nutrients in decapods. The first critical step was to ensure appropriate fixation of the target tissue. Bell and Lightner's (1988) fixation protocol (injection of Davidson's fixative), widely used for routine histology of paraffin sections, had not been optimized for image analysis and no protocol for frozen sections was described in literature. Therefore the aim of Chapter 1 was to optimize the fixation of the HP from whiteleg shrimp for both paraffin sections (for morphology) and frozen sections (for lipid detection) using a semi-quantitative scoring system. For paraffin sections, four injection volumes and three injection methods, and for frozen sections four freezing methods and four fixation methods were compared. For paraffin sections optimal fixation was achieved by increasing three fold the fixative volume

recommended by Bell and Lightner, from 10% to 30% of the shrimp body weight, combined with single injection into the HP. Optimal fixation for frozen sections was achieved by freezing the cephalothorax with liquid nitrogen, followed by fixation of the section with 60% isopropanol. The aim of Chapter 2 was then to develop CAIA in whiteleg shrimp for the study of HP. Paraffin sections were immunohistochemically stained with monoclonal antibodies WSH8 against haemocytes and counterstained with Mayer's haematoxylin for detection of haemocytes and B-cell vacuoles, and modified Toluidine Blue protocol was used for detection of F-cells; frozen sections were stained with Oil Red O for detection of lipid droplets within R-cells. Visiopharm® software was used to develop and validate protocols for the quantification of morphological parameters (areas of haemocyte infiltration, F-cells, B-cell vacuoles, lipid droplets and their ratios to total tissue area and total lumen area). These protocols were then used for determination of the nutritional condition of the HP. Under normal farming conditions, shrimp can experience starvation periods attributable to disease outbreaks or adverse environmental conditions. Starvation leads to significant morphological changes in the HP. In literature, limited research has described the effect on the HP of periods of starvation followed by refeeding, and none in whiteleg shrimp using CAIA. Chapter 3 described the effect of starvation and starvation followed by refeeding on the HP of whiteleg shrimp using CAIA. Visiopharm® software was used to quantify the following morphological parameters, measured as ratio to the total tissue area (TTA): total lumen area (TLA:TTA), haemocytic infiltration area in the intertubular spaces (HIA:TTA), B-cell vacuole area (VBA:TTA), lipid droplet area within R-cells (LDA:TTA), and F-cell area (FCA:TTA). Significant changes were measured for HIA:TTA and LDA:TTA during starvation (increase of HIA:TTA

associated with decreased of LDA:TTA) and starvation followed by refeeding (decrease of HIA:TTA associated with increase of LDA:TTA). Chapter 4 described the ultrastructural changes in the HP of whiteleg shrimp occurring during starvation and refeeding using transition electron microscopy. Starvation induced a progressive increase of cellular immunity (haemocytic infiltration, both hyaline and granular/semigranular haemocytes), potential indicators of necrosis (swelling of organelles and cytolysis), and autophagy (formation of phagophores, autophagosomes, multivesicular and residual bodies). The complete depletion of lipid droplets and a few signs of apoptosis (chromatin condensation and nuclear fragmentation) were observed during starvation. Refeeding did not result in a complete recovery of the HP. The present findings should contribute in the future to better understand the impact of starvation on the HP and shrimp health, and describe the different cell death types occurring in crustaceans during disease outbreaks and adverse environmental conditions.

Since its first description in 1848, many names have been given to the key organ of the gastro-intestinal tract of Decapoda, which have caused much confusion. Even the most commonly accepted name, “hepatopancreas,” is inappropriate because this organ inherently differs from the liver and pancreas of vertebrates. In Chapter 5 we briefly discussed the embryology, gross anatomy, histology, and physiology of the “hepatopancreas.” The names “perigastric organ” and “perigaster” (from the Greek *peri-* for “around” and “enclosing,” and *gaster* for “stomach”) were proposed as a replacement of “hepatopancreas.”

In the General discussion, the main findings of each chapter were critically discussed and conclusions were drawn. The optimization of fixation methods and staining and the

development of CAIA for the HP represented a solid background for future use of CAIA in crustaceans. In the future, the technical knowledge generated in this thesis could be used in a pre-emptive manner to monitor the health of the HP, facilitate early diagnosis of diseases and study the pathophysiology of the organ

Samenvatting

De aquacultuur van Penaeidae-garnalen is de laatste drie decennia enorm in omvang toegenomen. Maar reeds vanaf het prille begin had de sector te kampen met ongunstige omstandigheden en ziekte uitbraken, met serieuze economische verliezen tot gevolg. Het klinisch onderzoek van deze garnalen is voor een groot stuk gebaseerd op histologisch onderzoek, wat toch tijdrovend en enigszins subjectief is. Computergestuurde beeldanalyse (computer-assisted image analysis, CAIA) daarentegen is sneller, objectief, en geschikt voor een eerste routine screening. Een belangrijke voorwaarde echter is dat alle stappen in dit proces volgens een gestandaardiseerde methode dienen te verlopen.

In de Algemene Inleiding wordt de anatomie, histologie en fysiologie van het gastro-intestinaal kanaal van de Witpootgarnaal *Penaeus vannamei* beschreven, waarbij voornamelijk de hepatopancreas (HP), in Decapoda verantwoordelijk voor de vertering, absorptie en opslag van nutriënten, besproken wordt. Een eerste belangrijke stap is een efficiënte fixatie van dit orgaan. Het fixatieprotocol van Bell en Lightner (1988) dat op dit ogenblik het meest gebruikt wordt voor het vervaardigen van paraffinecoupes, is echter niet geoptimaliseerd voor het gebruik van computergestuurde beeldanalyse van deze weefselcoupes. Bovendien is een gestandaardiseerd protocol voor het maken van vriescoupes niet voorhanden.

Daarom werd in Hoofdstuk 1 de procedure voor het fixeren van de hepatopancreas voor het maken van zowel paraffinecoupes als vriescoupes die beiden gebruikt kunnen worden voor computergestuurde beeldanalyse, geoptimaliseerd. Voor het vervaardigen van paraffinecoupes werden drie injectiemethoden en vier injectievolumes getest en vergeleken; voor het maken van vriescoupes werden vier invriesmethoden en vier

fixatieven gebruikt. In het geval van de paraffinecoupes werd de beste fixatie bekomen door driemaal zoveel fixatief als beschreven door Bell en Lightner (namelijk 30% in plaats van 10% van het lichaamsgewicht) te injecteren als één dosis in de hepatopancreas. De optimale invriesmethode voor het maken van vriescoupes bestond erin de cephalothorax als dusdanig onder te dompelen in vloeibare stikstof en nadien de vriescoupes te fixeren in 60% isopropanol. In Hoofdstuk 2 wordt vervolgens de ontwikkeling van de protocols voor de computergestuurde beeldanalyse van de histologische coupes van de hepatopancreas beschreven. Hiervoor werden paraffinecoupes immunohistochemisch gekleurd, gebruik makend van de antistoffen WSH8, voor het aankleuren van de haemocyten, en tegengekleurd met Mayer's haematoxyline voor de detectie van de vacuolen in de B-cellen. Een gemodificeerde toluidineblauw kleuring werd toegepast op paraffinecoupes om de F-cellen aan te tonen. Op de vriescoupes werd een Oil Red O kleuring toegepast om de vetvacuolen, aanwezig in de R-cellen te kleuren. De software Visiopharm® werd gebruikt om de volgende morfologische parameters automatisch te kwantificeren, uitgedrukt in oppervlakte-eenheid: totale lumen (total lumen area, TLA), haemocyten-infiltratie in de intertubulaire ruimte (haemocytic infiltration area, HIA), B-cel vacuolen (vacuoles B-cell area, VBA), vetvacuolen in de R-cellen (lipid droplet area, LDA), en de F-cellen (F-cell area, FCA). Al deze parameters werden vervolgens uitgedrukt als een verhouding tot het totale weefsel oppervlak (total tissue area, TTA). Deze beeldanalyseprotocols werden vervolgens gebruikt om de morfologie van de hepatopancreas bij bepaalde nutritionele condities te evalueren. In aquacultuuromstandigheden worden garnalen regelmatig geconfronteerd met periodes van uithongering. Deze uithongering kan tot significante morfologische veranderingen

leiden ter hoogte van de hepatopancreas. In Hoofdstuk 3 wordt dan ook het effect van gecontroleerde uithongering en uithongering gevolgd door voederen, op de hepatopancreas van de Witpootgarnaal beschreven. Significante verschillen werden opgemerkt voor de HIA:TTA en LDA:TTA verhoudingen tijdens het uithongeren (namelijk een toename van de HIA:TTA verhouding na verloop van tijd, geassocieerd met een afname van de LDA:TTA verhouding), en tijdens het uithongeren gevolgd door voederen (namelijk een afname van de HIA:TTA verhouding en een toename van de LDA:TTA verhouding). In Hoofdstuk 4 worden de ultrastructurele veranderingen ter hoogte van de hepatopancreas van de Witpootgarnaal beschreven, zowel tijdens uithongeren als uithongeren gevolgd door voederen. Uithongering induceert een progressieve toename van de cellulaire immuniteit (infiltratie van zowel hyaliene als granulaire en semigranulaire haemocyten), necrose (zwellen van verschillende organellen, cytolyse), en autofagie (vorming van fagoforen, autofagosomen, multivesiculaire lichaampjes, en residuele lichaampjes). Bovendien verdwenen de vetvacuolen volledig tijdens uithongeren en werden enkele tekenen van apoptose waargenomen (chromatine condensatie, nucleaire fragmentatie). Opnieuw voederen resulteerde niet in een volledig herstel van de hepatopancreas.

Sinds de eerste beschrijving in 1848 werden verschillende namen gegeven aan het belangrijke orgaan in het gastro-intestinaal kanaal van Decapoda, wat vaak leidde tot verwarring. Zelfs de meest gebruikte benaming “hepatopancreas” is eigenlijk niet geschikt, aangezien dit orgaan duidelijk verschilt van de lever en pancreas van vertebraten. In Hoofdstuk 5 wordt kort de embryologie, anatomie, histologie en fysiologie van de “hepatopancreas” aangehaald. De namen “perigastrisch orgaan” en “perigaster”

(gebaseerd op het Grieks *peri-* wat “rondom” en “omheen” betekent, en *gaster* wat “maag” betekent) werden voorgesteld als nieuwe benaming voor de hepatopancreas.

In de Algemene Discussie tenslotte worden de belangrijkste bevindingen van elk hoofdstuk kritisch bediscussieerd en worden enkele conclusies getrokken. Het optimaliseren van de fixatiemethodes en kleurprotocols enerzijds, en het ontwikkelen van enkele automatische computergestuurde beeldanalyseprocessen anderzijds, vormt een soliede basis voor het verder gebruik van deze beeldanalyse. In de nabije toekomst kan deze knowhow gebruikt worden om op een preventieve manier de gezondheidsstatus van garnalen te monitoren, en vroegtijdig ongunstige leefomstandigheden en zelfs ziekte uitbraken te detecteren.

Aknowledgements

I would like to thank Skretting ARC and the Research Council of Norway for sponsoring this research project. In particular, dr. Charles McGurk, dr. Alex Obach and all Skretting colleagues who supported me during these three years.

I would like to thank prof. Wim Van den Broeck for his support, availability and valuable, constructive help throughout these years. Many thanks to Lobke De Bels, Jurgen De Craene, Liesbeth Couck and and Bart De Pauw for their excellent technical assistance.

I would like to thank prof. Geert Wiegertjes from Wageningen University and dr. Karin van Den Braak for their collaboration and for providing monoclonal antibodies.

Many thanks to my family and close friends for their support and love.

Curriculum vitae

Fabio Cervellione was born on August 4th, 1980.

He took his degree in Veterinary Medicine at the University of Milan in 2004 with a thesis entitled “Experimental infection with *Flavobacterium psychrophilum* in rainbow trout (*Oncorhynchus mykiss*) by intraperitoneal and bath challenges”. Then he moved to Scotland, where he took the title of MSc in Aquatic Veterinary Studies at the University of Stirling in 2005, with a thesis entitled “Detection of aquatic mycobacteria using single and duplex PCR”. From 2005 to 2014, he worked for Skretting Italy (fish and shrimp feed company) as veterinarian- technical and sales advisor for fresh water species. In same the period, from 2008 to 2010, he attended a three-year post-graduate course for veterinarians at the University of Milan, getting the title of Specialist in food inspection, safety, breeding and disease of aquatic animals and their products, with a thesis entitled “Red Mark syndrome in rainbow trout (*Oncorhynchus mykiss*) farmed in North Italy: anatomopathology, histology and aetiology”. In 2014 he moved to Norway and joined Skretting Aquaculture Research Center as junior researcher for the Health Department, as PhD candidate at Ghent University.

Presenter at six international conferences, co-author of seven peer-reviewed papers, two conference proceedings and four posters.

Bibliography

Publications:

Manfrin, A., Tonon, P., Cervellione, F., Qualtieri, K., Selli, L. & Bovo G. (2005) Experimental infection with *Flavobacterium psychrophilum* in rainbow trout (*Oncorhynchus mykiss*) by intraperitoneal and bath challenges. *Ittiopatologia*, 2: 171-182.

Pourahmad, F., Cervellione, F., Thompson, KD, Taggart, JB, Adams, A. & Richards, RH (2008) *Mycobacterium stomatepieae* sp. nov., a slowly growing, non-chromogenic species isolated from fish. *International Journal of Systemic and Evolutionary Microbiology*, 58 (12): 2821-7.

Salogni, C., Cervellione, F., Guarnera, S., Mioso, PM, Zanoni, M., Giovannini, S. & Alborali, GL (2010) Gram positive cocci infections in *Acipenser baeri* reared in the Po Valley. *Ittiopatologia*, 7: 25-32.

Cervellione, F., McGurk, C., Silva, P., Owen, MAG & Van den Broeck, W. (2016) Optimization of fixation methods for image analysis of the hepatopancreas in whiteleg shrimp, *Penaeus vannamei* (Boone). *Journal of Fish Diseases*, doi:10.1111/jfd.12531.

Cervellione, F., McGurk, C., Berger Eriksen, T. & Van den Broeck, W. (2016) Use of computer-assisted image analysis for semi-quantitative histology of the hepatopancreas in whiteleg shrimp *Penaeus vannamei* (Boone). *Journal of Fish Diseases*, doi:10.1111/jfd.12599.

Cervellione, F., McGurk, C. & Van den Broeck, W. (2017) Effect of starvation and refeeding on the hepatopancreas of whiteleg shrimp *Penaeus vannamei* (Boone) using computer-assisted image analysis. *Journal of Fish Diseases*, doi:10.1111/jfd.12599.

Cervellione, F., McGurk, C. & Van den Broeck, W. (2017) “Perigastric organ”: a replacement name for the “hepatopancreas” of Decapoda. *Journal of Crustacean Biology*, doi: 10.1093/jcbiol/rux020.

Oral presentations:

Cervellione, F., Rogato, F., Sarti, M. & Luzzana U. (2013) Protec: a nutritional approach for controlling nodavirus in sea bass (*Dicentrarchus labrax*). *XIX National Conference S.I.P.I.*, 35, Siracusa, Italy.

Cervellione, F., Rogato, F., Sarti, M., Luzzana, U. & Zarza Araque, C. (2011) Preliminary investigations on usage of rapid test for stress assessment in field. *XVII National Conference S.I.P.I.*, 36, Ostuni, Italy.

Sarti, M., Cervellione, F., Giusto, C., Manzano, M., Pecchini, A. & Luzzana U. (2008) Gut microflora modulation as a control strategy for rainbow trout gastro enteric syndrome (RTGE). *XV National Conference S.I.P.I.*, 23, Erice, Italy.

Cervellione, F., McGurk, C., Berger Eriksen, T. & Van den Broeck, W. (2016) Use of image analysis on paraffin and frozen sections of the hepatopancreas in whiteleg shrimp *Penaeus vannamei*. *The Crustacean Society Mid-year meeting*, 31, Singapore.

Cervellione, F., McGurk, C., Berger Eriksen, T. & Van den Broeck, W. (2016) Effect of starvation on the hepatopancreas of whiteleg shrimp *Penaeus vannamei* using computer-assisted image analysis on paraffin and frozen sections. *3rd International Conference on Aquaculture & Fisheries*, 62, London.

Cervellione, F., McGurk, C., Berger Eriksen, T. & Van den Broeck, W. (2017) Development of computer-assisted image analysis for semi-quantitative histology of the hepatopancreas for monitoring health in whiteleg shrimp (*Penaeus vannamei*). *18th EAFP International Conference on Diseases of Fish and Shellfish*, Belfast. Sept 2017.

Conference Proceedings:

Salogni, C., Cervellione, F., Alborali, GL, Gibelli, L. & Gelmetti, D. (2013) Atypical outbreak of Rainbow Trout Gastro Enteric Syndrome (RTGE). *XIX National Conference S.I.P.I.*, 39, Siracusa, Italy.

Salogni, C., Cervellione, F., Zanoni, M., Gelmetti, D. & Alborali GL (2008) Description of an outbreak of *Mycobacterium marinum* in rainbow trout (*Oncorhynchus mykiss*). *XV National Conference S.I.P.I.*, 29, Erice, Italy.

Posters:

Cervellione, F., Salogni, C., Mioso, PM, Alborali, GL & Gelmetti, D. (2011) Red Mark Syndrome in rainbow trout (*Oncorhynchus mykiss*) farmed in North Italy: anatomopathology, histology and aetiology. *XVII National Conference S.I.P.I.*, 46, Ostuni Italy.

Cervellione, F., McGurk, C., Silva, P., & Van den Broeck, W. (2015) Comparison of different fixatives and fixation methods for light microscopic examination of the gastrointestinal tract of Pacific white shrimp (*Penaeus vannamei*). *17th EAFP International Conference on Diseases of Fish and Shellfish*, 352, Gran Canaria.

Silva, P., Berger Eriksen, T., Owen, MAG, Lightner, DV, Noble, BL, Cervellione, F. & McGurk, C. (2015) Development of a quantitative semi-automated system, for hepatopancreas histology assessment in penaeid shrimp, using image analysis. *17th EAFP International Conference on Diseases of Fish and Shellfish*, 386, Gran Canaria.

Cervellione, F., McGurk, C., Berger Eriksen, T. & Van den Broeck, W. (2017) Development Effect of starvation and refeeding on the hepatopancreas morphology in whiteleg shrimp (*Penaeus vannamei*) using light and electron microscopy. *18th EAFP International Conference on Diseases of Fish and Shellfish*, Belfast. Sept 2017.

Lectures:

Strawberry disease and Red Mark Syndrome (2011). Faculty of Veterinary Medicine, School of Food inspection, safety, breeding and disease of aquatic animals and their products. University of Padova, Italy.